KoG

SCIENTIFIC-PROFESSIONAL JOURNAL OF CROATIAN SOCIETY
FOR GEOMETRY AND GRAPHICS

No. 14. (2010)
ISSN 1331-1611

KoG

Official publication of the Croatian Society for Geometry and Graphics publishes scientific and professional papers from the fields of geometry, applied geometry and computer graphics.

Founder and Publisher

Croatian Society for Geometry and Graphics

Design

Miroslav Ambruš-Kiš

Layout

Sonja Gorjanc, Ema Jurkin

Cover

Georg Glaeser: *"Reflecting Beauty", photography* (A jellyfish photographed in Kravjačica bay on the island of Kornat)

Print

"O-TISAK", d.o.o., Zagreb

URL address

http://www.hdgg.hr/kog
http://hrcak.srce.hr

Edition

150

Published annually

Guide for authors

Please, see the last page.

KoG is cited in: Mathematical Reviews, MathSciNet, Zentralblatt für Mathematik

---

This issue has been financially supported by The Ministry of Science, Education and Sport of the Republic of Croatia.

ISSN 1331–1611

KoG

No. 14
Zagreb, 2010

SCIENTIFIC AND PROFESSIONAL JOURNAL OF
CROATIAN SOCIETY FOR GEOMETRY AND GRAPHICS

CONTENTS

ISSN 1331–1611

KoG

BROJ 14
Zagreb, 2010

ZNANSTVENO-STRUČNI ČASOPIS
HRVATSKOG DRUŠTVA ZA GEOMETRIJU I GRAFIKU

SADRŽAJ

PREGLEDNI RAD

IZVORNI ZNANSTVENI RADOVI

Review
Accepted 24. 11. 2010.

NORMAN JOHN WILDBERGER

Universal Hyperbolic Geometry II: A pictorial overview

Universal Hyperbolic Geometry II: A pictorial overview

ABSTRACT

This article provides a simple pictorial introduction to universal hyperbolic geometry. We explain how to understand the subject using only elementary projective geometry, augmented by a distinguished circle. This provides a completely algebraic framework for hyperbolic geometry, valid over the rational numbers (and indeed any field not of characteristic two), and gives us many new and beautiful theorems. These results are accurately illustrated with colour diagrams, and the reader is invited to check them with ruler constructions and measurements.

Key words: hyperbolic geometry, projective geometry, rational trigonometry, quadrance, spread, quadrea

MSC 2010: 51M10, 14N99, 51E99

Univerzalna hiperbolička geometrija II: slikovni pregled

SAŽETAK

Članak pruža jednostavan slikovni uvod u univerzalnu hiperboličku geometriju. Objašnjava se kako razumjeti sadržaj koristeći samo osnovnu projektivnu geometriju, proširenu jednom istaknutom kružnicom. Na taj se način dobiva potpuno algebarski okvir za hiperboličku geometriju, koji vrijedi nad poljem racionalnih brojeva (i u biti nad bilo kojim poljem karakteristike različite od 2) i daje mnoge nove lijepe teoreme. Ovi su rezultati prikazani crtežima u boji, a čitatelj je pozvan provjeriti ih konstruktivno i računski.

Ključne riječi: hiperbolička geometrija, projektivna geometrija, racionalna geometrija, kvadranca, širina, kvadrea

1 Introduction

This paper introduces *hyperbolic geometry* using only elementary mathematics, without any analysis, and in particular without transcendental functions. Classical hyperbolic geometry, (see for example [6], [7], [8], [9], [10], [11], [15], [17], [23]), is usually an advanced topic studied in the senior years of a university mathematics program, often built up from a foundation of differential geometry. In recent years, a new, simpler and completely algebraic understanding of this subject has emerged, building on the ideas of *rational trigonometry* ([18] and [19]). This approach is called *universal hyperbolic geometry*, because it extends the theory to more general settings, namely to arbitrary fields (usually characteristic not two), and because it generalizes to other quadratic forms (see [21]).

The basic reference is *Universal Hyperbolic Geometry I: Trigonometry* ([22]), which contains accurate definitions, many formulas and complete proofs, but no diagrams. This paper complements that one, providing a pictorial introduction to the subject with a minimum of formulas and no proofs, essentially relying only on planar projective geometry. The reader is encouraged to verify theorems by making explicit constructions and measurements; aside from a single base (null) circle, with only a ruler one can check most of the assertions of this paper in special cases. Alternatively a modern geometry program such as The Geometer's Sketchpad, C.A.R., Cabri, GeoAlgebra or Cinderella illustrates the subject with a little effort.

Our approach extends the classical *Cayley Beltrami Klein*, or *projective*, model of hyperbolic geometry, whose underlying space is the interior of a disk, with lines being straight line segments. In our formulation we consider also the boundary of the disk, which we call the *null circle*, also points outside the disk, and also points at infinity. The lines are now complete lines in the sense of projective geometry, not segments, and include also *null lines* which are tangent to the null circle, and lines which do not meet the null circle, including the line at infinity. This orientation is familiar to classical geometers (see for example [2], [3], [4], [5], [14]), but it is not well-known to students because of the current dominance of the differential geometric point of view. A novel aspect of this paper is that we introduce our metrical concepts—*quadrance*, *spread* and *quadrea*—

purely in projective terms. It means that only high school algebra suffices to set up the subject and make computations. The proofs however rely generally on computer calculations involving polynomial or rational function identities; some may be found in ([22]), others will appear elsewhere.

Many of the results are illustrated with two diagrams, one illustrating the situation in the classical setting using interior points of the null circle, and another with more general points. The fundamental metrical notions of *quadrance* between points and *spread* between lines are undefined when null points or null lines are involved, but most theorems involving them apply equally to points and lines interior or exterior of the null circle. The reader should be aware that in more advanced work the distinction between these two types of points and lines also becomes significant. Instead of area of hyperbolic triangles, we work with a rational analog called *quadrea*.

With this algebraic approach we can develop geometry over the *rational numbers*—in my view, always the most important field. The natural connections between geometry and number theory are then not suppressed, but enrich both subjects. Later in the series we will also illustrate hyperbolic geometry over *finite fields*, in the direction of [1] and [16], where *counting* becomes important.

2 The projective plane

Hyperbolic geometry may be visualized as the geometry of the projective plane, augmented by a distinguished circle c (in fact a more general conic may also be used). Since projective geometry is not these days as familiar as it was in former times, we begin by reviewing some of the basic notions. The starting point is the affine plane—familiar from Euclidean geometry and Cartesian coordinate geometry—containing the usual points $[x,y]$ and (straight) lines with equations $ax+by=c$. The affine plane is augmented by introducing a *new point* for every family of parallel lines. In this introductory section we use *parallel* in the usual sense of Euclidean geometry, so that the lines with equations $a_1x+b_1y=c_1$ and $a_2x+b_2y=c_2$ are parallel precisely when $a_1b_2-a_2b_1=0$. Later on we will see that there is a different, hyperbolic meaning of 'parallel' (which is different from the usage in classical hyperbolic geometry!) The new point, one for each family of parallel lines, is a '*point at infinity*'. We also introduce one *new line*, the '*line at infinity*', which passes through every point at infinity.

Algebraically the projective plane may be defined without reference to the Euclidean plane, with points specified by homogeneous coordinates, or proportions, of the form $[x:y:z]$. Points $[x:y:1]$ correspond to the affine plane, and points at infinity are of the form $[x:y:0]$. The lines also are specified by homogeneous coordinates, now of the form $(a:b:c)$, with the pairing between the point $[x:y:z]$ and the line $(a:b:c)$ given by

$$ax+by-cz=0. \tag{1}$$

This particular relation is the characterizing equation for hyperbolic geometry; for spherical/elliptic geometry a different convention between points and lines is used, where the line $\langle a:b:c\rangle$ passes through the point $[x:y:z]$ precisely when $ax+by+cz=0$. Note that we use round brackets for lines in hyperbolic geometry.

We will visualize the projective plane as an extension of the affine plane, with the usual property that any two distinct points a and b determine exactly one line which passes through them both, called the **join** of a and b, and denoted by ab, and with the *new* property that any two lines L and M determine exactly one point which lies on them both, called the **meet** of L and M, and denoted by LM.

In projective geometry, the notion of parallel lines disappears, since now *any* two lines meet. Familiar measurements, such as distance and angle, are also absent. It is really the *geometry of the straightedge*.

Despite its historical importance, intrinsic beauty and simplicity, projective geometry is these days sadly neglected in the school and university curriculum. Perhaps the wider realization that it actually underpins hyperbolic geometry will lead to a renaissance of the subject! Most readers will know the two basic theorems in the subject, which are illustrated in Figure 1.

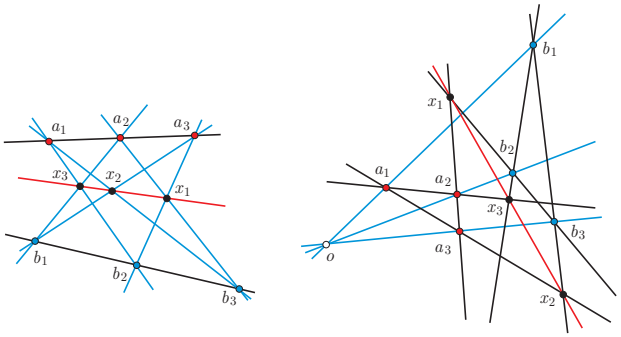

Figure 1: *Theorems of Pappus and Desargues*

Pappus' theorem asserts that if a_1, a_2 and a_3 are collinear, and b_1,b_2 and b_3 are collinear, then $x_1\equiv(a_2b_3)(a_3b_2)$, $x_2\equiv(a_3b_1)(a_1b_3)$ and $x_3\equiv(a_1b_2)(a_2b_1)$ are collinear. *Desargues' theorem* asserts that if a_1b_1, a_2b_2 and a_3b_3 are concurrent, then $x_1\equiv(a_2a_3)(b_2b_3)$, $x_2\equiv(a_3a_1)(b_3b_1)$ and $x_3\equiv(a_1a_2)(b_1b_2)$ are collinear. This is often stated in the form that if two triangles are perspective from a point, then they are also perspective from a line.

A further important notion concerns four collinear points a,b,c and d on a line L, in any order. Suppose we choose

affine coordinates on L so that the coordinates of a, b, c and d are respectively x, y, z and w. Then the **cross-ratio** is defined to be the extended number (possibly ∞) given by the ratio of ratios:

$$(a, b : c, d) \equiv \left(\frac{a-c}{b-c}\right) / \left(\frac{a-d}{b-d}\right).$$

This is independent of the choice of affine coordinates on L.

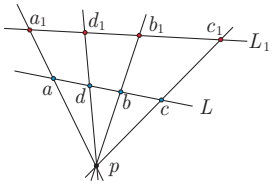

Figure 2: *Projective invariance of cross-ratio:* $(a, b : c, d) = (a_1, b_1 : c_1, d_1)$

Moreover it is also projectively invariant, meaning that if a_1, b_1, c_1 and d_1 are also collinear points on a line L_1 which are perspective to a, b, c and d from some point p, as in Figure 2, then $(a, b : c, d) = (a_1, b_1 : c_1, d_1)$.

The cross ratio is the most important invariant in projective geometry, and will be the basis of *quadrance* between points and *spread* between lines, but we give also analytic expressions for these quantities in homogeneous coordinates; both are *rational functions* of the inputs. The actual values assumed by the cross-ratio depend ultimately on the field over which our geometry is based, which is in principle quite arbitrary. To start it helps to restrict our attention to the *rational numbers*, invariably the most natural, familiar and important field. So we will adopt a scientific approach, identifying our sheet of paper with (part of) the *rational number plane*.

Here are a few more basic definitions. A **side** $\overline{a_1 a_2} = \{a_1, a_2\}$ is a set of two points. A **vertex** $\overline{L_1 L_2} = \{L_1, L_2\}$ is a set of two lines. A **couple** $\overline{aL} = \{a, L\}$ is a set consisting of a point a and a line L. A **triangle** $\overline{a_1 a_2 a_3} = \{a_1, a_2, a_3\}$ is a set of three points which are not collinear. A **trilateral** $\overline{L_1 L_2 L_3} = \{L_1, L_2, L_3\}$ is a set of three lines which are not concurrent. Every triangle $\overline{a_1 a_2 a_3}$ has three sides, namely $\overline{a_1 a_2}$, $\overline{a_2 a_3}$ and $\overline{a_1 a_3}$, and similarly any trilateral $\overline{L_1 L_2 L_3}$ has three vertices, namely $\overline{L_1 L_2}$, $\overline{L_2 L_3}$ and $\overline{L_1 L_3}$.

Since the points of a triangle and the lines of a trilateral are distinct, any triangle $\overline{a_1 a_2 a_3}$ determines an **associated trilateral** $\overline{L_1 L_2 L_3}$ where $L_1 \equiv a_2 a_3$, $L_2 \equiv a_1 a_3$ and $L_3 \equiv a_1 a_2$. Conversely any trilateral $\overline{L_1 L_2 L_3}$ determines an **associated triangle** $\overline{a_1 a_2 a_3}$ where $a_1 \equiv L_2 L_3$, $a_2 \equiv L_1 L_3$ and $a_3 \equiv L_1 L_2$.

3 Duality via polarity

We are now ready to introduce the **hyperbolic plane**, which is just the projective plane which we have just been describing, augmented by a distinguished Euclidean circle c in this plane, called the **null circle,** which appears in our diagrams always in blue. The points lying on c have a distinguished role, and are called **null points**. The lines tangent to c have a distinguished role, and are called **null lines**.

All other points and lines, including the points at infinity and the line at infinity, are for the purposes of elementary universal hyperbolic geometry treated in a non-preferential manner. In particular we do *not* restrict our attention to only **interior points** lying inside the circle c; this is a big difference with classical hyperbolic geometry; **exterior points** lying outside the circle are equally important. Similarly we do *not* restrict our attention to only **interior lines** which meet c in two points; **exterior lines** which do not meet c are equally important. Note also that these notions can be defined purely projectively once the null circle c has been specified: interior points do not lie on null lines, while exterior points do, and interior lines pass through null points, while exterior lines do not.

For those who prefer to work with coordinates, we may choose our circle to have homogeneous equation $x^2 + y^2 - z^2 = 0$, or in the plane $z = 1$ with coordinates $X \equiv x/z$ and $Y \equiv y/z$, simply the unit circle $X^2 + Y^2 = 1$.

The presence of the distinguished null circle c has as its main consequence a *complete duality* between points and lines of the projective plane, in the sense that every point a has associated to it a particular line $a^\perp$ and conversely. This duality is one of the ways in which universal hyperbolic geometry is very different from classical hyperbolic geometry, and it arises from a standard construction in projective geometry involving the distinguished null circle c—the notion of *polarity*. How polarity defines duality is central to the subject.

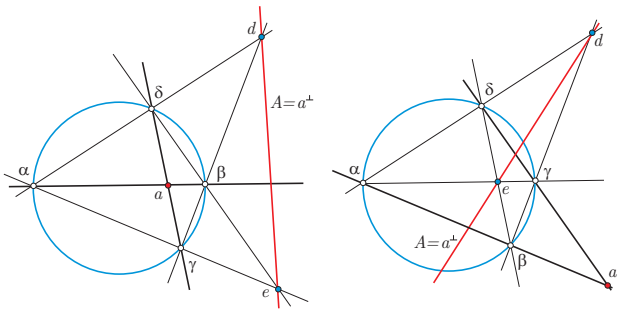

Figure 3: *Duality and pole-polar pairs*

To define the polar of a point a with respect to the null circle c, draw any two lines through a which each both pass through c in two distinct points, say α, β and γ, δ respectively; this is always possible. Now here is a beautiful fact from projective geometry: *if d and e are the other two diagonal points of the quadrilateral $\alpha\beta\gamma\delta$, then the line de does not depend on the two chosen lines through a, but only on a itself.* So we say that $de = A \equiv a^\perp$ is the **dual line** of the point a, and conversely $a = A^\perp$ is the **dual point** of the line A.

The picture is as in Figure 3, showing two different possible configurations for which the above prescriptions both hold. In case a is external to the circle, it is also possible to construct $A \equiv a^\perp$ from the tangents to the null circle c passing through a as in Figure 4, but this does not work for an interior point such as b.

The construction shows that there is in fact a symmetry between the initial point a and the diagonal points d and e, so that if we started with the point d, its dual would be the line ae, and if we started with the point e, its dual would be the point ad. So this shows another fundamental fact: *if d lies on the dual $a^\perp$ of the point a, then a lies on the dual $d^\perp$ of the point d.*

So to invert the construction, given a line A, choose two points d and e on it, find the dual lines $d^\perp$ and $e^\perp$, and define $a \equiv A^\perp = d^\perp e^\perp$. It is at this point that we need the projective plane, with its points and line at infinity, for if $d^\perp$ and $e^\perp$ were Euclidean parallel, then $d^\perp e^\perp$ would be a point at infinity. This situation occurs if we take our line A to be a diameter of the null circle c, in the sense of Euclidean geometry.

What happens when the point a is null? In that case the quadrilateral in the above construction degenerates, and the polar line $a^\perp$ is the null line tangent to the null circle at a. So every null line is dual to the unique null point which lies on it, as shown also in Figure 4.

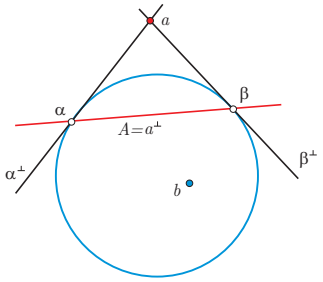

Figure 4: *Null points α, β and their dual null lines*

The duality between points and lines is surprisingly simple to describe in terms of homogeneous coordinates. The pole of the point $a \equiv [x : y : z]$ is just the line $a^\perp \equiv (x : y : z)$, so duality amounts to simply changing from one kind of brackets to the other! This explains why we chose the hyperbolic form of the pairing (1).

In the previous section we saw that every triangle $\overline{a_1a_2a_3}$ has an associated trilateral $\overline{L_1L_2L_3}$ and conversely. Now we see that there is another natural trilateral associated to $\overline{a_1a_2a_3}$, namely the **dual trilateral** $a_1^\perp a_2^\perp a_3^\perp$. Conversely to any trilateral $\overline{L_1L_2L_3}$ there is associated the **dual triangle** $L_1^\perp L_2^\perp L_3^\perp$.

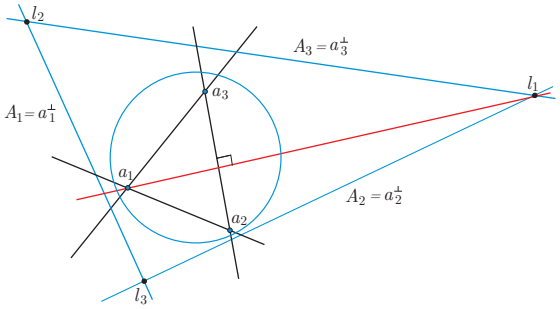

Figure 5: *A triangle $\overline{a_1a_2a_3}$ and its dual trilateral $\overline{A_1A_2A_3}$*

We also say that a couple $\overline{aL}$ is **dual** precisely when a and L are dual, and is otherwise **non-dual**.

So to summarize: *in (planar) universal hyperbolic geometry, duality implies that points and lines are treated completely symmetrically*. This is a significant departure both from Euclidean geometry and from classical hyperbolic geometry—in both of those theories, points and lines play quite different roles. In universal hyperbolic geometry, the above duality principle implies that every theorem can be dualized to create a (possibly) new theorem. We will state many theorems together with their duals, but to keep the length of this paper reasonable we will not extend this to all the theorems; the reader is encouraged to find statements and draw pictures of the dual results in these other cases.

4 Perpendicularity

The notions of perpendicular and parallel differ dramatically between Euclidean and hyperbolic geometries. In the affine geometry on which Euclidean geometry is based, the notion of *parallel lines* is fundamental, while *perpendicular lines* are determined by a quadratic form. In hyperbolic geometry, the situation is reversed—perpendicularity is more fundamental, and in fact parallelism is defined in terms of it!

Another novel feature is that perpendicularity applies not only to lines, but *also to points*. This is a consequence of the fundamental duality we have already established between points and lines.

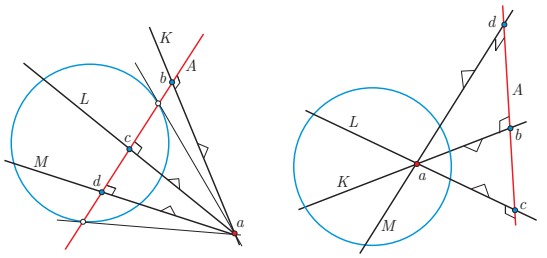

Figure 6: *Perpendicular points and lines*

Perpendicularity in the hyperbolic setting is easy to introduce once we have duality. We say that a point b is **perpendicular** to a point a precisely when b lies on the dual line $a^\perp$ of a. This is equivalent to a lying on the dual line $b^\perp$ of b, so the relation is symmetric, and we write

$$a \perp b.$$

Dually a line L is perpendicular to a line M precisely when L passes through the dual point $M^\perp$ of M. This is equivalent to M passing through the dual point $L^\perp$ of L, and we write

$$L \perp M.$$

Figure 6 shows our pictorial conventions for perpendicularity: the line A is dual to the point a, so points b, c and d lying on A are perpendicular to a, and this is recorded by a small (right) corner placed on the join of the perpendicular points, and between them. Also the lines K, L and M pass through a, so are perpendicular to A, and this is recorded as usual by a small parallelogram at the meet of the perpendicular lines.

Our first theorem records two basic facts that are obvious from the definitions so far.

Theorem 1 (Altitude line and point) *For any non-dual couple $\overline{aL}$, there is a unique line N which passes through a and is perpendicular to L, namely $N \equiv aL^\perp$, and there is a unique point n which lies on L and is perpendicular to a, namely $n \equiv a^\perp L$. Furthermore N and n are dual.*

We call N the **altitude line** to L through a, and n the **altitude point** to a on L. In case a and L are dual, any line through a is perpendicular to L, and any point lying on L is perpendicular to a. While the former idea is familiar, the latter is not. Figure 7 shows that if we restrict ourselves to the inside of the null circle, altitude points are invisible, so it is no surprise that the concept is missing from classical hyperbolic geometry. Remember that we are obliged to respect the balance which duality provides us!

If a triangle $\overline{a_1a_2a_3}$ has say a_1 dual to a_2a_3, then any line through a_1 will be perpendicular to the opposite line a_2a_3,

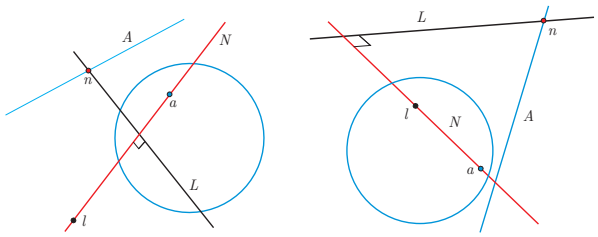

Figure 7: *Altitude line N and altitude point n of a couple $\overline{aL}$*

and we say the triangle is **dual**. A triangle is **non-dual** precisely when each of its points is not dual to the opposite line. Similar definitions apply to trilaterals.

Somewhat surprisingly, the next result is *not true* in classical hyperbolic geometry—a very conspicuous absence that too often goes unmentioned in books on the subject! The reason is that the orthocenter of a triangle of interior points might well be an exterior point, as the left diagram in Figure 8 shows. The absence of a distinguished orthocenter partially explains why the study of triangles in classical hyperbolic geometry is relatively undeveloped. With universal hyperbolic geometry, triangle geometry enters a rich new phase.

Theorem 2 (Orthocenter and ortholine) *The altitude lines of a non-dual triangle meet at a unique point o, called the **orthocenter** of the triangle. The altitude points of a non-dual trilateral join along a unique line O, called the **ortholine** of the trilateral. The ortholine O of the dual trilateral of a triangle is dual to the orthocenter o of the triangle.*

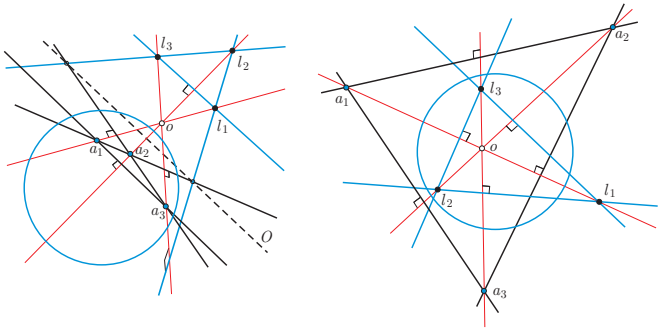

Figure 8: *Orthocenter o and ortholine O of a triangle $\overline{a_1a_2a_3}$ and its dual trilateral*

Figure 8 shows a triangle $\overline{a_1a_2a_3}$, its dual trilateral with associated triangle $\overline{l_1l_2l_3}$, and the corresponding orthocenter o and ortholine O.

5 Null points and lines

In modern treatments of hyperbolic geometry, points at infinity have a somewhat ambiguous role, and what we call null lines are rarely discussed, because they are essentially invisible in the Beltrami Poincaré models built from differential geometry. However earlier generations of classical geometers were well aware of them (see for example [14]).

In universal hyperbolic geometry null points and null lines play a particularly interesting and important role. Here is a first example, whose name comes from the definition that a triangle is **triply nil** precisely when each of its points is null.

Theorem 3 (Triply nil altitudes) *Suppose that α_1, α_2 and α_3 are distinct null points, with b any point lying on $\alpha_1\alpha_2$. Then the altitude lines to $\alpha_1\alpha_3$ and $\alpha_2\alpha_3$ through b are perpendicular.*

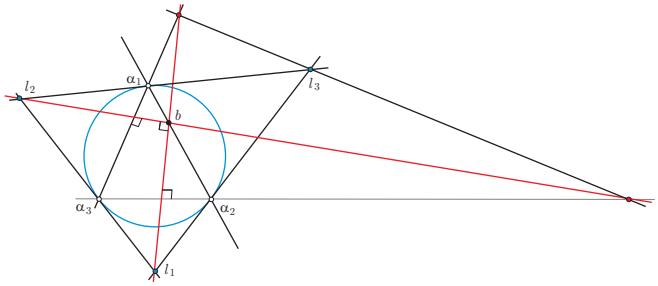

Figure 9: *The Triply nil altitudes theorem: $bl_1 \perp bl_2$*

Figure 9 shows that the Triply nil altitudes theorem may be recast in projective terms: if l_1, l_2 and l_3 are the poles of the lines of the triangle $\overline{\alpha_1\alpha_2\alpha_3}$ with respect to the conic c, then the points $(\alpha_1\alpha_3)(bl_1) = (bl_2)^\perp$, $(\alpha_2\alpha_3)(bl_2) = (bl_1)^\perp$ and l_3 are collinear.

In keeping with triangles and trilaterals, a (cyclic) set of four points is called a **quadrangle**, and a (cyclic) set of four lines a **quadrilateral**. The next result restates some facts that we already know about polarity of cyclic quadrilaterals in terms of perpendicularity.

Theorem 4 (Nil quadrangle diagonal) *Suppose that $\alpha_1, \alpha_2, \alpha_3$ and α_4 are distinct null points, with diagonal points $e \equiv (\alpha_1\alpha_2)(\alpha_3\alpha_4)$, $f \equiv (\alpha_1\alpha_3)(\alpha_2\alpha_4)$ and $g \equiv (\alpha_1\alpha_4)(\alpha_2\alpha_3)$. Then the lines ef, eg and fg are mutually perpendicular, and the points e, f and g are also mutually perpendicular.*

In classical hyperbolic geometry the null points $\alpha_1, \alpha_2, \alpha_3$ and α_4 would be considered to be 'at infinity', while the external diagonal points f and g in Figure 10 would be invisible. Let us repeat: *for us internal and external points are equally interesting.*

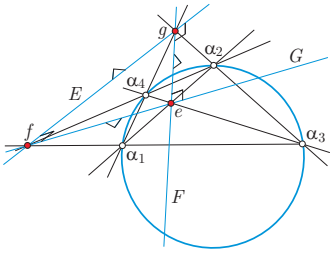

Figure 10: *Triply right diagonal triangle $\overline{efg}$*

6 Couples, parallels and bases

Points and lines are the basic objects in planar hyperbolic geometry. Given one point a, we may construct its dual line $A \equiv a^\perp$, and conversely given a line A we may construct its dual point $a \equiv A^\perp$. After that, there is in general nothing more to construct. For two objects, namely couples, sides and vertices, the situation is considerably more interesting, and gives us a chance to introduce some important additional concepts.

Given a non-dual couple $\overline{aL}$ we know we can construct the dual line $A \equiv a^\perp$ and the dual point $l \equiv L^\perp$, and the altitude line N and the altitude point n. Now we introduce another major point of departure from classical hyperbolic geometry, which provides an ironic twist to the oft-repeated history of hyperbolic geometry as a development arising from Euclid's Parallel Postulate.

Theorem 5 (Parallel line and point) *For any non-dual couple $\overline{aL}$ there is a unique line P which passes through a and is perpendicular to the altitude line N of $\overline{aL}$, namely $P \equiv a\left(a^\perp L\right)$, and there is a unique point p which lies on $a^\perp$ and is perpendicular to the altitude point n of $\overline{aL}$, namely $p \equiv a^\perp\left(aL^\perp\right)$. Furthermore P and p are dual.*

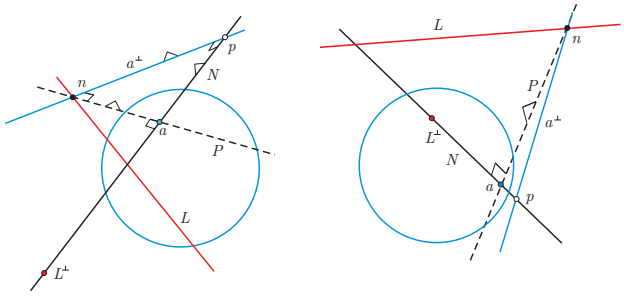

Figure 11: *Parallel line P and parallel point p of the couple $\overline{aL}$*

The line P is the **parallel line** of the couple $\overline{aL}$, and the point p is the **parallel point** of the couple $\overline{aL}$. These are shown in Figure 11. We may also refer to P as the **parallel line to the line** L **through** a. This is how we will henceforth use the term *parallel* in universal hyperbolic geometry—we do not say that *two lines are parallel*.

Theorem 6 (Base point and line) *For any non-dual couple $\overline{aL}$ there is a unique point b which lies on both L and the altitude line N of $\overline{aL}$, namely $b \equiv (aL^{\perp})\,L$, and there is a unique line B which passes through both $L^{\perp}$ and the altitude point n of $\overline{aL}$, namely $B \equiv (a^{\perp}L)\,L^{\perp}$. Furthermore B and b are dual.*

The point b is the **base point** of the couple $\overline{aL}$, and the line B is the **base line** of the couple $\overline{aL}$. These are shown in Figure 12.

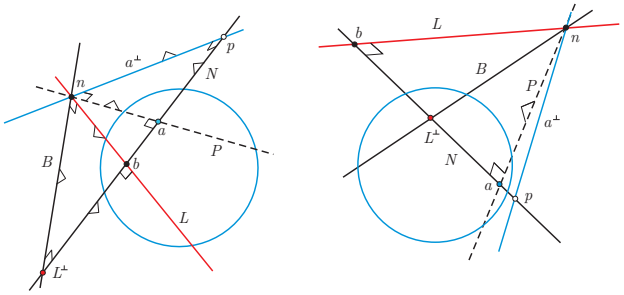

Figure 12: *Base point b and base line B of the couple $\overline{aL}$*

7 Sides, vertices and conjugates

There are also constructions for sides and vertices, and in fact the complete pictures associated with the general couple, side and vertex are essentially the same, but with different objects playing different roles.

Figure 13 shows the constructions possible if we start with a side $\overline{a_1a_2}$. Note that in this example one of these points is internal and one is external. A bit more terminology: we say that the side $\overline{a_1a_2}$ is **null** precisely when a_1a_2 is a null line, and **nil** precisely when at least one of a_1, a_2 is a null point. The vertex $\overline{L_1L_2}$ is **null** precisely when L_1L_2 is a null point, and **nil** precisely when at least one of L_1, L_2 is a null line.

Theorem 7 (Side conjugate points and lines) *For any side $\overline{a_1a_2}$ which is not both nil and null, there is a unique point $b_1 \equiv (a_1a_2)\,a_1^{\perp}$ which lies on a_1a_2 and is perpendicular to a_1, and there is a unique point $b_2 \equiv (a_1a_2)\,a_1^{\perp}$ which lies on a_1a_2 and is perpendicular to a_2.*

The points b_1 and b_2 are the **conjugate points** of the side $\overline{a_1a_2}$. The duals of these points are the lines $B_1 \equiv a_1\,(a_1a_2)^{\perp}$ and $B_2 \equiv a_2\,(a_1a_2)^{\perp}$, which are the **conjugate lines** of the side $\overline{a_1a_2}$. These relations are involutory: if the side $\overline{b_1b_2}$ is conjugate to the side $\overline{a_1a_2}$, then $\overline{a_1a_2}$ is also conjugate to $\overline{b_1b_2}$.

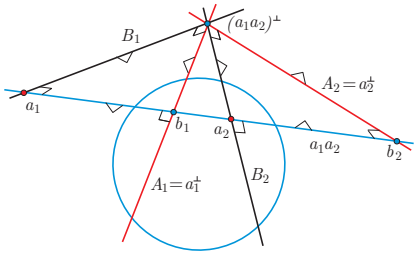

Figure 13: *Conjugate points and conjugate lines of the side $\overline{a_1a_2}$*

The same picture can also be reinterpreted by starting with a vertex.

Theorem 8 (Vertex conjugate points and lines) *For any vertex $\overline{A_1A_2}$ which is not both nil and null, there is a unique line $B_1 \equiv (A_1A_2)\,A_1^{\perp}$ which passes through A_1A_2 and is perpendicular to A_1, and there is a unique line $B_2 \equiv (A_1A_2)\,A_1^{\perp}$ which passes through A_1A_2 and is perpendicular to A_2.*

The lines B_1 and B_2 are the **conjugate lines** of the vertex $\overline{A_1A_2}$. The duals of these lines are the points $b_1 \equiv A_1\,(A_1A_2)^{\perp}$ and $b_2 \equiv A_2\,(A_1A_2)^{\perp}$, which are the **conjugate points** of the vertex $\overline{A_1A_2}$. This relation is also involutory: if the vertex $\overline{B_1B_2}$ is conjugate to the vertex $\overline{A_1A_2}$, then $\overline{A_1A_2}$ is also conjugate to $\overline{B_1B_2}$. This is shown also in Figure 14, which is essentially the same as Figures 12 and 13.

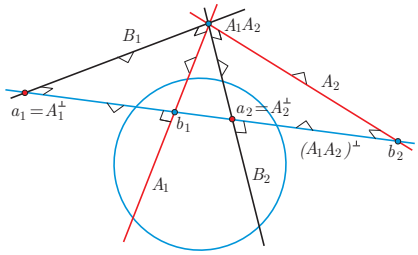

Figure 14: *Conjugate points and conjugate lines of the vertex $\overline{A_1A_2}$*

Furthermore the exact same configuration results if we had started with one of the sides $\overline{a_1b_2}$, or $\overline{a_2b_1}$, or $\overline{b_1b_2}$, or with one of the vertices $\overline{A_1B_2}$, or $\overline{A_2B_1}$, or $\overline{B_1B_2}$. However if we had started with a **right side**, meaning that the two

points are perpendicular, such as $\overline{a_1b_1}$, then we would obtain $L = a_1b_1$ and its dual point l. But then the conjugate side of $\overline{a_1b_1}$ would coincide with $\overline{a_1b_1}$, and similarly the conjugate vertex of a right vertex such as $\overline{A_1B_1}$ would coincide with $\overline{A_1B_1}$.

8 Reflections

The basic symmetries of hyperbolic geometry are *reflections*, but they have a somewhat different character from Euclidean reflections. Hyperbolic reflections send points to points and lines to lines, preserving incidence, in other words they are *projective transformations*. There are two seemingly different notions, the reflection σ_a in a (non-null) point a, and the reflection σ_L in a (non-null) line L. It is an important fact that these two notions end up agreeing, in the sense that

$$\sigma_a = \sigma_A$$

when $A = a^\perp$.

The transformation σ_a is defined first by its action on null points, and then by its action on more general points and lines.

For a non-null point a, the reflection σ_a sends a null point α to the other null point α' on the line αa. We write

$$\alpha' = \alpha\sigma_a.$$

In case $a\alpha$ is a null line, in other words a tangent to the null circle c, then $\alpha' \equiv \alpha$. Note that if a was itself a null point, then this definition would yield a transformation that would send every null point to a, which will not be a symmetry in the sense we wish. However such transformations can still be useful.

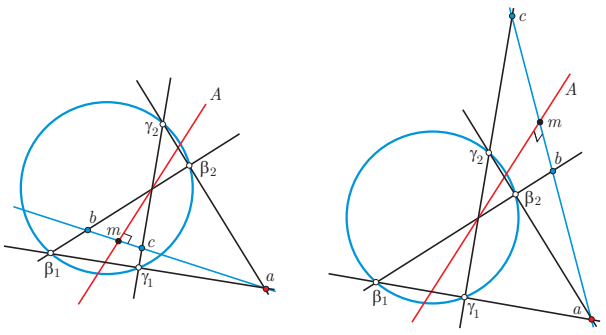

Figure 15: *Reflection in the point a or the dual line* $A \equiv a^\perp$

Once the action of a projective transformation on null points is known, it is determined on all points and lines, first of all on lines through two null points, and then on an arbitrary point by means of two such lines passing through it, and then on arbitrary lines. Figure 15 shows the reflection σ_a and its action on a point b to get $c \equiv b\sigma_a$. First find a line through b meeting the null circle at points β_1 and β_2, then construct $\gamma_1 \equiv \beta_1\sigma_a$ and $\gamma_1 \equiv \beta_1\sigma_a$, and then set

$$c \equiv b\sigma_a \equiv (ab)(\gamma_1\gamma_2).$$

For the reflection σ_L in a line L, the idea is dual to the above. It is defined first by its action on null lines, and then by its action on more general points and lines. For a non-null line L, the reflection σ_L sends a null line Π to the other null line Π' passing through the point $L\Pi$. We write

$$\Pi' = \Pi\sigma_L.$$

In case $L\Pi$ is a null point, $\Pi' \equiv \Pi$.

Once the action of a projective transformation on null lines is known, it is determined on all points and lines, since it is first of all determined on points lying on two null lines, and then on an arbitrary line by means of two such points lying on it, and then on arbitrary points.

Of course there is also a linear algebra/matrix approach to defining reflections. If $a = [u : v : w]$ then the action of $\sigma_a = \sigma_{a^\perp}$ on a point $b \equiv [x : y : z]$ is given by the projective matrix product

$$b\sigma_a = [x : y : z] \begin{bmatrix} u^2 - v^2 + w^2 & 2uv & 2uw \\ 2uv & -u^2 + v^2 + w^2 & 2vw \\ -2uw & -2vw & u^2 + v^2 - w^2 \end{bmatrix}$$

where the entries are only determined up to a scalar. The move to three dimensions simplifies the discussion.

9 Midpoints, midlines, bilines and bipoints

The notion of the *midpoint* of a side can be defined once we have the notion of a reflection. It also has a metrical formulation in terms of quadrance, which we have not yet introduced. There are three other closely related concepts, that of *midline*, *biline* and *bipoint*. Midpoints and midlines refer to sides, while bilines and bipoints refer to vertices. The existence of these objects reduces to questions in number theory—-whether or not certain quadratic equations have solutions.

If $c = b\sigma_d$ then we say d is a **midpoint** of the side $\overline{bc}$. In this case the point $e \equiv d^\perp(bc)$ is also a midpoint of $\overline{bc}$, and the two midpoints d and e of $\overline{bc}$ are perpendicular. The dual line $D \equiv d^\perp$ is a **midline** of $\overline{bc}$, meaning that it meets bc perpendicularly in a midpoint, namely e. The reflection σ_D in D of b is also c. Similarly the dual line $E \equiv e^\perp$ is also a midline of $\overline{bc}$. In Euclidean geometry midlines are called *perpendicular bisectors*. In hyperbolic geometry there are generally either zero or two midpoints between any two points, and so also zero or two midlines.

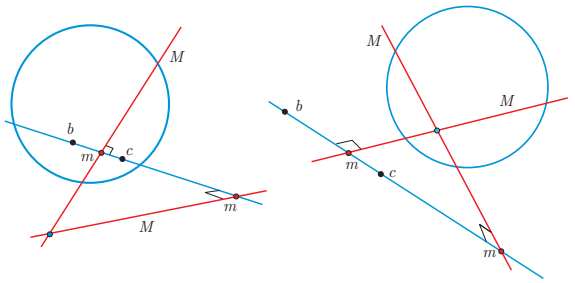

Figure 16: *Midpoints and midlines of* $\overline{bc}$

Figure 16 shows the midpoints m and midlines M of a side $\overline{bc}$. Figure 17 shows how to construct the midpoints and midlines of the side $\overline{bc}$ when such exist. For the midpoints of $\overline{bc}$ we first join b and c to the point $a \equiv (bc)^{\perp}$ to form lines M and N. If these are both interior lines, then their meets with the null circle give a completely nil quadrangle one of whose diagonal points is a, and the other two diagonal points d and e lie on bc and are the required midpoints. The duals D and E of d and e respectively are the midlines of $\overline{bc}$.

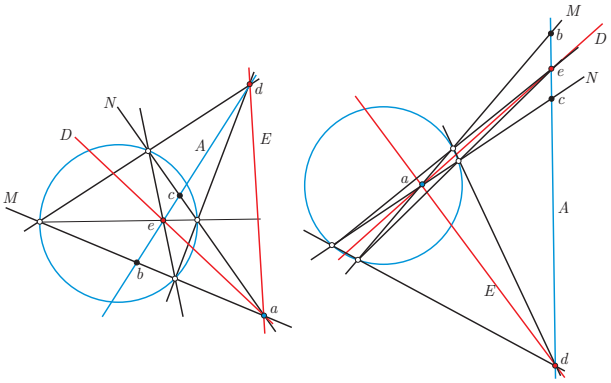

Figure 17: *Midpoints* d *and* e *of* $\overline{bc}$*, or bilines* D *and* E *of* $\overline{MN}$

The dual notions to midpoints and midlines of sides are the notions of bilines and bipoints of vertices. If M and N are lines and $M = N\sigma_D$ then the line D is a **biline** of the vertex $\overline{MN}$. In this case the line $E \equiv D^{\perp}\,(MN)$ is also a biline of $\overline{MN}$, and the two bilines D and E of $\overline{MN}$ are perpendicular.

The dual point $d \equiv D^{\perp}$ is a **bipoint** of $\overline{MN}$, and it joins MN perpendicularly in a biline, namely E. This implies that the reflection σ_d in d of M is also N. Similarly the dual point $e \equiv E^{\perp}$ is also a bipoint of $\overline{MN}$. In Euclidean geometry, bilines are called vertex bisectors or angle bisectors. Bipoints have no Euclidean analog.

Figure 17 can equally well be interpreted as illustrating the process of obtaining bilines D and E and bipoints d and e of the vertex $\overline{MN}$.

10 Hyperbolic triangle geometry

The richness of Euclidean triangle geometry is not reflected in the classical hyperbolic setting, but the situation is remedied with universal hyperbolic geometry. Here we give just a quick glimpse in this fascinating direction, which will be the focus of a subsequent paper in this series (see also [17]).

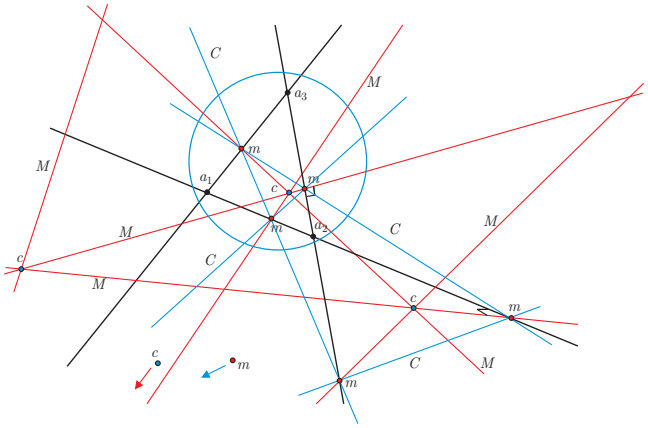

Figure 18: *Circumcenters and circumlines of a triangle* $\overline{a_1a_2a_3}$

Figure 18 shows a triangle $\overline{a_1a_2a_3}$ together with its six midpoints m (one is off the page) and corresponding six midlines M. The midpoints are collinear three at a time on four lines C called **circumlines**. The midlines are concurrent three at a time on four points c called **circumcenters**. The circumcenters are dual to the circumlines. Although we have not defined circles yet, a triangle generally has zero or four circumcircles, whose centers are at its circumcenters, if these exist.

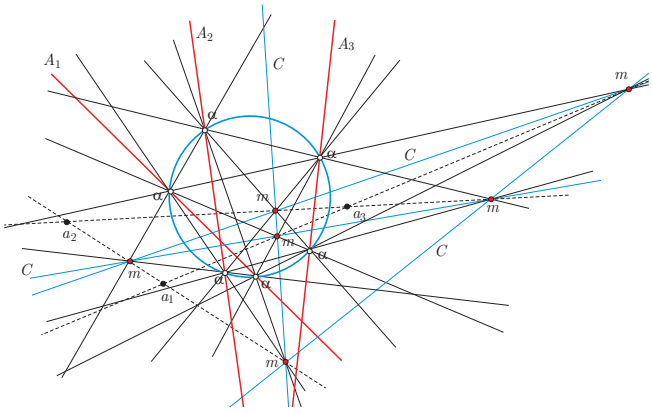

Figure 19: *Pascal's theorem via hyperbolic geometry*

An important application of circumlines is to *Pascal's theorem*, one of the great classical results of geometry. Figure 19 shows three lines A_1, A_2 and A_3 which meet the null

circle at six null points α. The dual points of A_1, A_2 and A_3 are a_1, a_2 and a_3 respectively. The triangle $\overline{a_1a_2a_3}$ has six midpoints m (red) and the four circumlines C (blue) pass through three midpoints each.

Two of the original three lines, such as A_1 and A_2, determine four null points α, and the other two diagonal points formed by such a quadrangle of null points, not including A_1A_2, give two midpoints m, in this case of the side $\overline{a_1a_2}$. So Pascal's theorem is here seen as a consequence of the fact that the *six midpoints of a triangle are collinear three at a time* forming the circumlines.

The six null points α can be partitioned into three sets of two in 15 ways. By different choices of the lines A_1, A_2 and A_3, there are altogether 15 such diagrams associated to the same six null points, and 60 possible circumlines C playing the role of Pascal's line. Such a large configuration has many remarkable features, some of them projective, some of them metrical.

11 Parallels and the doubled triangle

Given a triangle $\overline{a_1a_2a_3}$, the **double triangle** $\overline{d_1d_2d_3}$ is the triangle whose lines are the parallels P_1, P_2 and P_3 to the lines L_1, L_2 and L_3 of $\overline{a_1a_2a_3}$ through the points a_1, a_2 and a_3 respectively. We retain the usual notational conventions, so that $d_1 = P_2P_3$ etc. The situation is shown in Figure 20.

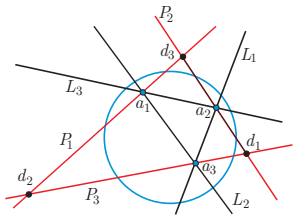

Figure 20: *A triangle $\overline{a_1a_2a_3}$ and its double triangle $\overline{d_1d_2d_3}$.*

The next theorem is surprising to me, and seems to require a somewhat involved computation.

Theorem 9 (Double median triangle) *If $\overline{d_1d_2d_3}$ is the double triangle of a triangle $\overline{a_1a_2a_3}$, then a_1, a_2 and a_3 are midpoints of the sides of $\overline{d_1d_2d_3}$.*

In Euclidean geometry the points in the next two theorems would both be the centroid of the triangle.

Theorem 10 (Double point) *If $\overline{d_1d_2d_3}$ is the double triangle of a triangle $\overline{a_1a_2a_3}$, then the lines a_1d_1, a_2d_2 and a_3d_3 are concurrent in a point x.*

Theorem 11 (Second double point) *If $\overline{d_1d_2d_3}$ is the double triangle of a triangle $\overline{a_1a_2a_3}$, and $\overline{g_1g_2g_3}$ is the double triangle of $\overline{d_1d_2d_3}$, then the lines a_1g_1, a_2g_2 and a_3g_3 are concurrent in a point y.*

These are shown in Figure 21; x is the **double point** of the triangle $\overline{a_1a_2a_3}$, and y is the **second double point** of the triangle $\overline{a_1a_2a_3}$.

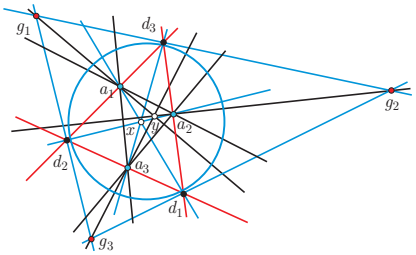

Figure 21: *First and second double points of a triangle $\overline{a_1a_2a_3}$*

It is not the case that the pattern continues in the obvious way: one cannot define a third double point in an analogous way. The study of the double triangle is clearly an interesting departure point from Euclidean triangle geometry.

12 Quadrance and spread

We now introduce the two basic measurements in universal hyperbolic geometry, the *quadrance* between points and the *spread* between lines. These are analogs of the corresponding notions in Euclidean *rational trigonometry*, but we assume no familiarity with this theory (although for a deeper understanding one should carefully compare the two). Our definition of quadrance and spread follows our projective orientation, and is given here in terms of the *cross-ratio* between four particular points or lines. The importance of this cross-ratio was shown in ([3]).

Suppose that a_1 and a_2 are points and that b_1 and b_2 are the conjugate points of the side $\overline{a_1a_2}$, as shown in Figure 22. Then define the **quadrance** between a_1 and a_2 to be the cross-ratio of points:

$$q(a_1, a_2) \equiv (a_1, b_2 : a_2, b_1).$$

The quadrance $q(a_1, a_2)$ is zero if $a_1 = a_2$. It is negative if a_1 and a_2 are both interior points, and approaches infinity as a_1 or a_2 approaches the null circle. It is undefined (or infinite) if one or both of a_1, a_2 is a null point. It is positive if one of a_1 and a_2 is an interior point and the other is an exterior point. It is negative if both a_1 and a_2 are exterior points and a_1a_2 is an interior line. It is zero if a_1a_2 is a null line. It is positive if both a_1 and a_2 are exterior points and a_1a_2 is an exterior line.

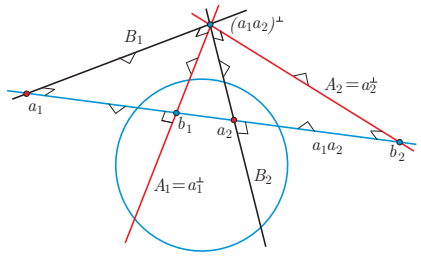

Figure 22: *Quadrance defined as cross-ratio:* $q(a_1,a_2) \equiv (a_1,b_2 : a_2,b_1)$

The usual distance $d(a_1,a_2)$ between a_1 and a_2 in the Klein model is also defined in terms of a cross-ratio, involving two *other* points: the meets of a_1a_2 with the null circle. This is problematic in three ways. First of all for two general points there may be no such meet, and so the Klein distance does not extend to general points. But even if the meets exist, it is not easy to separate them algebraically to get four points in a prescribed and canonical order to apply the cross-ratio. Finally to get a quantity that acts somewhat linearly, one is forced to introduce a logarithm or inverse circular function. This is much more complicated analytically, and makes extending the theory to finite fields, for example, more problematic.

In any case it turns out that if a_1 and a_2 are interior points, there is a relation between quadrance and the Klein distance:

$$q(a_1,a_2) = -\sinh^2(d(a_1,a_2)). \tag{2}$$

To define the spread between lines, we proceed in a dual fashion. In Figure 22, B_1 and B_2 are the conjugate lines of the vertex $\overline{A_1A_2}$. Define the **spread** between the lines A_1 and A_2 to be the cross-ratio of lines:

$$S(A_1,A_2) \equiv (A_1,B_2 : A_2,B_1).$$

This is positive if A_1 and A_2 are both interior lines that meet in an interior point. In fact if $\theta(A_1,A_2)$ is the usual angle between A_1 and A_2 in the Klein model, then it turns out that

$$S(A_1,A_2) = \sin^2(\theta(A_1,A_2)). \tag{3}$$

The relations (2) and (3) allow you to translate the subsequent theorems in this paper to formulas of classical hyperbolic trigonometry in the special case of interior points and lines.

The spread $S(A_1,A_2)$ between lines A_1 and A_2 is equal to the quadrance between the dual points, that is

$$S(A_1,A_2) = q\left(A_1^\perp,A_2^\perp\right).$$

So the basic duality between points and lines extends to the two fundamental measurements.

A **circle** is given by an equation of the form $q(x,a) = k$ for some fixed point a called the **center**, and a number k called the **quadrance**.

Here we show the circles centered at a point a of various quadrances. Figure 23 shows circles centered at a point a when a is an interior point. Figure 24 shows circles centered at an exterior point a. Both of these diagrams should be studied carefully. Note that the dual line $a^\perp$ of a is such a circle, of quadrance 1. Also note that the situation is dramatically different for a interior or a exterior. In the case of a an exterior point, there is a non-trivial circle of quadrance 0, namely the two null lines through a, and all circles meet the null circle at the two points where the dual line $a^\perp$ meets it. In classical hyperbolic geometry such curves are known as *constant width curves*—however from our point of view they are just circles.

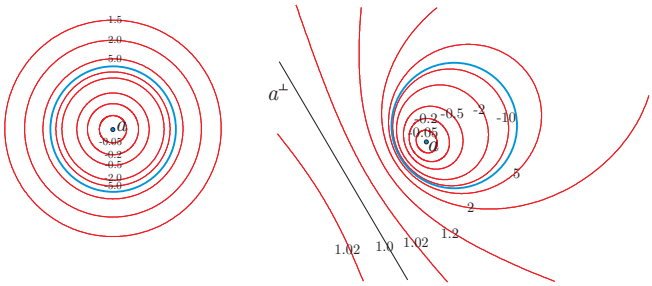

Figure 23: *Circles centered at a (interior)*

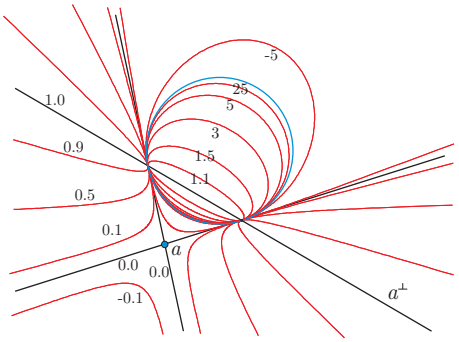

Figure 24: *Circles centered at a (exterior)*

There is a dual approach to circles where we use the relation $S(X,L) = k$ for a fixed line L and a variable line X. We leave it to the reader to show that we obtain the envelope of a circle as defined in terms of points. So the notion of a circle is essentially self-dual.

13 Basic trigonometric laws

For most calculations, we need explicit analytic formulae for the main measurements.

Theorem 12 *The* ***quadrance*** *between points* $a_1 \equiv [x_1 : y_1 : z_1]$ *and* $a_2 \equiv [x_2 : y_2 : z_2]$ *is*

$$q(a_1, a_2) = 1 - \frac{(x_1x_2 + y_1y_2 - z_1z_2)^2}{(x_1^2 + y_1^2 - z_1^2)(x_2^2 + y_2^2 - z_2^2)}.$$

Theorem 13 *The* ***spread*** *between lines* $L_1 \equiv (l_1 : m_1 : n_1)$ *and* $L_2 \equiv (l_2 : m_2 : n_2)$ *is*

$$S(L_1, L_2) = 1 - \frac{(l_1l_2 + m_1m_2 - n_1n_2)^2}{(l_1^2 + m_1^2 - n_1^2)(l_2^2 + m_2^2 - n_2^2)}.$$

These expressions are not defined if one or more of the points or lines involved is null, and reinforce the fact that the duality between points and lines extends to quadrances and spreads, and so every metrical result can be expected to have a dual formulation.

For a triangle $\overline{a_1a_2a_3}$ with associated trilateral $\overline{L_1L_2L_3}$ we will use the usual convention that $q_1 \equiv q(a_2, a_3)$, $q_2 \equiv q(a_1, a_3)$ and $q_3 \equiv q(a_1, a_2)$, and $S_1 \equiv S(L_2, L_3)$, $S_2 \equiv S(L_1, L_3)$ and $S_3 \equiv S(L_1, L_2)$. This notation will also be used in the degenerate case when a_1, a_2 and a_3 are collinear, or L_1, L_2 and L_3 are concurrent.

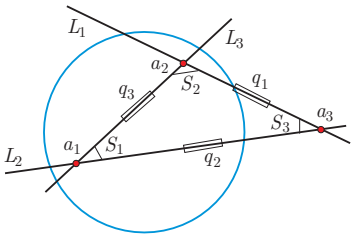

Figure 25: *Quadrance and spreads in a hyperbolic triangle*

With this notation, here are the main trigonometric laws in the subject. These are among the most important formulas in mathematics.

Theorem 14 (Triple quad formula) *If* a_1, a_2 *and* a_3 *are collinear points then*

$$(q_1 + q_2 + q_3)^2 = 2(q_1^2 + q_2^2 + q_3^2) + 4q_1q_2q_3.$$

Theorem 15 (Triple spread formula) *If* L_1, L_2 *and* L_3 *are concurrent lines then*

$$(S_1 + S_2 + S_3)^2 = 2(S_1^2 + S_2^2 + S_3^2) + 4S_1S_2S_3.$$

Theorem 16 (Pythagoras) *If* L_1 *and* L_2 *are perpendicular lines then*

$$q_3 = q_1 + q_2 - q_1q_2.$$

Theorem 17 (Pythagoras' dual) *If* a_1 *and* a_2 *are perpendicular points then*

$$S_3 = S_1 + S_2 - S_1S_2.$$

Theorem 18 (Spread law)

$$\frac{S_1}{q_1} = \frac{S_2}{q_2} = \frac{S_3}{q_3}.$$

Theorem 19 (Spread dual law)

$$\frac{q_1}{S_1} = \frac{q_2}{S_2} = \frac{q_3}{S_3}.$$

Theorem 20 (Cross law)

$$(q_1q_2S_3 - (q_1 + q_2 + q_3) + 2)^2 = 4(1 - q_1)(1 - q_2)(1 - q_3).$$

Theorem 21 (Cross dual law)

$$(S_1S_2q_3 - (S_1 + S_2 + S_3) + 2)^2 = 4(1 - S_1)(1 - S_2)(1 - S_3).$$

There are three symmetrical forms of Pythagoras' theorem, the Cross law and their duals, obtained by rotating indices. A proper appreciation for the beauty and power of these formulas requires some familiarity with rational trigonometry in the plane (see [18]), together with rolling up one's sleeves and solving many trigonometric problems in the hyperbolic setting. For students of geometry, this is an excellent undertaking.

14 Right triangles and trilaterals

Right triangles and trilaterals have some additional important properties besides the fundamental Pythagoras theorem we have already mentioned. We leave the dual results to the reader. Thales' theorem shows that there is an aspect of similar triangles in hyperbolic geometry. It also helps explain why spread is the primary measurement between lines in rational trigonometry.

Theorem 22 (Thales) *Suppose that* $\overline{a_1a_2a_3}$ *is a right triangle with* $S_3 = 1$. *Then*

$$S_1 = \frac{q_1}{q_3} \qquad \text{and} \qquad S_2 = \frac{q_2}{q_3}.$$

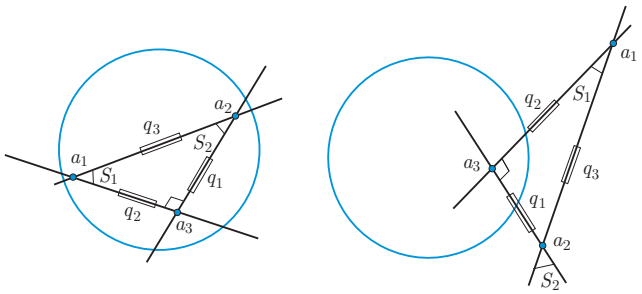

Figure 26: *Thales' theorem:* $S_1 = q_1/q_3$

The Right parallax theorem generalizes, and dramatically simplifies, a famous formula of Bolyai and Lobachevsky (see [6]) which usually requires exponential and circular functions, hence a prior understanding of real numbers.

Theorem 23 (Right parallax) *If a right triangle* $\overline{a_1a_2a_3}$ *has spreads* $S_1 = 0$, $S_2 = S$ *and* $S_3 = 1$, *then it will have only one defined quadrance* $q_1 = q$ *given by*

$$q = \frac{S-1}{S}.$$

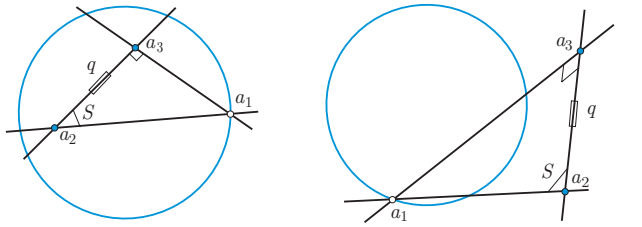

Figure 27: *Right parallax theorem:* $q = (S-1)/S$

We may restate this result in the form

$$S = \frac{1}{1-q}.$$

Napier's Rules are much simpler in the universal setting, where only high school algebra is required.

Theorem 24 (Napier's Rules) *Suppose a right triangle* $\overline{a_1a_2a_3}$ *has quadrances* q_1, q_2 *and* q_3, *and spreads* S_1, S_2 *and* $S_3 = 1$. *Then any two of the five quantities* S_1, S_2, q_1, q_2 *and* q_3 *determine the other three, solely by the three basic equations from Thales' theorem and Pythagoras' theorem:*

$$S_1 = \frac{q_1}{q_3} \qquad S_2 = \frac{q_2}{q_3} \qquad q_3 = q_1 + q_2 - q_1q_2.$$

15 Triangle proportions and barycentric coordinates

The following theorems implicitly involve barycentric coordinates. These are quite useful both in universal and classical hyperbolic geometry, see for example [17].

Theorem 25 (Triangle proportions) *Suppose that* $\overline{a_1a_2a_3}$ *is a triangle with quadrances* q_1, q_2 *and* q_3, *corresponding spreads* S_1, S_2 *and* S_3, *and that* d *is a point lying on the line* a_1a_2, *distinct from* a_1 *and* a_2. *Define the quadrances* $r_1 \equiv q(a_1, d)$ *and* $r_2 \equiv q(a_2, d)$, *and the spreads* $R_1 \equiv S(a_3a_1, a_3d)$ *and* $R_2 \equiv S(a_3a_2, a_3d)$. *Then*

$$\frac{R_1}{R_2} = \frac{S_1}{S_2}\frac{r_1}{r_2} = \frac{q_1}{q_2}\frac{r_1}{r_2}.$$

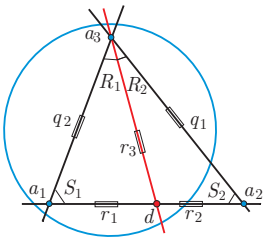

Figure 28: *Triangle proportions:* $R_1/R_2 = (S_1/S_2) \times (r_1/r_2)$

Theorem 26 (Menelaus) *Suppose that* $\overline{a_1a_2a_3}$ *is a non-null triangle, and that* L *is a non-null line meeting* a_2a_3, a_1a_3 *and* a_1a_2 *at the points* b_1, b_2 *and* b_3 *respectively. Define the quadrances*

$$\begin{aligned} r_1 &\equiv q(a_2, b_1) & t_1 &\equiv q(b_1, a_3) \\ r_2 &\equiv q(a_3, b_2) & t_2 &\equiv q(b_2, a_1) \\ r_3 &\equiv q(a_1, b_3) & t_3 &\equiv q(b_3, a_2). \end{aligned}$$

Then $r_1r_2r_3 = t_1t_2t_3$.

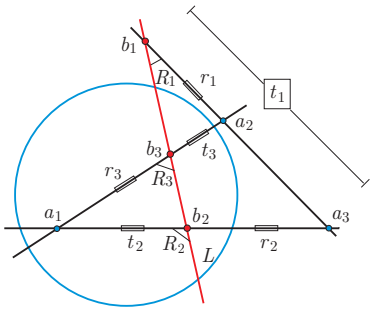

Figure 29: *Menelaus' theorem:* $r_1r_2r_3 = t_1t_2t_3$

Theorem 27 (Menelaus' dual) *Suppose that $\overline{A_1A_2A_3}$ is a non-null trilateral, and that l is a non-null point joining A_2A_3, A_1A_3 and A_1A_2 on the lines B_1, B_2 and B_3 respectively. Define the spreads*

$$R_1 \equiv S(A_2,B_1) \qquad T_1 \equiv S(B_1,A_3)$$
$$R_2 \equiv S(A_3,B_2) \qquad T_2 \equiv S(B_2,A_1)$$
$$R_3 \equiv S(A_1,B_3) \qquad T_3 \equiv S(B_3,A_2).$$

Then $R_1R_2R_3 = T_1T_2T_3$.

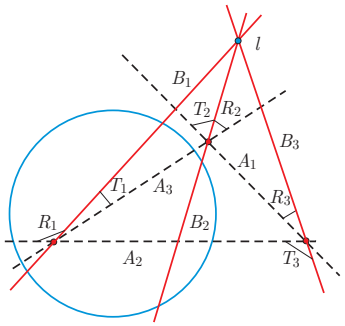

Figure 30: *Menelaus dual theorem: $R_1R_2R_3 = T_1T_2T_3$*

Theorem 28 (Ceva) *Suppose that the triangle $\overline{a_1a_2a_3}$ has non-null lines, that a_0 is a point distinct from a_1, a_2 and a_3, and that the lines a_0a_1, a_0a_2 and a_0a_3 meet the lines a_2a_3, a_1a_3 and a_1a_2 respectively at the points b_1, b_2 and b_3. Define the quadrances*

$$r_1 \equiv q(a_2,b_1) \qquad t_1 \equiv q(b_1,a_3)$$
$$r_2 \equiv q(a_3,b_2) \qquad t_2 \equiv q(b_2,a_1)$$
$$r_3 \equiv q(a_1,b_3) \qquad t_3 \equiv q(b_3,a_2).$$

Then $r_1r_2r_3 = t_1t_2t_3$.

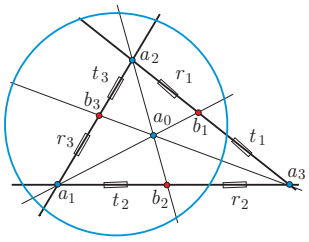

Figure 31: *Ceva's theorem: $r_1r_2r_3 = t_1t_2t_3$*

Theorem 29 (Ceva dual) *Suppose that the trilateral $\overline{A_1A_2A_3}$ is non-null, and that A_0 is a line distinct from A_1, A_2 and A_3, and that the points A_0A_1, A_0A_2 and A_0A_3 join the points A_2A_3, A_1A_3 and A_1A_2 respectively on the lines B_1, B_2 and B_3. Define the spreads*

$$R_1 \equiv S(A_2,B_1) \qquad T_1 \equiv S(B_1,A_3)$$
$$R_2 \equiv S(A_3,B_2) \qquad T_2 \equiv S(B_2,A_1)$$
$$R_3 \equiv S(A_1,B_3) \qquad T_3 \equiv S(B_3,A_2).$$

Then $R_1R_2R_3 = T_1T_2T_3$.

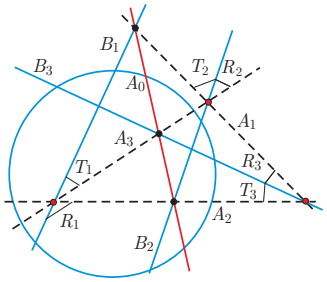

Figure 32: *Ceva's dual theorem: $R_1R_2R_3 = T_1T_2T_3$*

16 Isosceles triangles

Theorem 30 (Pons Asinorum) *Suppose that the non-null triangle $\overline{a_1a_2a_3}$ has quadrances q_1, q_2 and q_3, and corresponding spreads S_1, S_2 and S_3. Then $q_1 = q_2$ precisely when $S_1 = S_2$.*

Theorem 31 (Isosceles right) *If $\overline{a_1a_2a_3}$ is an isosceles triangle with two right spreads $S_1 = S_2 = 1$, then also $q_1 = q_2 = 1$ and $S_3 = q_3$.*

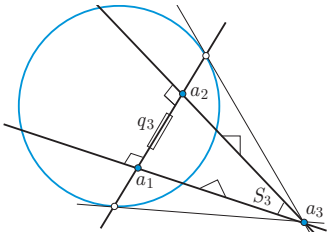

Figure 33: *Isosceles right triangle: $q_1 = q_2 = 1$ and $S_3 = q_3$*

Theorem 32 (Isosceles triangle) *Suppose a non-null isosceles triangle $\overline{a_1a_2a_3}$ has quadrances $q_1 = q_2 \equiv q$ and q_3, and corresponding spreads $S_1 = S_2 \equiv S$ and S_3. Then the following relations hold:*

$$q_3 = \frac{4(1-S)q(1-q)}{(1-Sq)^2} \qquad \text{and} \qquad S_3 = \frac{4S(1-S)(1-q)}{(1-Sq)^2}.$$

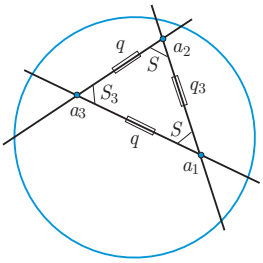

Figure 34: *An isosceles triangle: $q_1 = q_2 = q$, $S_1 = S_2 = S$*

Theorem 33 (Isosceles parallax) *If $\overline{a_1a_2a_3}$ is an isosceles triangle with a_1 a null point, $q_1 \equiv q$ and $S_2 = S_3 \equiv S$, then*

$$q = \frac{4(S-1)}{S^2}.$$

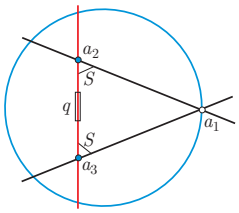

Figure 35: *Isosceles parallax: $q = 4(S-1)/S^2$*

17 Equilateral triangles

Theorem 34 (Equilateral quadrance spread) *Suppose that a triangle $\overline{a_1a_2a_3}$ is equilateral with common quadrance $q_1 = q_2 = q_3 \equiv q$, and with common spread $S_1 = S_2 = S_3 \equiv S$. Then*

$$(1-Sq)^2 = 4(1-S)(1-q).$$

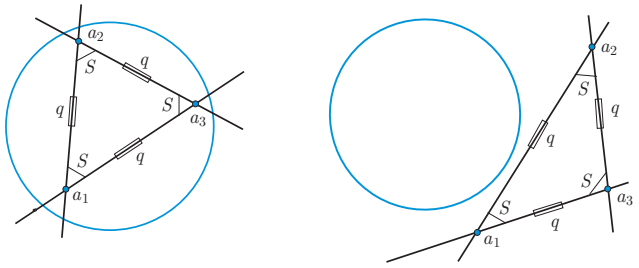

Figure 36: *Equilateral quadrance spread theorem:* $(1-Sq)^2 = 4(1-S)(1-q)$

18 Lambert quadrilaterals

Theorem 35 (Lambert quadrilateral) *Suppose a quadrilateral $\overline{abcd}$ has all three spreads at a, b and c equal to 1. Suppose that $q \equiv q(a,b)$ and $p \equiv q(b,c)$. Then*

$$q(c,d) = y = \frac{q(1-p)}{1-qp} \qquad q(a,d) = x = \frac{p(1-q)}{1-qp}$$

$$q(a,c) = s = q+p-qp \qquad q(b,d) = r = \frac{q+p-2qp}{1-qp}$$

and

$$S(ba,bd) = \frac{x}{r} \qquad S(bc,bd) = \frac{y}{r}$$

$$S(ac,ab) = \frac{p}{s} \qquad S(cb,ca) = \frac{q}{s}$$

$$S(ac,ad) = \frac{q(1-p)}{s} \qquad S(ca,cd) = \frac{p(1-q)}{s}$$

and

$$S(da,dc) = S = 1-pq.$$

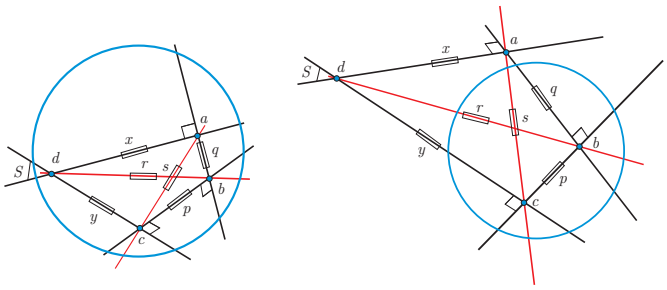

Figure 37: *Lambert quadrilateral $\overline{abcd}$*

19 Quadrea and triangle thinness

If $\overline{a_1a_2a_3}$ is a triangle with quadrances q_1, q_2 and q_3, and spreads S_1, S_2 and S_3, then from the Spread law the quantity

$$\mathcal{A} \equiv S_1q_2q_3 = S_2q_1q_3 = S_3q_1q_2$$

is well-defined, and called the **quadrea** of the triangle $\overline{a_1a_2a_3}$. It is the analog of the squared area in universal hyperbolic geometry. In Figure 38 several triangles with their associated quadreas are shown. Note that the quadrea is positive for a triangle of internal points, but may also be negative otherwise.

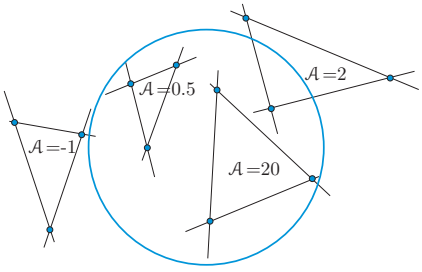

Figure 38: *Examples of triangles with quadreas* $\mathcal{A} = -1, 0.5, 20$ *and* 2

An interesting aspect of hyperbolic geometry is that *triangles are thin*. Here are two ways of giving meaning to this, both involving the quadrea of a triangle.

Theorem 36 (Triply nil Cevian thinness) *Suppose that* $\overline{\alpha_1\alpha_2\alpha_3}$ *is a triply nil triangle, and that* a *is a point distinct from* α_1, α_2 *and* α_3. *Define the cevian points* $c_1 \equiv (a\alpha_1)(\alpha_2\alpha_3)$, $c_2 \equiv (a\alpha_2)(\alpha_1\alpha_3)$ *and* $c_3 \equiv (a\alpha_3)(\alpha_1\alpha_2)$. *Then* $\mathcal{A}(\overline{c_1c_2c_3}) = 1$.

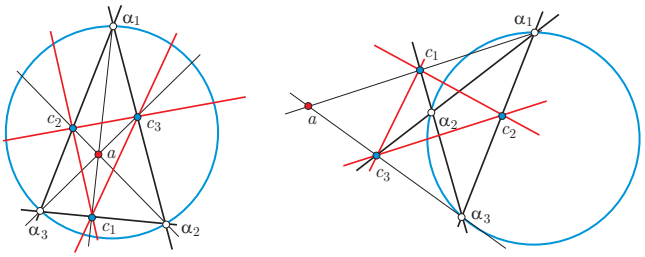

Figure 39: *Cevian triangle thinness:* $\mathcal{A}(\overline{c_1c_2c_3}) = 1$

Theorem 37 (Triply nil altitude thinness) *Suppose that* $\overline{\alpha_1\alpha_2\alpha_3}$ *is a triply nil triangle and that* a *is a point distinct from the duals of the lines. If the altitudes to the lines of this triangle from* a *meet the lines respectively at base points* b_1, b_2 *and* b_3, *then* $\mathcal{A}(\overline{b_1b_2b_3}) = 1$.

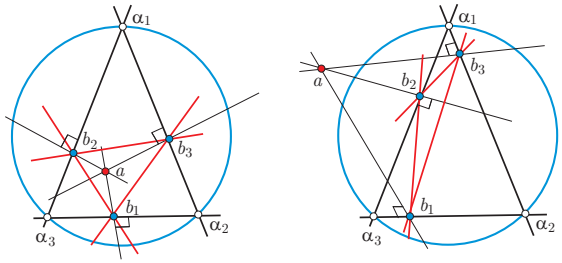

Figure 40: *Altitude triangle thinness:* $\mathcal{A}(\overline{b_1b_2b_3}) = 1$

20 Null perspective and null subtended theorems

There are many trigonometric results that prominently feature *null points* and *null lines*. We give a sample of these now. For some we include the dual formulations, for others these are left to the reader.

Theorem 38 (Null perspective) *Suppose that* α_1, α_2 *and* α_3 *are distinct null points, and* b *is any point on* $\alpha_1\alpha_3$ *distinct from* α_1 *and* α_3. *Suppose further that* x *and* y *are points lying on* $\alpha_1\alpha_2$, *and that* $x_1 \equiv (\alpha_2\alpha_3)(xb)$ *and* $y_1 \equiv (\alpha_2\alpha_3)(yb)$. *Then*

$$q(x,y) = q(x_1,y_1).$$

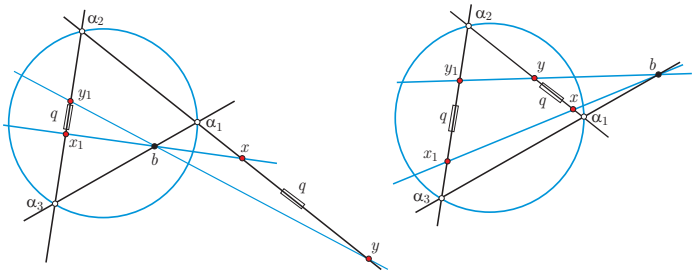

Figure 41: *Null perspective theorem:* $q(x,y) = q(x_1,y_1)$

Theorem 39 (Null subtended) *Suppose that the line* L *passes through the null points* α_1 *and* α_2. *Then for any other null point* α_3 *and any line* M, *let* $a_1 \equiv (\alpha_1\alpha_3)M$ *and* $a_2 \equiv (\alpha_2\alpha_3)M$. *Then* $q \equiv q(a_1,a_2)$ *and* $S \equiv S(L,M)$ *are related by*

$$qS = 1.$$

In particular q *is independent of* α_3.

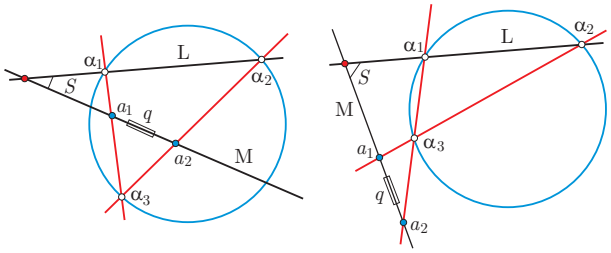

Figure 42: *Null subtended theorem:* $qS = 1$

Figure 42 shows two different examples; note that M need not pass through any null points. The Null subtended theorem allows you to create a hyperbolic ruler using just a straight-edge, in the sense that you can use it to repeatedly duplicate a given segment on a given line. Here is the dual result.

Theorem 40 (Null subtended dual) *Suppose that the point* l *lies on the null lines* Λ_1 *and* Λ_2. *Then for any other null line* Λ_3 *and any point* m, *let* $A_1 \equiv (\Lambda_1\Lambda_3)m$ *and* $A_2 \equiv (\Lambda_2\Lambda_3)m$. *Then* $S \equiv S(L_1,L_2)$ *and* $q \equiv q(l,m)$ *are related by*

$$Sq = 1.$$

Theorem 41 (Opposite subtended) *Suppose* $\overline{\alpha\beta\gamma\delta}$ *is a quadrangle of null points, and that* υ, μ *are also null points. Let* $a \equiv (\alpha\mu)(\gamma\delta)$, $b \equiv (\beta\mu)(\gamma\delta)$, $c \equiv (\gamma\upsilon)(\alpha\beta)$ *and* $d \equiv (\delta\upsilon)(\alpha\beta)$. *Then*

$$q(a,b) = q(c,d).$$

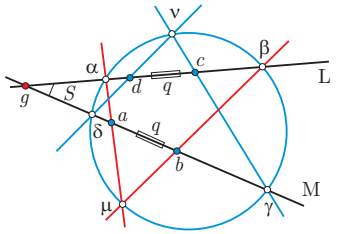

Figure 43: *Opposite subtended theorem:* $q(a,b) = q(c,d)$

Butterfly theorems have been investigated in the hyperbolic plane ([13]). The next theorems concern a related configuration of null points.

Theorem 42 (Butterfly quadrance) *Suppose that* $\overline{\alpha\beta\gamma\delta}$ *is a quadrangle of null points, with* $g \equiv (\alpha\gamma)(\beta\delta)$ *a diagonal point. Let* L *be any line passing through* g*, and suppose that* L *meets* $\alpha\delta$ *at* x *and* $\beta\gamma$ *at* y*. Then*

$$q(g,x) = q(g,y).$$

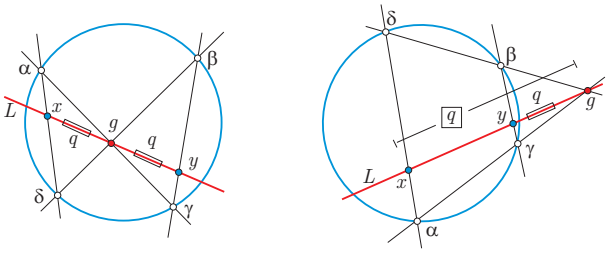

Figure 44: *Butterfly quadrance theorem:* $q(g,x) = q(g,y)$

Theorem 43 (Butterfly spread) *Suppose that* $\overline{\alpha\beta\gamma\delta}$ *is a quadrangle of null points, with* $g \equiv (\alpha\gamma)(\beta\delta)$ *a diagonal point. Let* L *be any line passing through* g*. Then*

$$S(L,\alpha\delta) = S(L,\beta\gamma).$$

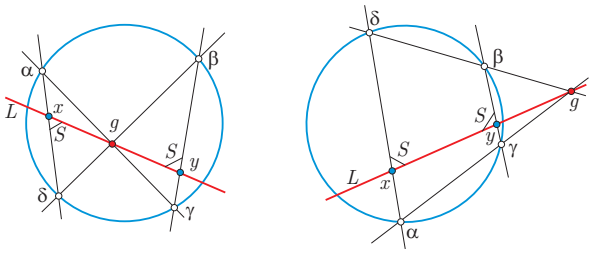

Figure 45: *Butterfly spread theorem:* $S(L,\alpha\delta) = S(L,\beta\gamma)$

21 The 48/64 theorems

In universal hyperbolic geometry we discover many constants of nature that express themselves in a geometrical way. Prominent among these are the numbers 48 and 64, but there are many others too!

Theorem 44 ($48/64$**)** *If the three spreads between opposite lines of a quadrangle* $\overline{\alpha_1\alpha_2\alpha_3\alpha_4}$ *of null points are* P,R *and* T*, then*

$$PR + RT + PT = 48$$

and

$$PRT = 64.$$

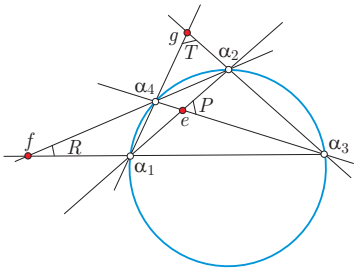

Figure 46: *The* $48/64$ *theorem:* $PR + RT + PT = 48$ *and* $PRT = 64$

It follows that

$$\frac{1}{R} + \frac{1}{S} + \frac{1}{T} = \frac{3}{4}.$$

In particular if we know two of these spreads, we get a linear equation for the third one.

Theorem 45 ($48/64$ **dual)** *If the three quadrances between opposite points of a quadrilateral* $\overline{\Lambda_1\Lambda_2\Lambda_3\Lambda_4}$ *of null lines are* p,r *and* t*, then*

$$pr + rt + pt = 48$$

and

$$prt = 64.$$

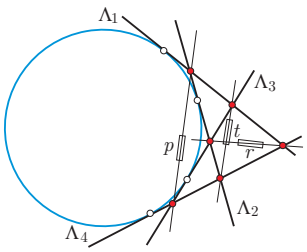

Figure 47: *The* $48/64$ *dual theorem:* $pr + rt + pt = 48$ *and* $prt = 64$

22 Pentagon theorems and extensions

The next theorem does not rely on null points, but is closely connected to a family of results that do.

Theorem 46 (Pentagon ratio) *Suppose* $\overline{a_1a_2a_3a_4a_5}$ *is a pentagon, meaning a cyclical list of five points, no three consecutive points collinear. Define* ***diagonal points***

$$\begin{array}{cc} b_1 \equiv (\alpha_2\alpha_4)(\alpha_3\alpha_5), & b_2 \equiv (\alpha_3\alpha_5)(\alpha_4\alpha_1), \\ b_3 \equiv (\alpha_4\alpha_1)(\alpha_5\alpha_2), & b_4 \equiv (\alpha_5\alpha_2)(\alpha_1\alpha_3), \\ \textit{and} & b_5 \equiv (\alpha_1\alpha_3)(\alpha_2\alpha_4), \end{array}$$

and subsequently ***opposite points***

$$\begin{array}{cc} c_1 \equiv (a_1b_1)(a_2a_5), & c_2 \equiv (a_2b_2)(a_3a_1), \\ c_3 \equiv (a_3b_3)(a_4a_2), & c_4 \equiv (a_4b_4)(a_5a_3), \\ \textit{and} & c_5 \equiv (a_5b_5)(a_1a_4). \end{array}$$

Then

$$q(b_1,c_4)\,q(b_2,c_5)\,q(b_3,c_1)\,q(b_4,c_2)\,q(b_5,c_3) = q(b_2,c_4)\,q(b_3,c_5)\,q(b_4,c_1)\,q(b_5,c_2)\,q(b_1,c_3).$$

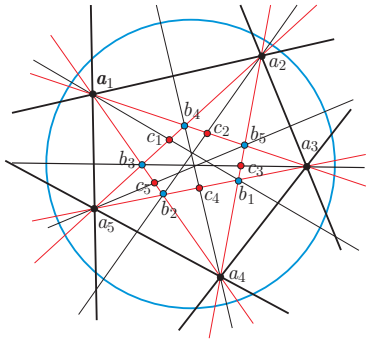

Figure 48: *Pentagon ratio theorem*

Since the pentagon is arbitrary, it follows by a scaling argument that *exactly the same theorem* holds in planar Euclidean geometry, where we replace the hyperbolic quadrance q with the Euclidean quadrance Q, since for five very close interior points, the hyperbolic quadrances and Euclidean quadrances are approximately proportional.

There are also some interesting additional features that occur in the special case of the pentagon when all the points a_i are null.

Theorem 47 (Pentagon null product) *Suppose* $\overline{\alpha_1\alpha_2\alpha_3\alpha_4\alpha_5}$ *is a pentagon of null points. Define diagonal points*

$$\begin{array}{cc} b_1 \equiv (\alpha_2\alpha_4)(\alpha_3\alpha_5), & b_2 \equiv (\alpha_3\alpha_5)(\alpha_4\alpha_1), \\ b_3 \equiv (\alpha_4\alpha_1)(\alpha_5\alpha_2), & b_4 \equiv (\alpha_5\alpha_2)(\alpha_1\alpha_3), \\ \textit{and} & b_5 \equiv (\alpha_1\alpha_3)(\alpha_2\alpha_4). \end{array}$$

Then

$$q(b_1,b_2)\,q(b_2,b_3)\,q(b_3,b_4)\,q(b_4,b_5)\,q(b_5,b_1) = -\frac{1}{4^5}.$$

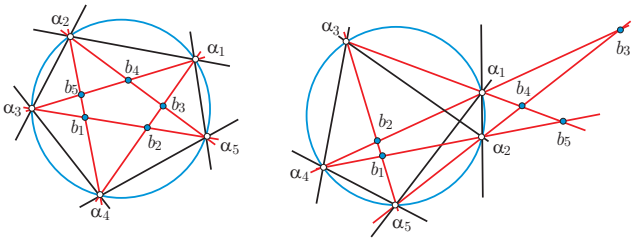

Figure 49: *Pentagon null product theorem:* $q(b_1,b_2)\,q(b_2,b_3)\,q(b_3,b_4)\,q(b_4,b_5)\,q(b_5,b_1) = -\frac{1}{4^5}$

Theorem 48 (Pentagon null symmetry) *With notation as in the Pentagon ratio theorem, suppose that* $\overline{\alpha_1\alpha_2\alpha_3\alpha_4\alpha_5}$ *is a pentagon of null points, then*

$$\begin{array}{cc} q(b_1,c_4) = q(b_5,c_2), & q(b_2,c_5) = q(b_1,c_3), \\ q(b_3,c_1) = q(b_2,c_4), & q(b_4,c_2) = q(b_3,c_5) \\ \textit{and} & q(b_5,c_3) = q(b_4,c_1). \end{array}$$

Furthermore if we fix $\alpha_2,\alpha_3,\alpha_4$ *and* α_5*, then the quadrance* $q(b_4,c_2) = q(b_3,c_5)$ *is constant, independent of* α_1*.*

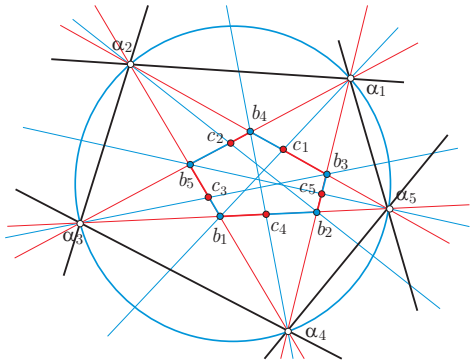

Figure 50: *Pentagon null symmetry theorem:* $q(b_1,c_4) = q(b_5,c_2)$ *etc*

Since five points determine a conic, here is an analog to the Pentagon ratio theorem for general septagons.

Theorem 49 (Septagon conic ratio) *Suppose* $\overline{\alpha_1\alpha_2\alpha_3\alpha_4\alpha_5\alpha_6\alpha_7}$ *is a septagon of points lying on a conic. Define diagonal points*

$$\begin{array}{cc} b_1 \equiv (\alpha_3\alpha_5)(\alpha_4\alpha_6), & b_2 \equiv (\alpha_4\alpha_6)(\alpha_5\alpha_7), \\ b_3 \equiv (\alpha_5\alpha_7)(\alpha_6\alpha_1), & b_4 \equiv (\alpha_6\alpha_1)(\alpha_7\alpha_2), \\ b_5 \equiv (\alpha_7\alpha_2)(\alpha_1\alpha_3), & b_6 \equiv (\alpha_1\alpha_3)(\alpha_2\alpha_4), \\ \textit{and} & b_7 \equiv (\alpha_2\alpha_4)(\alpha_3\alpha_5), \end{array}$$

and opposite points

$$\begin{array}{cc} c_1 \equiv (\alpha_1b_1)(\alpha_7\alpha_2), & c_2 \equiv (\alpha_2b_2)(\alpha_1\alpha_3), \\ c_3 \equiv (\alpha_3b_3)(\alpha_2\alpha_4), & c_4 \equiv (\alpha_4b_4)(\alpha_3\alpha_5), \\ c_5 \equiv (\alpha_5b_5)(\alpha_4\alpha_6), & c_6 \equiv (\alpha_6b_6)(\alpha_5\alpha_7), \\ \textit{and} & c_7 \equiv (\alpha_7b_7)(\alpha_6\alpha_1). \end{array}$$

Then

$$q(c_1,b_5)\,q(c_2,b_6)\,q(c_3,b_7)\,q(c_4,b_1)\,q(c_5,b_2)\,q(c_6,b_3)\,q(c_7,b_4)$$
$$= q(c_1,b_4)\,q(c_2,b_5)\,q(c_3,b_6)\,q(c_4,b_7)\,q(c_5,b_1)\,q(c_6,b_2)\,q(c_7,b_3).$$

Since the notion of a conic is projective, a scaling argument shows that the same theorem holds also in the Euclidean case. Figure 51 shows the special case of a septagon of null points (top), and a more general case where the septagon lies on a conic (bottom), in this case a Euclidean circle.

I conjecture that the Septagon conic ratio theorem extends to all odd polygons.

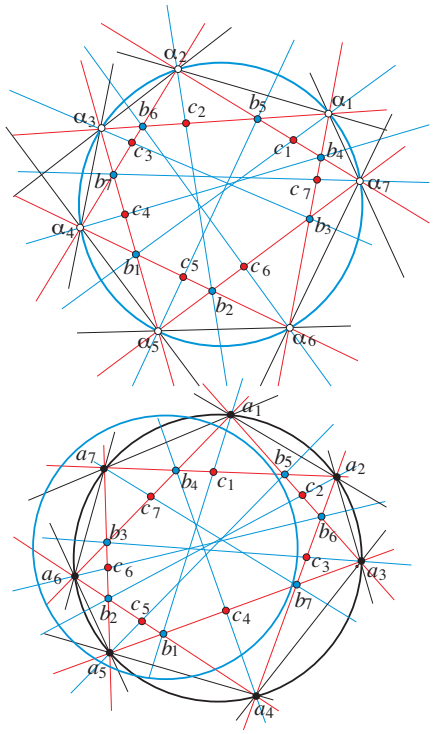

Figure 51: *Septagon conic ratio theorem*

23 Conics in hyperbolic geometry

The previous result used the fact that conics are well-defined in hyperbolic geometry, since they can be defined projectively, and we are working in a projective setting. A natural question is: can we also study conics metrically as we do in the Euclidean plane? In fact we can, and the resulting theory is both more intricate and richer than the Euclidean theory, nevertheless incorporating the Euclidean case as a limiting special case.

We have already mentioned (hyperbolic) circles and illustrated them in Figures 23 and 24. Let us now just briefly outline some results for a **(hyperbolic) parabola**, which may be defined as the locus of a point a satisfying $q(a,f) = q(a,D)$ where f is a fixed point called a **focus**, and D is a fixed line called a **directrix**, and where $q(a,D)$ is the quadrance from the point a to the base point b of the altitude to D through a. The following theorems summarize some basic facts about such a hyperbolic parabola, some similar to the Euclidean situation, others quite different. The situation is illustrated in Figure 52. Careful examination reveals many more interesting features of this situation, which will be discussed in a further paper in this series.

Theorem 50 (Parabola focus directrix pair) *If a (hyperbolic) parabola p has focus f_1 and directrix D_1, then it also has another focus $f_2 \equiv D_1^{\perp}$ and another directrix $D_2 \equiv f_1^{\perp}$.*

Theorem 51 (Parabola tangents) *Suppose that b_1 is a point on D_1 such that the two midlines of the side $\overline{b_1 f_1}$ exist. Then these midlines meet the altitude line to D_1 through b_1 at two points (both labelled a_1 in the Figure) lying on the parabola, and are the tangents to the parabola at those points.*

We note that in addition if the two midlines of the side $\overline{b_1 f_1}$ exist, then both midlines meet at the point $b_2 \equiv (b_1 f_1)^{\perp}$ lying on D_2 and the corresponding midlines of the side $\overline{b_2 f_2}$ meet the altitude line to D_2 through b_2 at two points (both labelled a_2 in the Figure) lying on the parabola, and themselves meet at b_1. This gives a pairing between some of the points b_1 lying on D_1 and some of the points b_2 lying on D_2. Of the four points labelled a_1 and a_2 lying on the parabola, one of the a_1 points and one of the a_2 points are (somewhat mysteriously) perpendicular. The entire situation is very rich, and emphasizes once again (see [20]) that the theory of conics is not a closed book, but rather a rich mine which has only been partly explored so far.

Recall that in Euclidean geometry the locus of a point a satisfying $q(a,f_1) + q(a,f_2) = k$ for two fixed points f_1 and f_2 and some fixed number k is a circle.

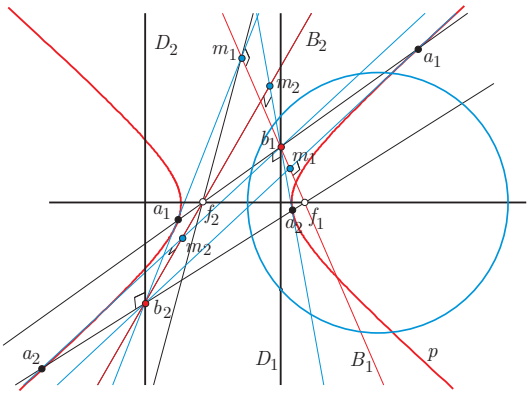

Figure 52: *Construction of a (hyperbolic) parabola*

Theorem 52 (Sum of two quadrances) *The (hyperbolic) parabola p described in the previous theorem may also be defined as the locus of those points a satisfying*

$$q(a, f_1) + q(a, f_2) = 1.$$

Many classical theorems for the Euclidean parabola hold also for the hyperbolic parabola p. Here are two, illustrated in Figure 53.

Theorem 53 (Parabola chord spread) *If a and b are two points on the hyperbolic parabola p with directrix D and focus f, and if c is the meet of D with the tangent of p at a, while d is the meet of D with the tangent to p at b, then $S(cf, fd) = S(af, fb)$.*

Theorem 54 (Parabola chord tangents perpendicular) *If a and b are two points on the hyperbolic parabola p with directrix D and focus f, and if e is the meet of D with ab, while g is the meet of the tangents to p at a and b, then ef is perpendicular to gf.*

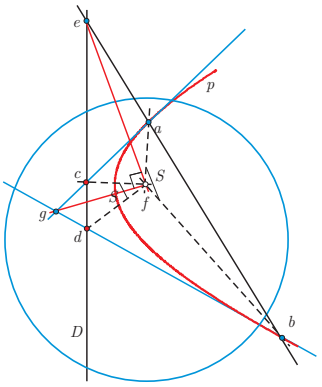

Figure 53: *Hyperbolic parabola with focus f and directrix D*

24 Bolyai's construction of limiting lines

Here is a universal version of a famous construction of J. Bolyai, to find the limiting lines U and V to an interior line L through a point a, where limiting means that U and V meet L on the null circle.

Start by constructing the altitude line K from a to L, meeting L at c, then the parallel line P through a to L, namely that line perpendicular to K. Now let m denote the midpoints of $\overline{ac}$, there are either two such points or none. If there are two, choose any point b on L, construct the altitude N to P through b, and reflect b in both midpoints m to get d and e on P. The side $\overline{ed}$ has a a midpoint, and the hyperbolic circle centered at a through d and e meets N at the points u and v. Then $U \equiv au$ and $V \equiv av$ are the required limiting lines as shown.

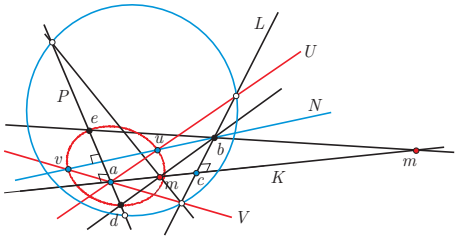

Figure 54: *A variant on J. Bolyai's construction of the limiting lines from a to L*

This construction seems to not be possible with only a straightedge, as we use a hyperbolic circle; this would correspond to the fact that there are two solutions. The question of what can and cannot be constructed with only a straightedge seems also an interesting one.

25 Canonical points

Both the Canonical points theorem in this section and the Jumping Jack theorem of the next section involve *cubic relations* between certain quadrances. I predict both will open up entirely new directions in hyperbolic geometry.

The Canonical points theorem has rather many aspects, one of which is a classical theorem of projective geometry.

Theorem 55 (Canonical points) *Suppose that α_1 and α_2 are distinct null points, and that x_3 and y_3 are points lying on $\alpha_1\alpha_2$. For any third null point α_3, and any point b_1 lying on $\alpha_2\alpha_3$, define $x_2 = (\alpha_1\alpha_3)(y_3b_1)$ and $y_2 = (\alpha_1\alpha_3)(x_3b_1)$. Similarly for any point b_2 lying on $\alpha_1\alpha_3$ define $x_1 = (\alpha_2\alpha_3)(y_3b_2)$ and $y_1 = (\alpha_2\alpha_3)(x_3b_2)$. Then $b_3 \equiv (x_1y_2)(x_2y_2)$ lies on $\alpha_1\alpha_2$. Now define points*

$$c_1 = (x_2x_3)(y_2y_3) \quad c_2 = (x_1x_3)(y_1y_3) \quad c_3 = (x_1x_2)(y_1y_2)$$

and corresponding points

$$\begin{aligned} z_3 &= (c_1b_1)(\alpha_1\alpha_2) & w_2 &= (c_1b_1)(\alpha_1\alpha_3) \\ z_1 &= (c_2b_2)(\alpha_2\alpha_3) & w_3 &= (c_2b_2)(\alpha_1\alpha_2) \\ z_2 &= (c_3b_3)(\alpha_1\alpha_3) & w_1 &= (c_3b_3)(\alpha_2\alpha_3). \end{aligned}$$

Then z_3 and w_3 depend only on x_3 and y_3, and not on α_3, b_1 and b_2. Furthermore b_1, z_2, w_3 are collinear, as are b_2, z_3, w_1, and b_3, z_1, w_2.

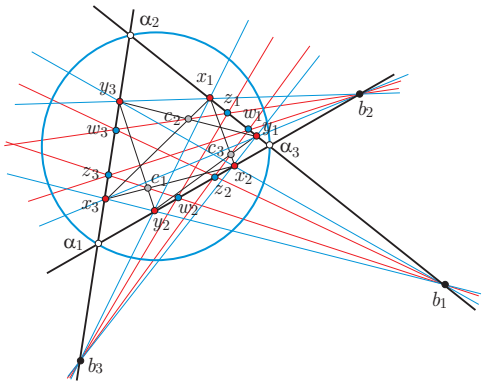

Figure 55: *Canonical points theorem:* $\overline{x_3y_3}$ *determines* $\overline{z_3w_3}$

In particular note that the theorem implies that any two points x and y whose join passes through two null points determine canonically two points z and w lying on xy in this fashion. We call z and w the **canonical points** of x and y. In Figure 55 z_3 and w_3 are the canonical points of x_3 and y_3, while z_1 and w_1 are the canonical points of x_1 and y_1, and z_2 and w_2 are the canonical points of x_2 and y_2.

Theorem 56 (Canonical points cubic) *With notation as above, the quadrances* $q \equiv q(x_3,y_3)$ *and* $r \equiv q(x_3,z_3)$ *satisfy the cubic relation*

$$(q-4r)^2 = 8qr(2r-q). \tag{4}$$

We call the algebraic curve

$$(x-4y)^2 = 8xy(2y-x)$$

the **Canonical points cubic**. The graph is shown in Figure 56. It is perhaps interesting that the point $[9/8,9/8]$ is the apex of one of the branches of this algebraic curve.

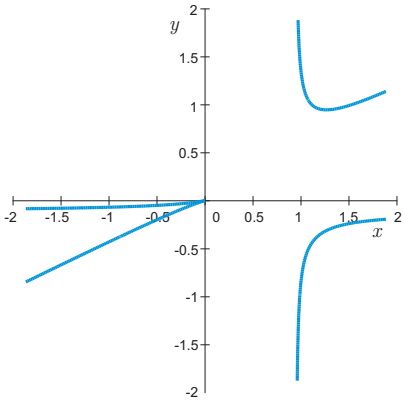

Figure 56: *The Canonical points cubic:* $(x-4y)^2 = 8xy(2y-x)$

26 The Jumping Jack theorem

Here is my personal favourite theorem. Although one can give a computational proof of it, the result begs for a conceptual framework that explains it, and points to other similar facts (if they exist!)

Theorem 57 (Jumping Jack) *Suppose that* $\overline{\alpha_1\alpha_2\alpha_3\alpha_4}$ *is a quadrangle of null points, with* $g \equiv (\alpha_1\alpha_3)(\alpha_2\alpha_4)$ *a diagonal point, and let* L *be any line through* g. *Then for an arbitrary null point* α_5, *define the meets* $x \equiv (\alpha_1\alpha_3)(\alpha_4\alpha_5)$, $y \equiv L(\alpha_4\alpha_5)$, $z \equiv (\alpha_2\alpha_4)(\alpha_3\alpha_5)$ *and* $w \equiv L(\alpha_3\alpha_5)$. *If* $r \equiv q(x,y)$ *and* $s \equiv q(z,w)$ *then*

$$16rs(3-4(s+r)) = 1.$$

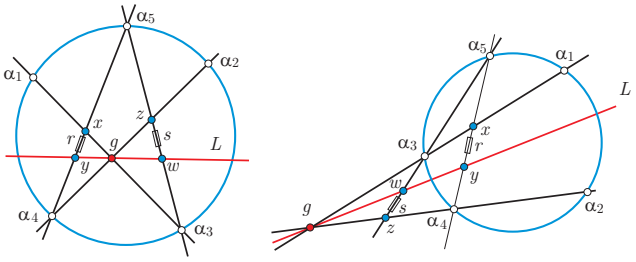

Figure 57: *Jumping Jack theorem:* $16rs(3-4(s+r)) = 1$

We call the algebraic curve

$$16xy(3-4(x+y)) = 1$$

the **Jumping Jack cubic**. The Jumping Jack theorem shows that it has an infinite number of rational solutions, which include a parametric description with 6 independent parameters.

The graph is shown in Figure 58. Note the isolated solution $[1/4,1/4]$, which is the centroid of the trilateral formed by the three asymptotes.

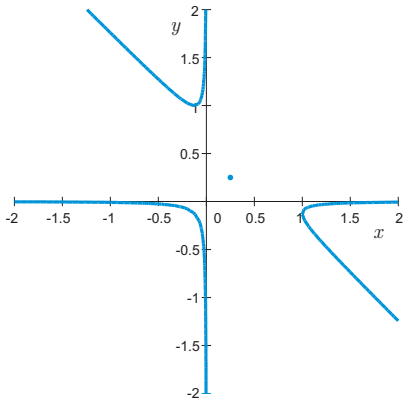

Figure 58: *Jumping Jack cubic:* $16xy(3-4(x+y)) = 1$

27 Conclusion

Universal hyperbolic geometry provides a new framework for a classical subject. It provides a more logical foundation for this geometry, as now analysis is not used, but only high school algebra with polynomials and rational functions. The main laws of trigonometry require only quadratic equations for their solutions. Theorems extend now beyond the familiar interior of the unit disk, and also to geometries over finite fields. Although we have not stressed this, it turns out that almost all the theorems we have described also hold in elliptic geometry! That is because the algebraic treatment turns out to be essentially independent of the projective quadratic form in the three dimensional space that is implicitly used to set up the theory in (1). We have shown how many classical results can be enlarged to fit into this new framework, and also described novel and interesting results.

So there are many opportunities for researchers to make essential discoveries at this early stage of the subject. When it comes to hyperbolic geometry, we are all beginners now.

References

[1] J. ANGEL, Finite upper half planes over finite fields, *Finite Fields and their Applications* **2** (1996), 62–86.

[2] W. BENZ, *Classical Geometries in Modern Contexts: Geometry of Real Inner Product Spaces*, Birkhäuser, Basel, 2007.

[3] H. BRAUNER, *Geometrie Projektiver Räume I, II*, Bibliographisches Institut, Mannheim, 1976.

[4] J. L. COOLIDGE, *The Elements of Non-Euclidean Geometry*, Merchant Books, 1909.

[5] H. S. M. COXETER, *Non-Euclidean Geometry*, 6th ed., Mathematical Association of America, Washington D. C., 1998.

[6] M. J. GREENBERG, *Euclidean and Non-Euclidean Geometries: Development and History*, 4th ed., W. H. Freeman and Co., San Francisco, 2007.

[7] R. HARTSHORNE, *Geometry: Euclid and Beyond*, Springer, New York, 2000.

[8] B. IVERSEN, *Hyperbolic Geometry*, London Mathematical Society Student Texts 25, Cambridge University Press, Cambridge, 1992.

[9] H. LENZ, *Nichteuklidische Geometrie*, Bibliographishes Institut, Mannheim, 1967.

[10] J. MCCLEARY, *Geometry from a Differentiable Viewpoint*, Cambridge University Press, New York, 1994.

[11] J. MILNOR, Hyperbolic Geometry—The First 150 Years, *Bulletin of the AMS* **6** (1982), 9-24.

[12] A. PRÉKOPA and E. MOLNAR, eds., *Non-Euclidean Geometries: János Bolyai Memorial Volume*, Springer, New York, 2005.

[13] A. SLIEPČEVIĆ and E. JURKIN, The Butterfly Theorems in the Hyperbolic Plane, *Annales Universitatis Scientiarum Budapestinensis* **48** (2005), 109–117.

[14] D. M. Y. SOMMERVILLE, *The Elements of Non-Euclidean Geometry*, G. Bell and Sons, Ltd., London, 1914, reprinted by Dover Publications, New York, 2005.

[15] J. STILLWELL, *Sources of Hyperbolic Geometry*, American Mathematical Society, Providence, R. I., 1996.

[16] A. TERRAS, *Fourier Analysis on Finite Groups and Applications*, Cambridge University Press, Cambridge,1999.

[17] A. UNGAR, *Hyperbolic Triangle Centers: The Special Relativistic Approach*, FTP, volume 166, Springer, 2010.

[18] N. J. WILDBERGER, *Divine Proportions: Rational Trigonometry to Universal Geometry*, Wild Egg Books, Sydney, 2005.

[19] N. J. WILDBERGER, One dimensional metrical geometry, *Geometriae Dedicata* **128** (1) (2007), 145–166.

[20] N. J. WILDBERGER, Chromogeometry and Relativistic Conics, *KoG* **13** (2009), 43–50.

[21] N. J. WILDBERGER, Affine and Projective Universal Geometry, to appear, *J. of Geometry*, `http://arxiv.org/abs/math/0612499v1`.

[22] N. J. WILDBERGER, Universal Hyperbolic Geometry I: Trigonometry, `http://arxiv.org/abs/0909.1377v1`.

[23] H. E. WOLFE, *Introduction to Non-Euclidean Geometry*, Holt, Rinehart and Winston, New York, 1945.

Norman John Wildberger
School of Mathematics and Statistics
UNSW Sydney 2052 Australia
e-mail: n.wildberger@unsw.edu.au

Original scientific paper
Accepted 1. 10. 2010.

ANA SLIEPČEVIĆ
EMA JURKIN

Snails in Hyperbolic Plane

Snails in Hyperbolic Plane

ABSTRACT

The properties of the limaçon of Pascal in the Euclidean plane are well known. The aim of this paper is to obtain the curves in the hyperbolic plane having the similar properties. That curves are named hyperbolic snails and defined as the circle pedal curves.
It is shown that all of them are circular quartics, while some of them are entirely circular.

Key words: limaçon of Pascal, hyperbolic plane, entirely circular 4-order curves

MSC 2010: 51M09, 51M10, 51M15

Puževi u hiperboličkoj ravnini

SAŽETAK

Dobro su poznata svojstva krivulje euklidske ravnine zvane Pascalov puž. U ovom se radu u hiperboličkoj ravnini konstruiraju krivulje sa sličnim svojstvima. Te su krivulje nazvane hiperboličkim puževima i definirane kao nožišne krivulje kružnica.
Pokazuje se da su svi hiperbolički puževi cirkularne kvartike, a neke od njih su čak potpuno cirkularne.

Ključne riječi: Pascalov puž, hiperbolička ravnina, potpuno cirkularne krivulje 4. reda

1 Introduction

The properties of the limaçon of Pascal in the Euclidean plane are well known. It is a bicircular curve of fourth order, that can be obtained as a circle pedal curve, ([5], pp. 133–134). The pedal point (pole) P is a node, cusp or isolated double point of this pedal curve depending on whether it is outside, on or inside the circle. The limaçon has cusps at the apsolute points and a singular focus that coincides with the midpoint of the segment OP, where O is the center of the circle. There are the limaçones of Pascal that have singular foci lying on them.
The limaçon of Pascal can also be obtained by the inversion of a conic if its focus coincides with the pole of the inversion, ([5], p. 122). The limaçon of Pascal possesses a node, cusp or isolated double point depending on whether the generating conic is a hyperbola, parabola or ellipse, respectively.
The limaçon of Pascal possesses an axis of symmetry.
One can ask himself if there is a curve in the hyperbolic plane having the similar properties.

Let a be the absolute conic for the Cayley-Klein model of the hyperbolic plane (H-plane) represented by a circle of classical Euclidean plane. The interior points of the absolute conic are called *real points*, exterior points are *ideal points* and points of the absolute conic are called *absolute points*, [4].

A perpendicularity in the H-plane is defined by the absolute polarity. This means that two lines are *perpendicular* iff one passes through the absolute pole of the other. The *pedal* of a given curve with respect to a point P is the locus of the foot of the perpendicular from the point P to the tangent line to the given curve, [4].
A curve in the H-plane is *circular* if it touches the absolute conic at least at one point. If a curve possesses a common tangent with the absolute conic (isotropic asymptote) at each intersection point, it is *entirely circular*, [6].
A curve having two touching points with the absolute conic, possess a singular focus defined as an intersection of isotropic tangent lines at the absolute points, [3].

2 Hyperbolic snail

Definition 1 *A hyperbolic snail (H-snail) is a circle pedal curve.*

There are three classes of circles in the H-plane. Therefore, different types of H-snail can be expected. The circles are classified into the hypercycles, cycles and horocycles depending on whether they touch the absolute conic at two different real points, at a pair of imaginary points, or whether their four absolute points coincide, respectively, [4].

Theorem 1 *H-snail is a fourth order curve touching the absolute conic at two points.*

Proof. Let us construct the pedal curve k^4 of a circle c_2. Let the given circle c_2 be e.g. a hypercycle with the center O and absolute touching points O_1 and O_2 and let P be the pole of the pedal transformation, Figure 1.
The construction should be made in the following way: The connecting line PT, where T is the absolute pole of the tangent line t of the circle c_2, intersects t in a point T_N lying on the required curve.
Absolute touching points O_1, O_2 obviously lie on the curve k^4 since they are the feet of the perpendiculars from the point P to the isotropic asymptotes OO_1 and OO_2.
Through each of the intersection points A_1, A_2 of the absolute conic a and the polar line p of the pole P with respect to a, pass two tangent lines to the hypercycle. Consequently, A_1, A_2 are double points of the required curve. According to Chasles correspondence principal, [9], k^4 is fourth order curve as it is the result of (1, 2)-correspondence between the first order pencil of lines (P) and the second order pencil (c_2) of the tangent lines of the conic c_2.
Two tangent lines to the hypercycle c_2 pass through the point P. Their poles are located on the polar line p. The connecting lines of those points with the point P are the tangent lines of k^4 at its double point P.
The constructed curve k^4 is the fouth order curve touching the absolute conic at O_1, O_2. It has three double points O, A_1, A_2, and a quadruple focus O.

If the given circle c_2 is cycle or horocycle, it is similar, Figure 2. The cycle touches the absolute conic at the pair of imaginary points, and the same holds for its pedal curve k^4. The horocycle pedal curve hyperosculates the absolute conic a at the touching point $O = O_1 = O_2$ with the intersection multiplicity 4. □

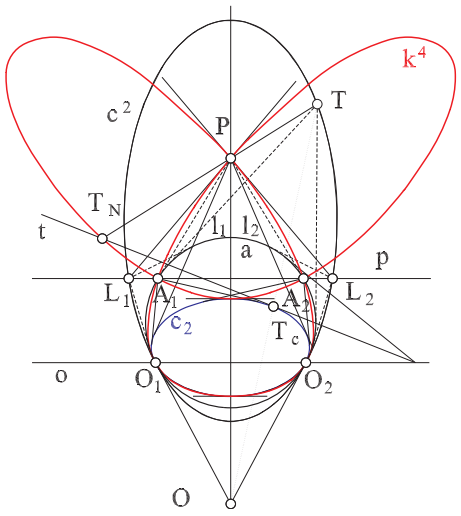

Figure 1

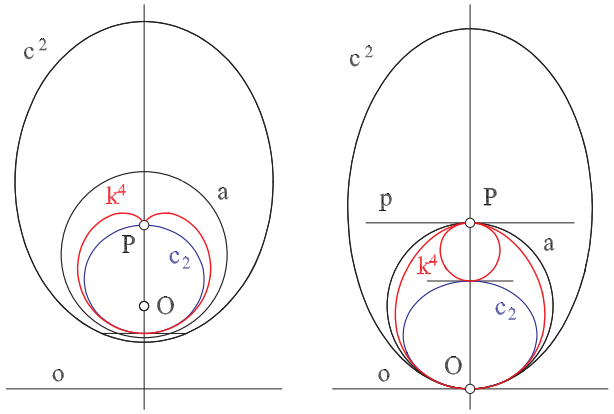

Figure 2

Corollary 1 *If the pole P of the pedal transformation is an absolute point, H-snail is an entirely circular fourth order curve.*

Proof. If the pole P lies on the absolute conic, three double points P, A_1, A_2 of H-snail coincide with the point P at which both tangents coincide with the line p, Figure 2.

Generally, an entirely circular quartic in the H-plane possesses six quadruple foci. The isotropic tangent lines OO_1, OO_2 of k^4 intersect the twice counted isotropic tangent line p at the points F_1, F_2, respectively. Therefore, entirely circular H-snail k^4 possesses two quadruple foci O, P, and two eightfold foci F_1, F_2. □

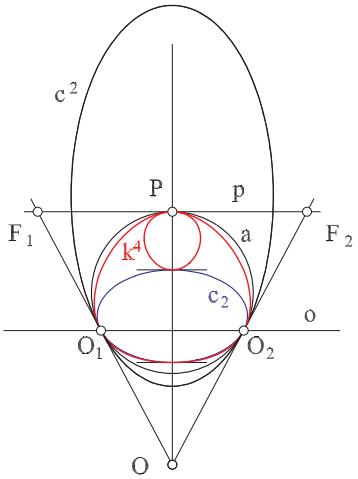

Figure 3

Remark 1 If the pedal point P is a real point, k^4 has two imaginary double points on the absolute conic. These are imaginary contact points of the absolute conic and tangents passing through the point P.
The pole P is a node, cusp or isolated double point depending on whether it is outside, on or inside the circle c_2, respectively.

Remark 2 Let us denote by c^2 the reciprocal curve of the circle c_2 in the absolute polarity, Figure 1. It's easy to see that the pedal curve k^4 of the circle c_2 is the inverse curve of the circle c^2 with respect to the same pole P, [8]. This fact simplifies derivation of some constructive and synthetic conclusions about H-snails.

The limaçon of Pascal possesses an axis of symmetry. The analogous statement holds in the hyperbolic plane.

Theorem 2 *Let the H-snail k^4 be the pedal curve of the circle c_2 with the center O with respect to the pedal point P. The line $s = OP$ is an axis of symmetry of the H-snail.*

Proof. The fact that every circle of the H-plane is a collinear image of the absolute conic a, [3], will be applied in the proof.
Let T_N be a point on k^4, obtained as the foot of the perpendicular from the pole P to the tangent line t, Figure 4. Let q be the line through T_N perpendicular to s. The connecting line $z = ST$ intersects the circle c^2 in the point T', being the pole of the tangent line t' and inverse of the point T_N'. By A and B the intersection points of line s with lines z and q are denoted.
A circle is a symmetric curve with respect to every diameter. In other words, the points T and T' are equally distanced from the line s and equality $(SA, TT') = -1$ holds. After connecting these four points with the pole P a harmonic quadruple of lines is obtained, [1]. Accordingly, $(SB, T_N T_N') = -1$. This finishes the proof. □

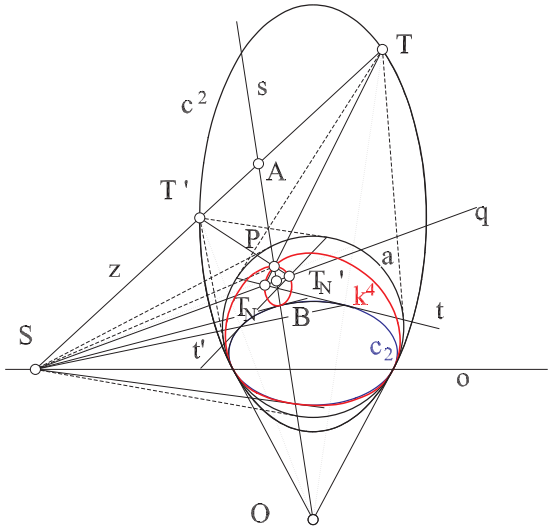

Figure 4

For further studies of the entirely circular quartics in the hyperbolic plane the papers [2], [7] and [8] can be consulted.

References

[1] H. S. M. COXETER, *Projektivna geometrija.* Školska knjiga, Zagreb, 1977.

[2] E. JURKIN, O. ROESCHEL, Envelopes of the Absolute Quadratic System of Conics of the Hyperbolic Plane I. *Mathematica Pannonica* **19** (2008), 1, 23–35

[3] D. PALMAN, Vollkommen zirkuläre Kurven 3. Ordnung in der hyperbolischen Ebene. *Glasnik MFA* **14** (1959), 19–74.

[4] L. RAJČIĆ, Obrada osnovnih planimetrijskih konstrukcija geometrije Lobačevskog sintetičkim sredstvima. *Glasnik MFA* **5** (1950), 57–120.

[5] A. A. SAVELOV, *Ravninske krivulje.* Školska knjiga, Zagreb, 1979.

[6] A. SLIEPČEVIĆ, V. SZIROVICZA, A Classification and Construction of Entirely Circular Cubics in the Hyperbolic Plane. *Acta Math. Hungar.* **104** (**3**) (2004), 185–201.

[7] V. SZIROVICZA, Entirely circular curves of 4th-order produced by quadratic inversion in the hyperbolic plane. *Rad HAZU.* **503** (2009), 1–6.

[8] V. SZIROVICZA, Vollkommen zirkuläre Fusspunktskurven der hyperbolischen Ebene. *Rad JAZU.* **408** (1984), 17–25.

[9] H. WIELEITNER, *Theorie der ebenen algebraischen Kurven höherer Ordnung.* G. J. Göschen'sche Verlagshandlung, Leipzig, 1905.

Ana Sliepčević
Faculty of Civil Engineering
Kačićeva 26, 10000 Zagreb, Croatia
e-mail: anas@grad.hr

Ema Jurkin
Faculty of Mining, Geology and Petroleum Engineering
Pierottijeva 6, 10000 Zagreb, Croatia
e-mail: ejurkin@rgn.hr

Original scientific paper
Accepted 30. 11. 2010.

MÁRTA SZILVÁSI-NAGY*

Surface Patches Constructed from Curvature Data

Surface Patches Constructed from Curvature Data

ABSTRACT

In this paper a technique for the construction of smooth surface patches fitted on triangle meshes is presented. Such a surface patch may replace a well defined region of the mesh, and can be used e.g. in re-triangulation, mesh-simplification and rendering.

The input data are estimated curvature values and principal directions computed from a circular neighborhood of a specified triangle face of the mesh.

Key words: triangle mesh, principal curvatures, local surface approximation

MSC 2010: 65D17, 68U07, 65D18, 68U05

Dijelovi plohe konstruirani iz podataka o zakrivljenosti

SAŽETAK

U ovom članku se prikazuje metoda za konstrukciju glatkih dijelova plohe koji odgovaraju mreži trokuta. Takav dio plohe može zamijeniti dobro definirano područje mreže, i može se upotrijebiti npr. u retriangulaciji, simplifikaciji mreže i renderiranju.

Ulazni podaci su procijenjene vrijednosti zakrivljenosti i glavni smjerovi izračunati iz kružne okoline određenog trokuta mreže.

Ključne riječi: mreža trokuta, glavne zakrivljenosti, lokalna aproksimacija plohe

1 Introduction

Triangle meshes are the most common surface representation in many computer graphics applications. In order to reduce a model's size, cut the storage space and decrease the time required to display the model, simplification algorithms are applied to the mesh. A simplification algorithm in [5] is based on iterative edge contraction analyzed on a tessellation of twice-differentiable surfaces. For local approximation ellipsoids at the mesh vertices are computed that characterize the local shape of the surface. These quadrics are elongated in directions of low curvature and thin in directions of higher curvature. Edge contractions are determined by minimizing the defined quadric metric which result in appropriately stretched triangles in the simplified mesh.

Also in point-based surface models some approximating geometric primitives are used for a compact representation. Piecewise constant surfaces in the form of circular discs, so-called splats have been proposed for rendering purposes in [8]. Splat radii depend on local curvature properties. From estimated normals at data points a smoothly varying normal field is generated for each patch, which is necessary for producing photo-realistic results in ray-tracing methods. For optimal local approximation to the underlying surface elliptical splats have been used in [7]. The two axes are aligned to the principal curvature directions and the radii are inversely proportional to the minimum and maximum curvatures. From sampled points of a surface analytic patches are constructed in a polynomial form in [6]. First, the principal curvatures and the Darboux frame are estimated using sampled points along three curves passing through the point of interest. The coefficients of the polynomial function describing the required patch are computed by a constrained surface fitting method using the total Gaussian curvature. A different type of surface elements, so-called surfel objects are used in [10]. Surfels are point primitives with attributes as surface normal, position, orientation and texture. They allow the creation of 3D graphic models with complex shapes.
Several methods have been developed for getting curvature information from discrete surface representations. A survey of results in discrete differential geometry and flexible tools to approximate important geometric attributes, including normal vectors and curvatures on arbitrary triangle meshes, also applications such as mesh smoothing

* Supported by a joint project between the TU Berlin and the BUTE.

are given in [9]. The quadratic paraboloid is the typical analytic regular surface used for local approximation of a mesh, which is usually computed by least squares method ([3]). The principal curvatures of the underlying surface are estimated by the principal curvatures of such a paraboloid. In [2] the quadric is extended by linear terms, and is fitted iteratively by correcting the surface normal, which leads to a new quadric in each step. The curvature estimation method in [11] uses biquadratic Bézier patches as a local fitting technique. One advantage in using parametric form of the locally approximating surface is the ability to add smoothing constraints when dealing with noisy data. A surface-based method is applied to point-based surfaces in [19]. The moving least-squares method is used to compute analytic surfaces locally fitting a point cloud, which provides direct curvature evaluation but also feature recognition and rendering applications.

Instead of fitting a smooth surface to a local set of points a different approach estimates the curvatures directly from the discrete data of the triangulation. A classical paper of Taubin ([17]) shows a normal-curvature based method. First, the normal curvatures are estimated in the direction of each edge leaving the mesh vertex of interest, then the second fundamental tensor is computed. The principal curvatures are determined as eigenvalues of this tensor defined at each vertex. The algorithm in [1] computes the normal curvatures by fitting circles at each vertex in three (or more) tangent directions using two neighboring points and applying the Meusnier theorem. Then the principal curvatures are computed on the base of Euler formula. A modification of this algorithm is shown in [4] which is adjusted to deal with real discrete noisy range data. A finite-differences approach for estimating curvatures on irregular triangle meshes is presented and used for computing derivatives of curvature and higher-order surface differentials in [12].

The objective of this work is to view a surface represented by a triangle mesh as a collection of local patches. In our algorithm a circular or elliptical surface patch is constructed around a specific triangle face of the mesh, and is represented by a trigonometric vector function. The input data are estimated curvature values and principal directions computed from a neighborhood of the given triangle in the following way ([14], [15]).

First a circular neighborhood is constructed around a specified triangle (Fig. 1). This bent disc laid onto the mesh is determined by a given arc length as "radius" r_g (see Fig. 2) which is measured in the normal sections of the mesh along the polygonal section lines. From the chord length of a "diameter", denoted by d, the radius r_n of the osculating circle in the actual normal plane is computed by a third order approximation method. By repeating this computation in sufficient many normal planes, curvature values can be ordered to the actual triangle face. The maximal and minimal diameters determine the principal directions T_1, T_2 and the curvature radii (Fig. 3) denoted by ρ_1 and ρ_2 in Fig. 4.

This construction and curvature estimation work also on triangle meshes, where the usual vertex-based methods cannot be applied. Such a mesh is shown in Fig. 7.

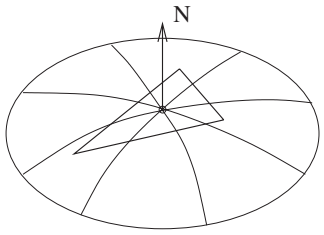

Figure 1: *Circular neighborhood of a face*

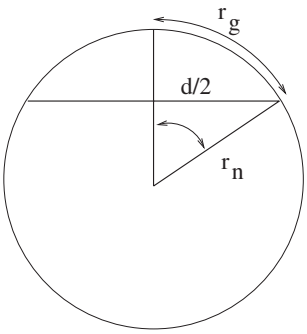

Figure 2: *The osculating circle in a normal plane*

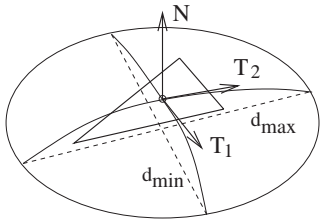

Figure 3: *Principal directions*

2 The approximating surface patch

Having the principal directions T_1 and T_2 at the barycenter P of the actual triangle face, a local basis is defined by $\{\mathbf{e}_1, \mathbf{e}_2, \mathbf{e}_3\} = \{T_1, T_2, N\}$ (Fig. 3). In the normal plane containing the first principal direction the osculating circle has the radius ρ_1, the central angle of the given arc length

is $\alpha = r_g/\rho_1$, $\rho_1 \neq 0$. In the second normal plane determined by the second principal direction, orthogonal to the first one, the curvature radius is ρ_2 and the central angle of the given arc length is $\beta = r_g/\rho_2$, $\rho_2 \neq 0$ (Fig. 4). An arbitrary point of the circles is Q_1 and Q_2, respectively. The position vector of these points, i.e. the vector equations of these circle arcs in the local coordinate systems are

$$\vec{PQ}_1 = \rho_1 \sin\vartheta \mathbf{e}_1 + (-\rho_1 + \rho_1 \cos\vartheta)\mathbf{e}_3,\ 0 \leq \vartheta \leq \alpha$$

for a negative principal curvature $\kappa_1 = -1/\rho_1$ and

$$\vec{PQ}_2 = \rho_2 \sin(\vartheta\frac{\beta}{\alpha})\mathbf{e}_2 + (\rho_2 - \rho_2 \cos(\vartheta\frac{\beta}{\alpha})\mathbf{e}_3,\ 0 \leq \vartheta \leq \alpha,$$

when the principal curvature $\kappa_2 = 1/\rho_2$ is positive. In Fig. 4 $\vartheta^* = \vartheta(\beta/\alpha)$.

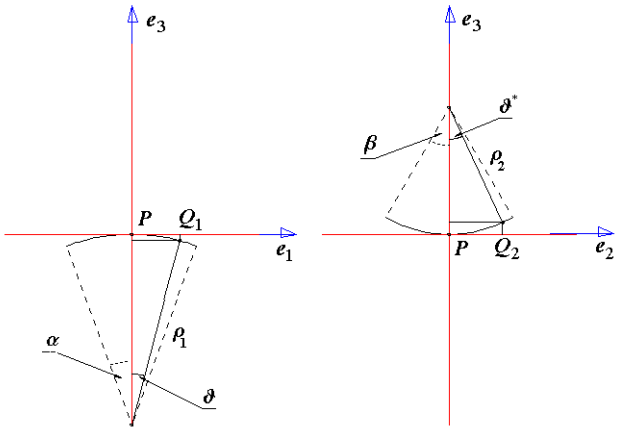

Figure 4: *Arcs of osculating circles in the principal normal sections of given length* $2r_g$

These circle arcs will determine the approximating surface patch around the point P. If they are of the same arc length, a circular patch will be generated.

In the construction of an elliptical patch we assume that $\rho_1 < \rho_2$, i.e. the neighborhood of the point P is more flat in the second principal direction. Then we enlarge the arc length of the osculating circle, in this way the patch to be generated will be stretched in this direction. If $\kappa_2 \to 0$, e.g. for a cylinder, then $\rho_2 \to \infty$ and $\beta \to \pi/2$. Consequently, the corresponding arc is a straight line segment of length $\to \infty$. This arc length should be limited in the construction. In our examples this limit has been set to $2.5 \cdot r_g$, and $\beta = min\{\alpha, 2.5 \cdot (r_g/\rho_2)\}$, $\rho_2 \neq 0$, while for circular patches $\beta = r_g/\rho_2$.

The vector equation of the surface patch is generated from the two circle arcs in the normal planes through the principal directions in such a way that the third coordinate of the arbitrary point of the patch is a convex combination of those of the points Q_1 and Q_2, while the normal plane is rotating around the normal vector with the angle φ.

$$\mathbf{q}(\vartheta,\varphi) = \mathbf{p} + \rho_1 \sin\vartheta\cos\varphi\mathbf{e}_1 + \rho_2 \sin(\vartheta\tfrac{\beta}{\alpha})\sin\varphi\mathbf{e}_2 + \left((-\rho_1 + \rho_1\cos\vartheta)\cos^2\varphi + (\rho_2 - \rho_2\cos(\vartheta\tfrac{\beta}{\alpha})\sin^2\varphi\right)\mathbf{e}_3,$$
$$0 \leq \vartheta \leq \alpha,\ 0 \leq \varphi \leq 2\pi.$$

In this equation the neighborhood of the point P is assumed to be of hyperbolic type. In the case of an elliptic neighborhood the third coordinates of the arc points Q_1 and Q_2 have to be computed by the same formula. In Fig. 5 the boundary curve of the generated surface patch is shown in a hyperbolic neighborhood of the point P.

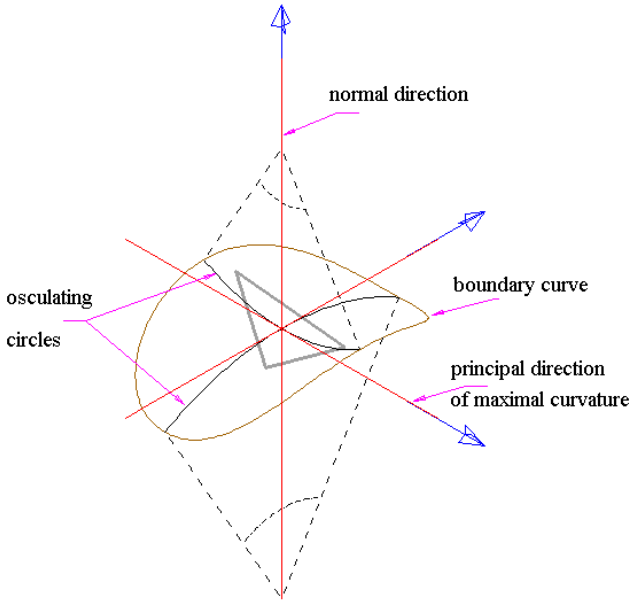

Figure 5: *The boundary curve of the surface patch*

If the neighborhood of the point P is of elliptic type, the constructed patch is situated tangential on the concave side of the mesh. Assuming that the mesh vertices are lying on the underlying surface approximated by the mesh, the position of this "inscribed" surface patch will be corrected by translating it in the normal direction. The measurement of this translation is computed as the mean value of the distances of the three vertex point of the base triangle to the generated patch.

3 Examples and analysis of the patch construction

In the examples circular and elliptical patches on "synthetic" and "real" meshed surfaces have been constructed. Synthetic meshes are generated by computing the mesh points from the vector equation of the surface on the corresponding triangulated parameter domain. Real meshes are chosen from an available collection offered for test purposes.

Computations in a normal plane require an appropriate polyhedral data structure adapted to the triangle mesh. Modeling systems usually store tesselated surfaces in STL format, which is a set of triangle faces, each described by three vertex points and a normal vector perpendicular to the face. In the implementation of our algorithms the STL data have been scanned for searching identical edges, hereby adjacent faces, and a polyhedral data structure based on a doubly linked edge system has been generated [13]. The polygonal line of intersections of the normal planes and the mesh, the estimation of normal curvatures and principal directions have been computed by the help of this data structure implemented in Java programming language. Then the mesh and the results of these computations have been transferred to the symbolical algebraic program package Mathematica [18]. The analytical description of the constructed patches, the error estimation and the figures have been made by Mathematica. The distance between a vertex point and the surface patch (Fig. 6) has been computed also by Mathematica.

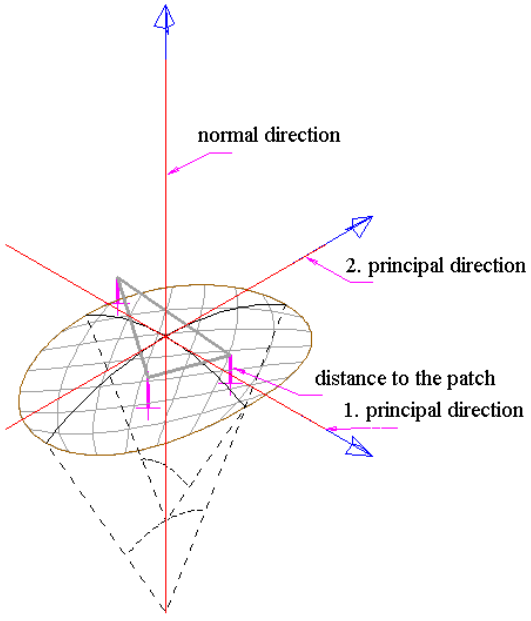

Figure 6: *Translation of the surface patch*

In Fig. 7 a synthetic mesh of a half cylinder is shown. In this triangulation all the mesh points are lying on the boundary circles, and no vertices are in the region of the construction. In such a case the vertex based algorithms do not work, but our face based curvature estimation resulted in accurate principal curvatures and principal directions ([14], [15]). The circular and elliptical patches are computed from these data. Series of the constructed patches may replace specified parts of the mesh (see Fig. 8).

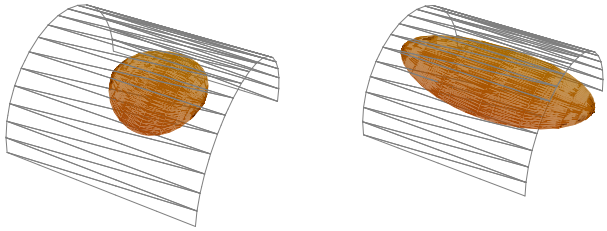

a b

Figure 7: *Circular and elliptical patch on a cylindrical meshed surface*

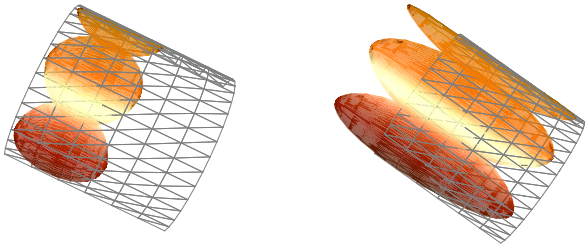

a b

Figure 8: *Series of patches on a dense mesh of the cylinder.*

The constructed patch approximates the mesh in a neighborhood of its center point. The approximation error is depending on the size of the constructed patch. Working on an analytic surface given by a vector equation, the input data of the patch construction, namely the principal directions and curvatures at the actual surface point are computed from the surface equation [16]. On triangle meshes these data are estimated values. In both cases the osculating circles in the principal directions approximate the corresponding normal sections of the meshed surface with an error. This error can be easily calculated at the end points of the circle arc. In this way the arc length r_g determining the size of the generated patch can be given using this error value as prescribed tolerance. The question is, how large is the difference between the patch boundary and the mesh in other normal sections. This difference has been computed by the distance of a testpoint on the boundary curve of the patch to the mesh. As the triangle faces lying in the actual

region of the construction are registered in the polyhedral data structure, the nearest face to the testpoint is selected for computing the error (Fig. 9).

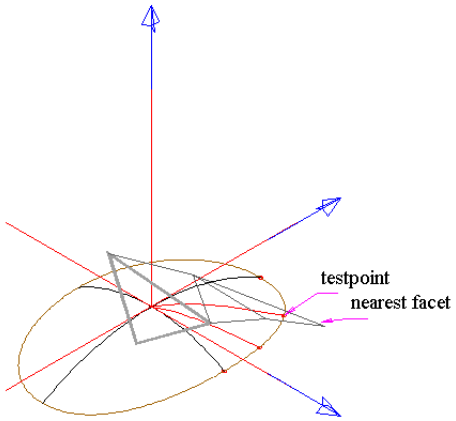

Figure 9: *Error estimation*

On a real mesh of the sphere (Fig. 10) four testpoints have been chosen on a quarter of the patch boundary, i.e. in the interval $\varphi \in [0, \pi/2]$. The relative errors to the given arc length of the osculating circle are for the smaller patch in turn 0.18%, 0.06%, 0.04%, 0.65% and for the larger patch accordingly 0.03%, 0.8%, 1.7%, 2.5%. For the smaller patch the order of these errors roughly equals to the approximation error of the input data. The error is growing fast by increasing the size of the patch. In our implementation an "optimal siz" of the patches has been chosen interactively.

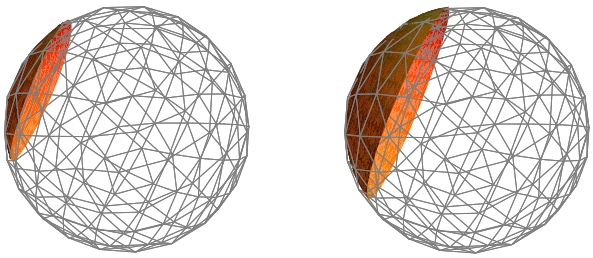

a b

Figure 10: *Circular patches on a "real" mesh of a sphere*

The measurements of the covered regions by circular and elliptical patches have been investigated on synthetic meshes of a saddle surface (Fig. 11) and a torus (Fig. 12).

In the case of "real objects" the size of approximating patches may vary strongly. A large elliptical patch is shown in Fig. 13.

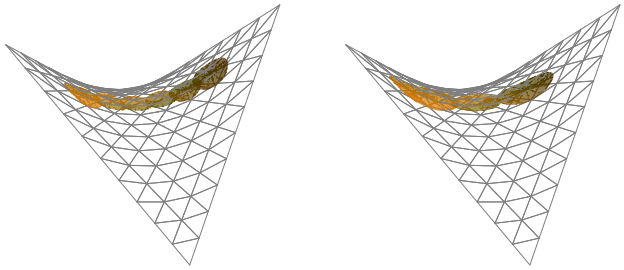

a b

Figure 11: *Circular and elliptical patches on a saddle surface*

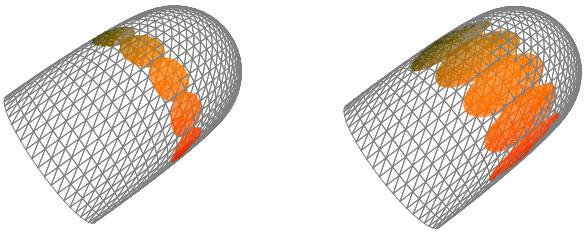

a b

Figure 12: *Circular and elliptical patches on a torus*

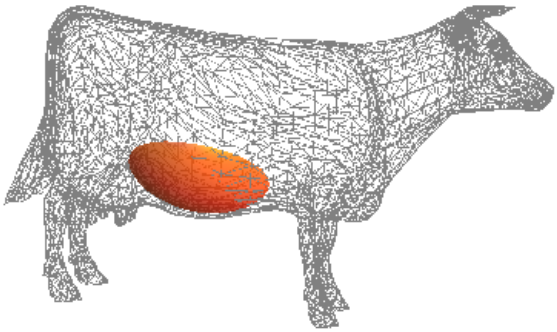

Figure 13: *Elliptical patch on the mesh of the cow*

4 Conclusions

A construction method for generating circular and elliptical surface patches has been presented for local approximation of triangle meshes. This is a novel, direct way for building a vector function of such analytical surfaces from estimated curvature data. The numerical analysis has been made on synthetic meshes of cylindrical and toroid surfaces. The implementation of the algorithm has been developed in Java programming language and by the help of the symbolical algebraic program package Mathematica.

References

[1] X. CHEN, F. SCHMITT, Intrinsic surface properties from surface triangulation. In *Proc. European Conf. Comp. Vision* 1992, 739–743.

[2] R.V. GARIMELLA, B.K. SWARTZ, Curvature estimation for unstructured triangulations of surfaces. *Technical Report, Los Alamos National Laboratory* 2003.

[3] B. HAMANN, Curvature approximation for triangulated surfaces. *In Geometric Modelling* (G. Farin at al., Eds.) Springer Verlag 1993, 139–153.

[4] E. HAMEIRI, I. SHIMSHONI, Estimating the principal curvature and the Darboux frame from real 3D range data. *IEEE Trans. Sys. Man. and Cyber.* **33** (2003), No.4, 626–637.

[5] P. S. HECKBERT, M. GARLAND, Optimal triangulation and quadric-based surface simplification. *Computational geometry* **14** (1999), No.1, 49-65.

[6] Y.-B. JIA, L. MI, J. TIAN, Surface patch reconstruction via curve sampling. *Proceedings 2006 IEEE International Conference on Robotics and Automation*, ICRA 2006.

[7] L. KOBBELT, M. BOTSCH, A survey of point-based techniques in computer graphics. *Computers & Graphics* **28** (2004), 801–814.

[8] L. LINSEN, K. MÜLLER, P. ROSENTHAL, Splat-based ray tracing of point clouds. *Journal of WSCG* **15** (2007), 1–3.

[9] M.MEYER, M. DESBRUN, P. SCHRÖDER, A.H. BARR, Discrete differential-geometry operators for triangulated 2-manifolds. In *Visualization and Mathematics III*, (H.-C. Hedge, K. Polthier Eds.) Springer-Verlag 2002, 35–57.

[10] H. PFISTER, M. ZWICKER, J. VAN BAAR, M. GROSS, Surfels: surface elements as rendering primitives. In *SIGGRAPH'00*, ACM Press/Addison-Wesley Publishing Co., NewYork 2000, 335–342.

[11] A. RAZDAN, M. BAE, Curvature estimation scheme for triangle meshes using biquadratic Bézier patches. *Computer-Aided Design* **37** (2005), 1481–1491.

[12] S. RUSINKIEWICZ, Estimating curvatures and their derivatives on triangle meshes. In *2nd International Symposium on 3D Data Processing*, September 2004, 486–493.

[13] M. SZILVÁSI-NAGY, GY. MÁTYÁSI, Analysis of STL Files. *Mathematical and Computer Modelling* **38** (2003), 945–960.

[14] M. SZILVÁSI-NAGY, About curvatures on triangle meshes. *KoG* **10** (2006), 13–18.

[15] M. SZILVÁSI-NAGY, Face-based estimations of curvatures on triangle meshes. *Journal for Geometry and Graphics* **12** (2008), No. 1, 63–73.

[16] M. SZILVÁSI-NAGY, Construction of circular splats on analytic surfaces. in *Fifth Hungarian Conference on Computer Graphics and Geometry*, Budapest 2010, 55–57.

[17] G. TAUBIN, Estimating the tensor of curvature of a surface from a polyhedral approximation. In *Proceedings of the Fifth International Conference on Computer Vision (ICCV 95)*, 1995, 852–857.

[18] S. WOLFRAM, *Mathematica. A System for Doing Mathematics by Computer. Second Edition*. Addison-Wesley, 1991.

[19] P. YANG, X. QIAN, Direct computing of surface curvatures for point-set surfaces. In *Eurographics Symposium on Point-Based Graphics (2007)*, (M. Botsch, R. Pajarola Eds.), 2007.

Márta Szilvási-Nagy

Dept. of Geometry, Budapest University of Technology and Economics

H-1521 Budapest, Hungary

e-mail: szilvasi@math.bme.hu

Original scientific paper
Accepted 20. 12. 2010.

JÁNOS PALLAGI
BENEDEK SCHULTZ
JENÖ SZIRMAI

Visualization of Geodesic Curves, Spheres and Equidistant Surfaces in $\mathbf{S}^2\times\mathbf{R}$ Space

Visualization of Geodesic Curves, Spheres and Equidistant Surfaces in $\mathbf{S}^2\times\mathbf{R}$ Space

ABSTRACT

The $\mathbf{S}^2\times\mathbf{R}$ geometry is derived by direct product of the spherical plane $\mathbf{S}^2$ and the real line $\mathbf{R}$. In [9] the third author has determined the geodesic curves, geodesic balls of $\mathbf{S}^2\times\mathbf{R}$ space, computed their volume and defined the notion of the geodesic ball packing and its density. Moreover, he has developed a procedure to determine the density of the geodesic ball packing for generalized Coxeter space groups of $\mathbf{S}^2\times\mathbf{R}$ and applied this algorithm to them.

E. MOLNÁR showed in [3], that the homogeneous 3-spaces have a unified interpretation in the projective 3-sphere $\mathcal{PS}^3(\mathbf{V}^4,V_4,\mathbf{R})$. In our work we shall use this projective model of $\mathbf{S}^2\times\mathbf{R}$ geometry and in this manner the geodesic lines, geodesic spheres can be visualized on the Euclidean screen of computer.

Furthermore, we shall define the notion of the equidistant surface to two points, determine its equation and visualize it in some cases. We shall also show a possible way of making the computation simpler and obtain the equation of an equidistant surface with more possible geometric meaning. The pictures were made by the Wolfram Mathematica software.

Key words: non-Euclidean geometries, projective geometry, geodesic sphere, equidistant surface

MSC 2010: 53A35, 51M10, 51M20, 52C17, 52C22

Vizualizacija geodetskih krivulja, sfera i ekvidistantnih ploha u prostoru $\mathbf{S}^2\times\mathbf{R}$

SAŽETAK

$\mathbf{S}^2\times\mathbf{R}$ geometrija izvodi se kao direktni produkt sferne ravnine $\mathbf{S}^2$ i realnog pravca $\mathbf{R}$. U članku [9], treći je autor odredio geodetske krivulje i geodetske kugle prostora $\mathbf{S}^2\times\mathbf{R}$, izračunao njihov volumen i definirao pojam popunjavanja geodetskim kuglama i njegovu gustoću. Pored toga, razvio je metodu određivanja gustoće popunjavanja geodetskim kuglama za generalizirane Coxeterove grupe prostora $\mathbf{S}^2\times\mathbf{R}$ i primijenio taj algoritam na njih.

U [3] je E. MOLNAR pokazao da homogeni 3-prostori imaju jedinstvenu interpretaciju u projektivnim 3-sferama $\mathcal{PS}^3(\mathbf{V}^4,V_3,\mathbf{R})$. U našem članku koristit ćemo projektivni model $\mathbf{S}^2\times\mathbf{R}$ geometrije te se na taj način geodetske linije i kugle mogu vizualizirati na euklidskom ekranu računala.

Nadalje, definirat ćemo pojam plohe jednako udaljene od dviju točaka, odrediti njezinu jednadžbu te je vizualizirati u pojedinim slučajevima. Također ćemo pokazati mogući način pojednostavljena računa i dobiti jednadžbe plohe s točnijim geometrijskim značenjem. Slike su napravljene u Wolframovom programu Mathematica.

Ključne riječi: neeuklidske geometrije, projektivna geometrija, geodetske sfere, ekvidistantne plohe

1 On $\mathbf{S}^2\times\mathbf{R}$ geometry

$\mathbf{S}^2\times\mathbf{R}$ is derived as the direct product of the spherical plane $\mathbf{S}^2$ and the real line $\mathbf{R}$. The points are described by (P,p) where $P\in\mathbf{S}^2$ and $p\in\mathbf{R}$. The isometry group $Isom(\mathbf{S}^2\times\mathbf{R})$ of $\mathbf{S}^2\times\mathbf{R}$ can be derived by the direct product of the isometry group of the spherical plane $Isom(\mathbf{S}^2)$ and the isometry group of the real line $Isom(\mathbf{R})$.

$$Isom(\mathbf{S}^2\times\mathbf{R}) := Isom(\mathbf{S}^2)\times Isom(\mathbf{R}); \tag{1.1}$$

The structure of an isometry group $\Gamma\subset Isom(\mathbf{S}^2\times\mathbf{R})$ is the following: $\Gamma := \{A_i\times\rho_i\}$, where $A_i\times\rho_i := A_i\times(R_i,r_i) := (g_i,r_i)$, $A_i\in Isom(\mathbf{S}^2)$, R_i is either the identity map $\mathbf{1}_\mathbf{R}$ of $\mathbf{R}$ or the point reflection $\overline{\mathbf{1}}_\mathbf{R}$. $g_i := A_i\times R_i$ is called the linear part of the transformation $(A_i\times\rho_i)$ and r_i is its translation part. The multiplication formula is the following:

$$(A_1\times R_1,r_1)\circ(A_2\times R_2,r_2) = ((A_1A_2\times R_1R_2, r_1R_2+r_2). \tag{1.2}$$

E. MOLNÁR has shown in [3], that the homogeneous 3-spaces have a unified interpretation in the projective 3-sphere $\mathcal{PS}^3(\mathbf{V}^4,V_4,\mathbb{R})$. In our work we shall use this projective model of $\mathbf{S}^2\times\mathbf{R}$ and the Cartesian homogeneous coordinate simplex $E_0(\mathbf{e}_0)$, $E_1^\infty(\mathbf{e}_1)$, $E_2^\infty(\mathbf{e}_2)$, $E_3^\infty(\mathbf{e}_3)$, $(\{\mathbf{e}_i\}\subset\mathbf{V}^4$ with the unit point $E(\mathbf{e}=\mathbf{e}_0+\mathbf{e}_1+\mathbf{e}_2+\mathbf{e}_3))$ which is distinguished by an origin E_0 and by the ideal points of coordinate axes, respectively. Moreover, $\mathbf{y}=c\mathbf{x}$ with $0<c\in\mathbb{R}$ (or $c\in\mathbb{R}\setminus\{0\}$) defines a point $(\mathbf{x})=(\mathbf{y})$ of the projective 3-sphere $\mathcal{PS}^3$ (or that of the projective space $\mathcal{P}^3$ where opposite rays $(\mathbf{x})$ and $(-\mathbf{x})$ are identified). The dual system $\{(e^i)\}\subset V_4$ describes the simplex planes, especially the plane at infinity $(e^0)=E_1^\infty E_2^\infty E_3^\infty$, and generally, $v=u\frac{1}{c}$ defines a plane $(u)=(v)$ of $\mathcal{PS}^3$ (or that of $\mathcal{P}^3$). Thus $0=\mathbf{x}u=\mathbf{y}v$ defines the incidence of point $(\mathbf{x})=(\mathbf{y})$ and plane $(u)=(v)$, as $(\mathbf{x})\mathrm{I}(u)$ also denotes it. Thus $\mathbf{S}^2\times\mathbf{R}$ can be visualized in the affine 3-space $\mathbf{A}^3$ (so in $\mathbf{E}^3$) as well.

In the later sections we will use some special types of $\mathbf{S}^2\times\mathbf{R}$ isometries, which transforms a fixed $P(1,\alpha,\beta,\gamma)$ point of $\mathbf{S}^2\times\mathbf{R}$ into $(1,1,0,0)$. This will be useful for determining the equidistant surfaces, so now we will compute this transformation.

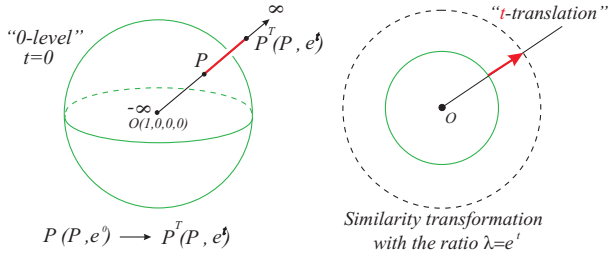

Figure 1: *Translation in* $\mathbf{S}^2\times\mathbf{R}$ *geometry*

$\mathcal{T}=(\mathbf{Id}.,T)$ is a fibre translation,

$$P(1,\alpha,\beta,\gamma)\to P^{\mathcal{T}}(1,\alpha',\beta',\gamma')=$$
$$=P^{\mathcal{T}}(1,\frac{\alpha}{\sqrt{\alpha^2+\beta^2+\gamma^2}},\frac{\beta}{\sqrt{\alpha^2+\beta^2+\gamma^2}},\frac{\gamma}{\sqrt{\alpha^2+\beta^2+\gamma^2}}). \tag{1.3}$$

($P^{\mathcal{T}}$ has 0 fibre coordinate), (see Fig. 1).

Similarly $\mathcal{R}_z=(\mathbf{R_z},0)$ is a special rotation about z axis with 0 fibre translation, which moves the point $(1,\alpha',\beta',\gamma')$ into the $[x,z]$ plane.

$$P^{\mathcal{T}}(1,\alpha',\beta',\gamma')\to P^{\mathcal{T}\mathcal{R}_z}(1,\alpha'',0,\gamma'')=$$
$$=P^{\mathcal{T}\mathcal{R}_z}(1,\sqrt{\alpha'^2+\beta'^2},0,\gamma'). \tag{1.4}$$

Finally $\mathcal{R}_y=(\mathbf{R_y},0)$ is a special rotation about y axis with 0 fibre translation, which moves the point $(1,\alpha'',0,\gamma'')$ into the $[x,y]$ plane.

$$P^{\mathcal{T}\mathcal{R}_z}(1,\alpha'',0,\gamma'')\to P^{\mathcal{T}\mathcal{R}_z\mathcal{R}_y}(1,1,0,0)=$$
$$=P^{\mathcal{T}\mathcal{R}_z\mathcal{R}_y}(1,\sqrt{\alpha''^2+\gamma''^2},0,0). \tag{1.5}$$

Remark 1.1 *More informations about the isometry group of* $\mathbf{S}^2\times\mathbf{R}$ *and about its discrete subgroups can be found in [1], [2] and [9].*

2 Geodesic curves and spheres of $\mathbf{S}^2\times\mathbf{R}$

E. Molnár [3] has introduced the natural the well-known infinitezimal arc-length square at any point of $\mathbf{S}^2\times\mathbf{R}$ as follows

$$(ds)^2=\frac{(dx)^2+(dy)^2+(dz)^2}{x^2+y^2+z^2}. \tag{2.1}$$

We shall apply the usual geographical coordiantes (ϕ,θ), $(-\pi<\phi\le\pi,\ -\frac{\pi}{2}\le\theta\le\frac{\pi}{2})$ of the sphere with the fibre coordinate $t\in\mathbf{R}$. We describe points in the above coordinate system in our model by the following equations:

$$x^0=1,\ x^1=e^t\cos\phi\cos\theta,\ x^2=e^t\sin\phi\cos\theta,\ x^3=e^t\sin\theta. \tag{2.2}$$

Then we have $x=\frac{x^1}{x^0}=x^1$, $y=\frac{x^2}{x^0}=x^2$, $z=\frac{x^3}{x^0}=x^3$, i.e. the usual Cartesian coordinates. We obtain by (2.1) and (2.2) that in this parametrization the infinitezimal arc-length square at any point of $\mathbf{S}^2\times\mathbf{R}$ is the following

$$(ds)^2=(dt)^2+(d\phi)^2\cos^2\theta+(d\theta)^2. \tag{2.3}$$

Hence we get the symmetric metric tensor field g_{ij} on $\mathbf{S}^2\times\mathbf{R}$ by components:

$$g_{ij}:=\begin{pmatrix}1&0&0\\0&\cos^2\theta&0\\0&0&1\end{pmatrix}, \tag{2.4}$$

The geodesic curves of $\mathbf{S}^2\times\mathbf{R}$ are generally defined as having locally minimal arc length between their any two (near enough) points. The equation systems of the parametrized geodesic curves $\gamma(t(\tau),\phi(\tau),\theta(\tau))$ in our model can be determined by the general theory of Riemann geometry:

By (2.4) the second order differential equation system of the $\mathbf{S}^2\times\mathbf{R}$ geodesic curve is the following [9]:

$$\ddot\phi-2\tan\theta\dot\phi\dot\theta=0,\ \ddot\theta+\sin\theta\cos\theta\dot\phi^2=0,\ \ddot t=0, \tag{2.5}$$

from which we get first an equator circle on $\mathbf{S}^2$ times a line on $\mathbf{R}$ each running with constant velocity c and ω, respectively:

$$t=c\cdot\tau,\ \theta=0,\ \phi=\omega\cdot\tau,\ c^2+\omega^2=1. \tag{2.6}$$

We can assume, that the starting point of a geodesic curve is $(1,1,0,0)$, because we can transform a curve into an arbitrary starting point, moreover, unit velocity can be assumed. Then we get the equation systems of a geodesic curve, visualized in Fig. 2 in our Euclidean model:

$$\begin{aligned} \tau &\to (x(\tau),y(\tau),z(\tau)),\\ x(\tau) &= e^{\tau\sin v}\cos(\tau\cos v),\\ y(\tau) &= e^{\tau\sin v}\sin(\tau\cos v)\cos u,\\ z(\tau) &= e^{\tau\sin v}\sin(\tau\cos v)\sin u,\\ \text{with fixed}\quad & -\pi<u\le\pi,\quad -\frac{\pi}{2}\le v\le\frac{\pi}{2}. \end{aligned} \tag{2.7}$$

Remark 2.1 *Thus we have also harmonized the scales along the base sphere and the fibre lines.*

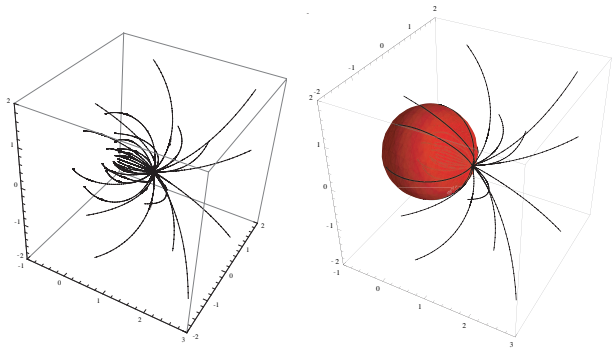

Figure 2: *Geodesic curves with the base sphere, ("the spider")*

Definition 2.2 *The distance $d(P_1,P_2)$ between the points P_1 and P_2 is defined by the arc length of the geodesic curve from P_1 to P_2.*

Definition 2.3 *The geodesic sphere of radius ρ (denoted by $S_{P_1}(\rho)$) with centre at the point P_1 is defined as the set of all points P_2 in the space with the condition $d(P_1,P_2)=\rho$. Moreover, we require that the geodesic sphere is a simply connected surface without selfintersection in $\mathbf{S}^2\times\mathbf{R}$ space.*

Remark 2.4 *We shall see that this last condition depends on radius ρ.*

Definition 2.5 *The body of the geodesic sphere of centre P_1 and of radius ρ in the $\mathbf{S}^2\times\mathbf{R}$ space is called geodesic ball, denoted by $B_{P_1}(\rho)$, i.e. $Q\in B_{P_1}(\rho)$ iff $0\le d(P_1,Q)\le\rho$.*

Remark 2.6 *Henceforth, typically we choose $(1,1,0,0)$ as centre of the sphere and its ball, by the homogeneity of $\mathbf{S}^2\times\mathbf{R}$.*

From (2.7) follows that $S(\rho)$ is a simply connected surface in $\mathbf{E}^3$ if and only if $\rho\in[0,\pi)$, because if $\rho\ge\pi$ then there is at least one $v\in[-\frac{\pi}{2},\frac{\pi}{2}]$ so that $y(\tau,v)=z(\tau,v)=0$, i.e. selfintersection would occur.

Thus we obtain the following

Proposition 2.7 *The geodesic sphere and ball of radius ρ (with the above requirements) exists in the $\mathbf{S}^2\times\mathbf{R}$ space if and only if $\rho\in[0,\pi]$.*

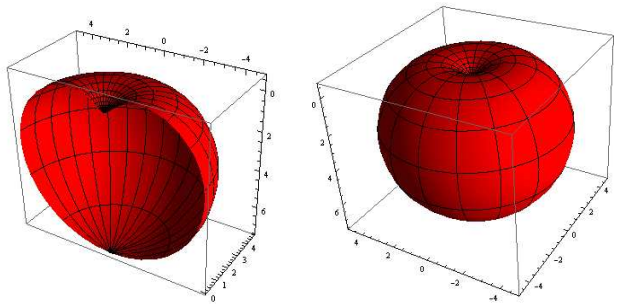

Figure 3: *Geodesic half sphere and sphere of radius $\rho=2$*

3 Equidistant surfaces in $\mathbf{S}^2\times\mathbf{R}$ geometry

3.1 What about parameters of a given geodesic curve?

It can be assumed by the homogeneity of $\mathbf{S}^2\times\mathbf{R}$ that one of endpoints of a given geodesic curve segment is $P_1(1,1,0,0)$ to simplify our calculations. The other endpoint is given by its homogeneous coordinates $P_2(1,a,b,c)$. We consider the geodesic curve segment $\mathcal{G}_{P_1P_2}$. Our first goal is to calculate parameters τ,u,v belonging to $\mathcal{G}_{P_1P_2}$. We get by (2.7) the following important observation:

$$\sqrt{a^2+b^2+c^2}=e^{\tau\sin v}. \tag{3.1}$$

We obtain from (2.7) and (3.1) the following equations and the parameter v :

$$\begin{aligned} &\sqrt{a^2+b^2+c^2}\cos(\tau\cos v)=a\ \Rightarrow\\ &\Rightarrow\tau\cos v=\arccos\left(\frac{a}{\sqrt{a^2+b^2+c^2}}\right), \end{aligned} \tag{3.2}$$

$$\log\sqrt{a^2+b^2+c^2}=\tau\sin v, \tag{3.3}$$

$$\tan v = \frac{\log\sqrt{a^2+b^2+c^2}}{\arccos\left(\frac{a}{\sqrt{a^2+b^2+c^2}}\right)} \Rightarrow$$
$$\Rightarrow v = \arctan\left(\frac{\log\sqrt{a^2+b^2+c^2}}{\arccos\left(\frac{a}{\sqrt{a^2+b^2+c^2}}\right)}\right), \tag{3.4}$$

if $P_2 \notin x \Leftrightarrow a \neq 0,\ b = c = 0$.

Remark 3.1 *If $P_2 \in x$, then $v = \frac{\pi}{2}$, $u = 0$ moreover the geodesic curve is the Euclidean segment P_1P_2, and its equidistant surface is a Euclidean sphere in our model.*

Thus we get the parameter τ from (3.1) and (3.3):

$$\tau = \frac{\log\sqrt{a^2+b^2+c^2}}{\sin v} \quad \text{if } v \neq 0. \tag{3.5}$$

The parameter u of the given geodesic curve $\mathcal{G}_{P_1P_2}$ can be expressed by (2.7):

$$\frac{z(\tau)}{y(\tau)} = \frac{c}{b} = \tan u \to u = \arctan\left(\frac{c}{b}\right). \tag{3.6}$$

Remark 3.2 *If $v = 0$ then*
$\tau = \arccos\left(\frac{a}{\sqrt{a^2+b^2+c^2}}\right) = \arccos(a)$ *and* $u = \arctan\left(\frac{c}{b}\right)$.

3.2 The equation of the equidistant surface

We want to find an equation for the surface $\mathcal{S}_{P_1P_2}$ consisting of all points that are equidistant from the point P_1 and P_2.

Definition 3.3 *An equidistant surface $\mathcal{S}_{P_1P_2}$ of two arbitrary given points $P_1, P_2 \in \mathbf{S}^2\times\mathbf{R}$ consists of all $X \in \mathbf{S}^2\times\mathbf{R}$ points, for which $d(P_1,X) = d(X,P_2)$ holds. Moreover, we require that this surface is a simply connected surface without selfintersection in $\mathbf{S}^2\times\mathbf{R}$ space.*

The varying point $X(1,x,y,z) \in \mathcal{S}_{P_1P_2}$ satisfies the following equation (see formulas (1.1), (1.2), (1.3), Fig. 4):

$$d(P_1,X) = d(X,P_2) = d(X^{\mathcal{T}\mathcal{R}_z\mathcal{R}_y}, P_2^{\mathcal{T}\mathcal{R}_z\mathcal{R}_y}) = \\ = d(X^{\mathcal{T}\mathcal{R}_z\mathcal{R}_y}, P_1),\ \ \forall X \in \mathcal{S}_{P_1P_2} \tag{3.7}$$

It is clear by the above equation (3.7), that the length of the geodesic curve $\mathcal{G}_{P_1,X}$ is equal to the length of the geodesic line $\mathcal{G}_{X_{\mathcal{S}_{P_1P_2}}^{\mathcal{T}\mathcal{R}_z\mathcal{R}_y},P_1}$, thus the τ parameters (can be determined by (3.5) and Remark 3.1) of the above geodesic curves are equal. Finally we have got the equation of the equaidistant surface $\mathcal{S}_{P_1P_2}$ after major simplification in model of $\mathbf{S}^2\times\mathbf{R}$ geometry:

$$4\arccos^2\left(\frac{ax+by+cz}{\sqrt{a^2+b^2+c^2}\sqrt{x^2+y^2+z^2}}\right) + \\ +\log^2\left(\frac{a^2+b^2+c^2}{x^2+y^2+z^2}\right) = \tag{3.8}$$
$$= 4\arccos^2\left(\frac{x}{\sqrt{x^2+y^2+z^2}}\right) + \log^2(x^2+y^2+z^2).$$

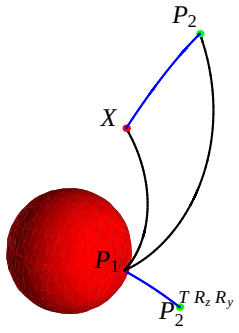

Figure 4: *It is clear, that $X \in \mathcal{S}_{P_1P_2}$ if and only if $d(P_1,X) = d(P_1,P_2^{\mathcal{T}\mathcal{R}_z\mathcal{R}_y})$ holds.*

Using formula (3.8) we can visualize the equidistant surface by computer (Fig. 5).

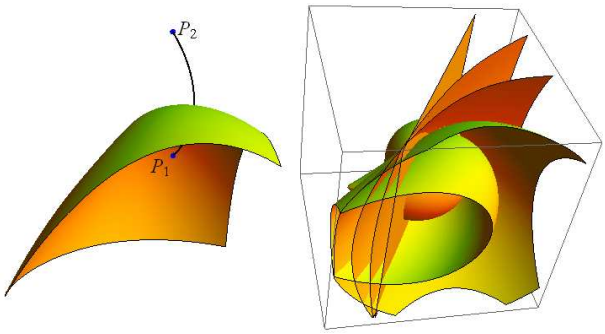

Figure 5: *An equidistant surface, and how to change the equidistant surfaces $\mathcal{G}_{P_1,P_2}$ with fixed $P_1(1,1,0,0)$ and varying $P_2 : (1,4,0,0) \to (1,-\frac{1}{2},\frac{\sqrt{3}}{2},0)$ along their geodesic curve.*

Remark 3.4 *The behavior of the equidistant surfaces at (and near) the origin requires more discussion.*

3.3 Further examination in Euclidean sense

Equation (3.8) can be simplified by using some Euclidean concepts and notations. In this subsection we will use these simplifications to find some Euclidean geometric meaning behind the equation.

Let us note the Euclidean location vectors of the points $P_1(1,1,0,0)$, $P_2(1,a,\ b,\ c)$ and $X(1,x,y,z)$ by $\mathbf{e}(1,0,0)$, $\mathbf{a}(a,b,c)$ and $\mathbf{x}(x,y,z)$ respectively. Substituting the usual denotation of Euclidean scalar product $\langle\ ,\ \rangle$ into equation (3.8) we obtain its following form:

$$4\arccos^2\left(\frac{\langle\mathbf{a},\mathbf{x}\rangle}{\sqrt{\langle\mathbf{a},\mathbf{a}\rangle}\sqrt{\langle\mathbf{x},\mathbf{x}\rangle}}\right)+\log^2\left(\frac{\langle\mathbf{a},\mathbf{a}\rangle}{\langle\mathbf{x},\mathbf{x}\rangle}\right)= \\ =4\arccos^2\left(\frac{\langle\mathbf{x},\mathbf{e}\rangle}{\sqrt{\langle\mathbf{x},\mathbf{x}\rangle}}\right)+\log^2\left(\langle\mathbf{x},\mathbf{x}\rangle\right). \tag{3.9}$$

If we apply the well known Euclidean angle formula then $\cos(\varepsilon)=\frac{\langle\mathbf{a},\mathbf{x}\rangle}{\sqrt{\langle\mathbf{a},\mathbf{a}\rangle\langle\mathbf{x},\mathbf{x}\rangle}}$ and $\cos(\delta)=\frac{x}{\sqrt{\langle\mathbf{x},\mathbf{x}\rangle}}$ where the angles ε and δ are the angles $\measuredangle(\mathbf{a},\mathbf{x})$ and $\measuredangle(\mathbf{x},\mathbf{e})$ in Euclidean sense ($0\le\varepsilon,\delta\le\pi$).

$$4\varepsilon^2+\log^2(\langle\mathbf{a},\mathbf{a}\rangle\langle\mathbf{x},\mathbf{x}\rangle^{-1})=4\delta^2+\log^2(\langle\mathbf{x},\mathbf{x}\rangle) \tag{3.10}$$

It is easy to examine some special cases using equation (3.10) of the equidistance surface.

Let us consider that case, where $P_2=(1,a,0,0)$ and $(a\neq 1)$, i.e. P_2 lies on the x-axis and $P_1\neq P_2$.

It is clear that in this case $\varepsilon=\delta$ holds and by (3.10) we obtain:

$$\log^2(\langle\mathbf{a},\mathbf{a}\rangle\langle\mathbf{x},\mathbf{x}\rangle^{-1})=\log^2(\langle\mathbf{x},\mathbf{x}\rangle)\Rightarrow \\ \Rightarrow\sqrt{\langle\mathbf{x},\mathbf{x}\rangle}=\langle\mathbf{a},\mathbf{a}\rangle^{1/4}. \tag{3.11}$$

Thus $\mathcal{S}_{P_1P_2}$ is an Euclidean sphere with centre in the origin of radius $\rho=\langle\mathbf{a},\mathbf{a}\rangle^{1/4}$.

Let us consider that case, where P_2 lies on the base sphere, e.g. $\langle\mathbf{a},\mathbf{a}\rangle=1$.

In this case we get by (3.10) the following equation:

$$4\varepsilon^2+\log^2(\langle\mathbf{x},\mathbf{x}\rangle^{-1})=4\delta^2+\log^2(\langle\mathbf{x},\mathbf{x}\rangle)\Leftrightarrow\varepsilon=\delta. \tag{3.12}$$

This means, if P_2 is on the base sphere, then $\mathcal{S}_{P_1P_2}$ is an Euclidean plane without the origin.

Our projective method gives us a way of investigating homogeneous spaces, which suits to study and solve similar problems (see [7], [8]).

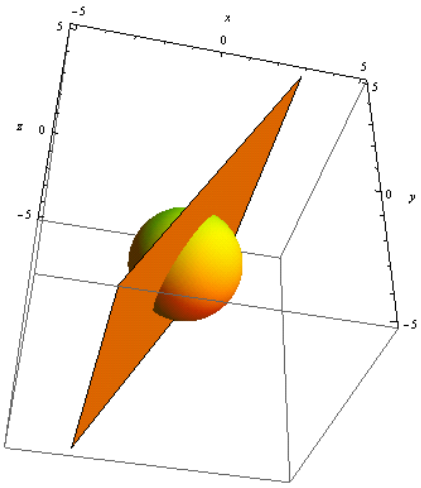

Figure 6: *The equidistant surface $\mathcal{S}_{P_1,P_2}$ with fixed $P_1(1,1,0,0)$ and $P_2:(1,4,0,0)$, in this case the equidistance surface is a spere in Euclidean sense and if $P_2(1,-\frac{1}{2},\frac{\sqrt{3}}{2},0)$, in this case the equidistant surface is a plane without origin in Euclidean sense. These are the special cases discussed in Subsection 3.3.*

References

[1] FARKAS, Z. J., The classification of $\mathbf{S}^2\times\mathbf{R}$ space groups. *Beiträge zur Algebra und Geometrie (Contributions to Algebra and Geometry)* **42**(2001) 235–250.

[2] FARKAS, Z. J., MOLNÁR, E., Similarity and diffeomorphism classification of $\mathbf{S}^2\times\mathbf{R}$ manifolds. *Steps in Diff. Geometry, Proc. of Coll. on Diff. Geom. 25–30 July 2000. Debrecen (Hungary)* (2001) 105–118.

[3] MOLNÁR, E., The projective interpretation of the eight 3-dimensional homogeneous geometries. *Beiträge zur Algebra und Geometrie (Contributions to Algebra and Geometry)* **38** (1997) No. 2, 261–288.

[4] MOLNÁR, E., PROK, I., SZIRMAI, J., Classification of tile-transitive 3-simplex tilings and their realizations in homogeneous spaces. *Non-Euclidean Geometries, János Bolyai Memorial Volume* Ed. PREKOPA, A. and MOLNÁR, E. Mathematics and Its Applications **581**, Springer (2006), 321–363.

[5] MOLNÁR, E., SZILÁGYI, B., Translation curves and their spheres in homogeneous geometries. (to appear in *Publicationes Math. Debrecen*).

[6] SCOTT, P., The geometries of 3-manifolds. *Bull. London Math. Soc.* **15** (1983) 401–487. (Russian translation: Moscow "Mir" 1986.)

[7] SZIRMAI, J., The densest geodesic ball packing by a type of **Nil** lattices. *Beiträge zur Algebra und Geometrie (Contributions to Algebra and Geometry)* **48** (2007), No. 2, 383–398.

[8] SZIRMAI, J., The densest translation ball packing by fundamental lattices in **Sol** space. *Beiträge zur Algebra und Geometrie (Contributions to Algebra and Geometry)*. **51** (2010), No. 2, 353–371.

[9] SZIRMAI, J., Geodesic ball packings in $\mathbf{S}^2\times\mathbf{R}$ space for generalized Coxeter space groups. (manuscript to *Beiträge zur Algebra und Geometrie (Contributions to Algebra and Geometry)*, 2010.)

[10] SZIRMAI, J., Geodesic ball packings in $\mathbf{H}^2\times\mathbf{R}$ space for generalized Coxeter space groups. (to appear in *Mathematical Communications*, 2010.)

[11] THURSTON, W. P. (and LEVY, S. editor), *Three-Dimensional Geometry and Topology.* Princeton University Press, Princeton, New Jersey, Vol **1** (1997).

Jáanos Pallagi
e-mail: jpallagi@math.bme.hu

Benedek Schultz
e-mail: schultz.benedek@gmail.com

Jenö Szirmai
e-mail: szirmai@math.bme.hu

Budapest University of Technology and Economics,
Institute of Mathematics, Department of Geometry
H-1521 Budapest, Hungary

Acknowledgement: We thank Prof. Emil Molnár for helpful comments to this paper.

Originälle wissenschaftliche Arbeit
Angenommen am 21.12.2010.

TIBOR DÓSA

Äquidistant-, Eigen-Äquidistant- und Selbst-Äquidistant-Kurven in der euklidischen Ebene

Equidistant-, Own-Equidistant- and Self-Equidistant-Curves in the Euclidean Plane

ABSTRACT

There are given two curves in the plane. We are looking for the equidistant-curve of both in the following sense: what is the geometric locus of the centers of the circles that are tangent to both given curves? These points are in the same distance from the two given curves. The own-equidistant curve of a given curve is the locus of the centers of the circles that are twice tangent to the curve. The self-equidistant curve of a given curve is the envelope curve of the circles that are tangent to the curve and their centers lay on the curve too. The inverse problem is inspected too, curves c_1 and c_e are given. Which is the curve c_2 so that c_e is the equidistant-curve of c_1 and c_2? About these curves few is known [3], [4], [5], perhaps because one needs for their calculation an efficient computer algebra program. We have investigated only curves of polinomial equation with coefficients of integer numbers in the Euclidean plane. We have used the computer program Mathematica 5.2.

Key words: equidistant curve

MSC 2000: 14H50

Ekvidistantne, vlastito-ekvidistantne i svojstveno-ekvidistantne krivulje u euklidskoj ravnini

SAŽETAK

U ravnini su dane dvije krivulje. Tražimo krivulju koja je od njih jednako udaljena u sljedećem smislu: što je geometrijsko mjesto središta kružnica koje diraju obje dane krivulje? Te točke su jednako udaljene od dviju danih krivulja. Vlastito-ekvidistantna krivulja dane krivulje je geometrijsko mjesto središta onih kružnica koje danu krivulju dodiruju dva puta. Svojstveno-ekvidistantna krivulja dane krivulje je anvelopa kružnica koje diraju danu krivulju, a njihova središta također leže na toj krivulji. Također se proučava i obrnuti problem, dane su krivulje c_1 i c_e. Koja je krivulja c_2 tako da je c_e ekvidistantna krivulja za c_1 i c_2? O ovim krivuljama se malo zna, npr. [3], [4], [5], možda zbog toga što njihovo izračunavanje zahtijeva efikasni algebarski program. Proučavali smo samo krivulje čije su jednadžbe polinomi sa cjelobrojnim koeficijentima u euklidskoj ravnini. Koristili smo program Mathematica 5.2.

Ključne riječi: ekvidistantna krivulja

1 Äquidistant-Kurven

Zwischen zwei Staaten gibt es einen See. Wir suchen die Grenzlinie durch den See, die von beiden Ufern die gleiche Entfernung besitzt. Im allgemeinen, seien zwei ebene Kurven gegeben. Wir suchen den geometrischen Ort der Mittelpunkte der Kreise, die zu beiden Kurven tangent sind. Diese Kurve ist die Äquidistant-Kurve der beiden anderen, weil deren Punkte gleich weit von den beiden entfernt sind.

Sei $G(x_0,y_0,d)$ die Distanz-Funktion einer Kurve, dass heisst $G(x_0,y_0,d)$ = 0, wenn der Punkt (x_0,y_0) von der Kurve in einer Distanz von d liegt. $G(x_0,y_0,d)$ ist eigentlich die Gleichung der Parallelkurve der Kurve mit Distanz d. Wir können die Funktion G einer Kurve C wie folgt bestimmen. Wenn die Kurve C nur aus dem Punkt $P(x,y)$ besteht, dann gilt:

$$G(x_0,y_0,d) = (x-x_0)^2+(y-y_0)^2-d^2 = 0.$$

Sei das Polynom $F(x,y) = 0$ mit ganzzahligen Koeffizienten die Gleichung der Kurve C. Die Gleichung des Kreises um den Punkt (x_0,y_0) ist: $(x-x_0)^2+(y-y_0)^2-d^2 = 0$. Wenn wir aus diesen beiden Gleichungen y elimieren, erhalten wir eine Gleichung $H(x,x_0,y_0,d) = 0$. Der entsprechende Mathematica Befehl ist:

$$H = Resultant[F(x,y),(x-x_0)^2+(y-y_0)^2-d^2,y].$$

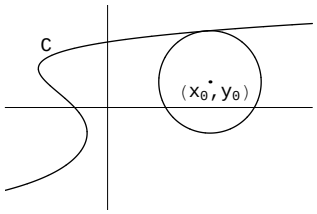

Abbildung 1

Weil der Kreis tangent zur Kurve C ist (Abb. 1), und der tangente Punkt als doppelter Schnittpunkt gilt, ist x eine doppelte Wurzel der Gleichung $H = 0$. Daraus folgt, dass x auch eine Wurzel der Gleichung $\partial H/\partial d = 0$ ist. Wenn aus diesen beiden Gleichungen x eliminiert wird, erhalten wir die Distanz-Funktion der Kurve C. Wenn zum Beispiel C eine Parabel ist, dann:

$$F(x,y) = y - x^2 = 0$$

$$H = (x-x_0)^2 + (x^2-y_0)^2 - d^2$$

$$G(x_0,y_0,d) =$$

$$16(d^2 - x_0^2 + y_0)^3 - (x_0^2 - y_0)^2(1+4y_0)^2 + 8d^4(1-10y_0-2y_0^2)$$

$$+d^2(1+4y_0)(1-12y_0+8y_0^2+4x_0^2(5+2y_0)) = 0$$

für alle Punkte (x_0,y_0) der Ebene.

Seien C_1, C_2 zwei Kurven und G_1, G_2 ihre Distanz-Funktion. Wenn wir aus den letzteren d eliminieren, erhalten wir die Gleichung der zu C_1 und C_2 gehörenden Äquidistant-Kurve. Es ist trivial, dass:

- die Äquidistant-Kurve von zwei Punkten die Streckenhalbierende ist;
- die Äquidistant-Kurve einer Linie und eines Punktes, der nicht auf der Linie liegt eine Parabel ist;
- die Äquidistant-Kurve eines schneidenden Geradenpaares die Winkelhalbierende ist;
- die Äquidistant-Kurven von zwei Kreisen Kegelschnitte sind.

Bei den folgenden Bildern sind die Grundkurven (C_1, C_2 oder C_1, P_1) grün, die Äquidistant-Kurven rot, die Tangent-Kreise blau. Der Einfachheit halber sind die trivialen Äquidistant-Punkte an den Achsen weggelassen.

1. Die Äquidistant-Kurve der Kardioide und des Nullpunktes ist ein Kreis, vgl. Abb. 2.

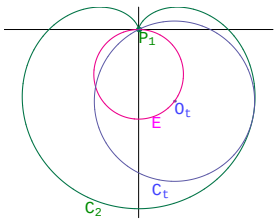

Abbildung 2

2. Die Äquidistant-Kurve der Lemniskate und des Nullpunktes ist eine Hyperbel, vgl. Abb. 3.

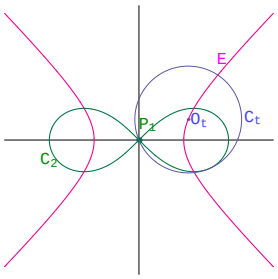

Abbildung 3

3. Die Äquidistant-Kurve der Konchoide $(x^2+y^2)(y-1)^2 = y^2$ und des Nullpunktes besteht aus zwei Kurven. Diese sind die Parallelkurven der Parabel (gelb) $y = -1/2x^2 + 1/2$ mit Abstand $\pm 1/2$. Ihre Gleichung lautet: $16x^6 + 4x^4(-11+16y+4y^2) + x^2(-1-60y+24y^2+64y^3) + y(y-1)(1+8y)^2 = 0$, vgl. Abb. 4.

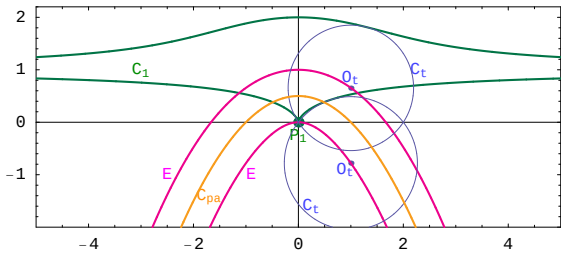

Abbildung 4

4. Die Äquidistant-Kurve des Zweiblattes $(x^2 + (y+1/2)^2)^2 = 4(y+1/2)x^2$ und seines Knotenpunktes $(0,-1/2)$ hat eine dreifache Symmetrie, ihre Gleichung ist: $16(x^2+y^2)^2 + 24x^2(3+8y) + 8y^2(9-8y) - 27 = 0$, vgl. Abb. 5.

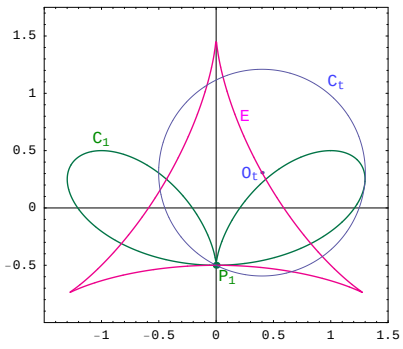

Abbildung 5

5. Die Äquidistant-Kurve der Ellipse $x^2+4y^2=4$ und der Linie $y=-1$ hat die Gleichung $x^6+x^4(-10+8y+14y^2)+x^2(9-132y-194y^2-68y^3+y^4)+108y-72y^3+32y^4-4y^5=0$, vgl. Abb. 6.

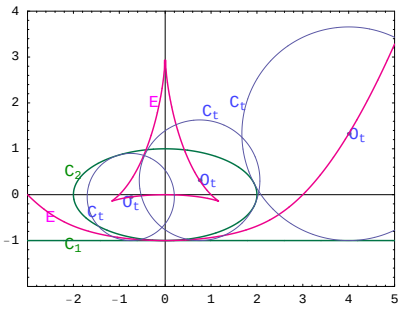

Abbildung 6

2 Eigen-Äquidistant-Kurven

Die Eigen-Äquidistant-Kurve einer gegebenen Kurve C ist der geometrische Ort der Mittelpunkte der Kreise, die zweimal zu C tangent sind. Sei $G(x,y,d)$ die Distanz-Funktion der Kurve C. Wenn für einen Punkt $P(x,y)$ d doppelte Wurzel von G ist, dann ist der Kreis um P mit Radius d zweimal tangent zu C, das heisst, P ist ein Punkt der Eigen-Äquidistant-Kurve. Wenn d die zweifache Wurzel von G ist, dann ist d auch eine Wurzel von $\partial H/\partial d=0$. Wenn wir d aus den beiden Gleichungen eliminieren, erhalten wir die Gleichung der Eigen-Äquidistant-Kurve. Der entsprechende Mathematica Befehl ist:

$Q = Resultant[G(x,y,d), D[G(x,y,d),d], d]$

Die Funktion $Q(x,y)$ besteht meistens aus mehreren Faktoren, relevant sind der von der Eigen-Äquidistant-Kurve und der von der Evolute. Die Evolute kann auch als degenerierte Eigen-Äquidistant-Kurve betrachtet werden, weil der Berührungspunkt des Krümmungskreises doppelt zählt.

1. Es ist bekannt, dass die Eigen-Äquidistant-Kurve der Strophoide $x^2(1+y)=y^2(1-y)$ die Parabel $y=1/4\,x^2$, sowie eine Halbgerade ist. Der Punkt P ist das Zentrum der maximalen Krümmung, vgl. Abb. 7.

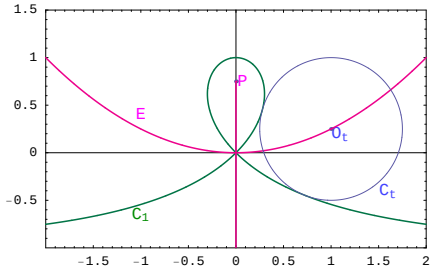

Abbildung 7

2. Die Eigen-Äquidistant-Kurve der Agnesi-Kurve $y(1+x^2)=1$. Auf dem oben gezeigten Weg erhalten wir die implizite Gleichung der Evolute

$11664x^8+x^6(48931-276y-15168y^2+7024y^3+96y^4-1536y^5+1024y^6)-12x^4(-6687+20367y+3718y^2-1908y^3-106y^4+524y^5-276y^6-44y^7+36y^8)-24x^2(-17253+7830y+2160y^2-13230y^3+5392y^4+600y^5-1424y^6+768y^7+64y^8)+16(-1+2y)^3(27+8y^3)^2=0,$

und der Eigen-Äquidistant-Kurve

$1048576x^{10}+16x^8(225333-208416y-86272y^2-38912y^3+8192y^4)+16x^6(288225-704106y+215010y^2+221768y^3+71872y^4+66016y^5-16192y^6-384y^7+256y^8)-8x^4(-257337+1462860y-2120256y^2+1203336y^3-110394y^4+151968y^5+214400y^6+32640y^7-18688y^8-512y^9+1024y^{10})+8x^2(-52488-400221y+1293975y^2-1900260y^3+2035854y^4-1343412y^5+901080y^6-377712y^7+202880y^8-27200y^9-2688y^{10}+1280y^{11}+512y^{12})-(5-4y+4y^2)^2(27+8y^3)^3=0.$

Die gelbe Kurve ist die Evolute, die Punkte P sind ihre Spitzen. Die rote Kurve ist die Eigen-Äquidistant-Kurve, aber nur die Punkte von den beiden Punkten P nach oben sind äquidistant, vgl. Abb. 8.

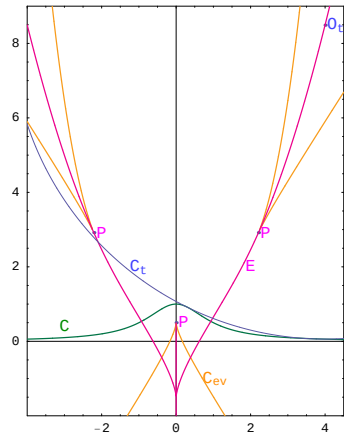

Abbildung 8

3. Nehmen wir die Lissajous-Kurve $x=\cos t$, $y=\sin 2t$. Ihre implicite Gleichung lautet $y^2=4x^2(1-x^2)$. Die gelbe Kurve ist die Evolute, vgl. Abb. 9. Triviale Äquidistant-Punkte sind die y-Achse und die Strecke $(-3,3)$ auf der x-Achse. Überraschenderweise gibt es eine sternförmige Kurve in der Mitte. Die Punkte ausserhalb von den Punkten P sind keine Eigen-Äquidistant-Punkte. Die Punkte P sind die Zentren der maximalen Krümmungen. Die Gleichung der roten Kurve ist $-68719476736y^{20}+<<56\,\text{Terme}>>+42845606719488x^{16}=0$, vgl. Abb. 10.

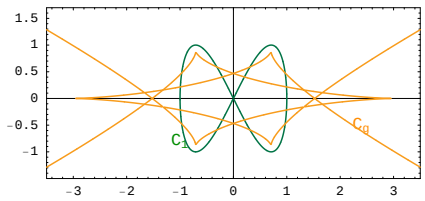

Abbildung 9

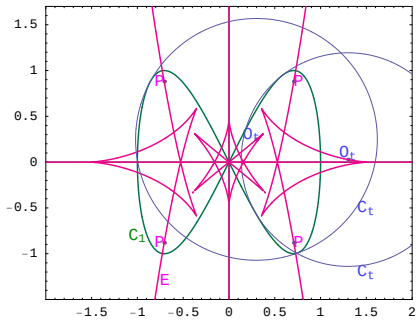

Abbildung 10

4. Die Eigen-Äquidistant-Kurve der einfachen Lamesche-Kurve $y^4+x^4=1$ bildet eine schöne sternförmige Kurve. Ihre Gleichung lautet $1073741824(x^{88}+y^{88})+$ << 527 Terme >>$=0$, vgl.Abb. 11.

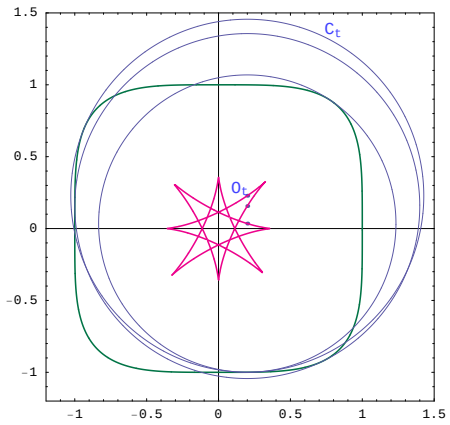

Abbildung 11

5. Nehmen wir noch die Lissajous-Kurve: $x=\sin 2t+1/4\cos 3t$, $y=-\cos 2t-1/4\sin 3t$. Ihre Eigen-Äquidistant-Kurve sieht noch dekorativer aus, die entsprechende Gleichung ist $78732x^{46}+$ << 568 Terme >> $+(246037500+1968300x^2)y^{44}=0$, vgl. Abb. 12.

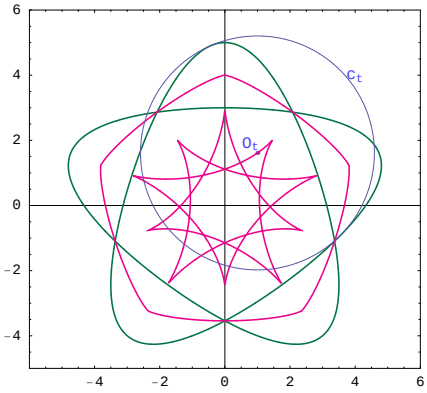

Abbildung 12

3 Selbst-Äquidistant-Kurven

Die Selbst-Äquidistant-Kurve einer Kurve C ist die Hüllkurve der Kreise, die tangent zu C sind und deren Mittelpunkte auf der Kurve C liegen. Sei F(x,y)=0 die Gleichung der Kurve C und $G(x_0,y_0,d)$ ihre Distanz-Funktion.

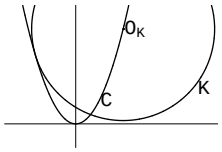

Abbildung 13

Die Gleichung des Kreises K ist $(x-x_0)^2+(y-y_0)^2=d^2$ wobei $F(x_0,y_0)=0$. Diese zwei Gleichungen definieren eine Kreisschar. Ihre Hüllkurve erhalten wir so:

- zuerst eliminieren wir d aus K und G, wir erhalten $H(x,y,x_0,y_0)$;
- dann eliminieren wir x_0 aus H und F, wir erhalten $J(x,y,y_0)$;
- schliesslich eliminieren wir y_0 aus J und $\partial J/\partial y_0$.

1. Die Selbst-Äquidistant-Kurve der Parabel $y=x^2$ hat die folgende Gleichung $x^4(1+2y)+2x^2(1+y)(-5-10y+y^2)-2(1+2y+3y^2)^2=0$, vgl. Abb. 14.

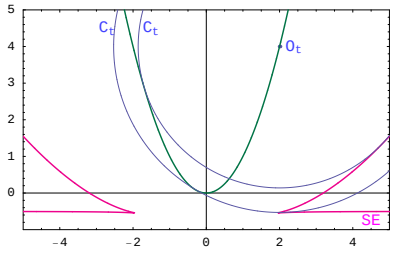

Abbildung 14

2. Zu der Ellipse $(x/2)^2 + y^2 = 1$ gehörende Selbst-Äquidistant-Kurve hat die folgende Gleichung $196y^{10} + y^8(-6132 + 953x^2) + 4y^6(9738 - 7179x^2 + 463x^4) + 2y^4(139212 + 109719x^2 - 24354x^4 + 899x^6) + 4y^2(-424683 - 176175x^2 + 86013x^4 - 8949x^6 + 218x^8) + (-36 + x^2)(441 - 138x^2 + 13x^4)^2 = 0$, vgl. Abb. 15.

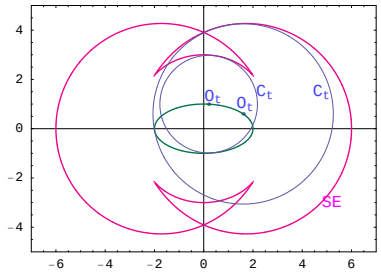

Abbildung 15

3. Die Selbst-Äquidistant-Kurve der Hyperbel $x^2 - y^2 = 1$ hat die folgende Gleichung $16y^{10} + 16y^8(7 + 3x^2) + 8y^6(-31 - 8x^2 + 4x^4) - 8y^4(-42 + 159x^2 + 44x^4 + 4x^6) - y^2(207 + 8x^2(-100 - 159x^2 + 8x^4 + 6x^6)) + (9 - x^2)(3 + 4x^2(1 + x^2))^2 = 0$, vgl. Abb. 16.

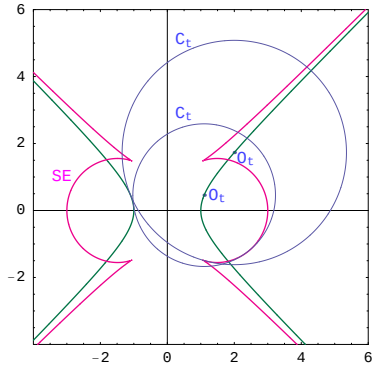

Abbildung 16

4. Die Gleichung der Selbst-Äquidistant-Kurve der Strophoide ist $4x^{30} + << 248 \text{ Terme} >> + 4y^{30} = 0$, vgl. Abb. 17.

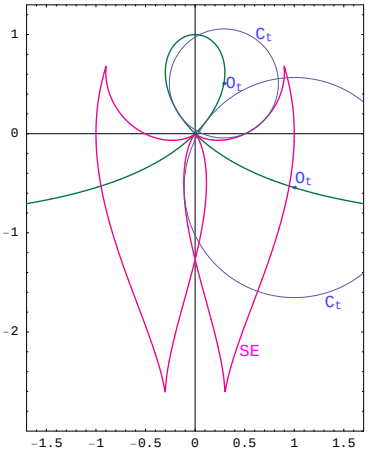

Abbildung 17

4 Inverse und offene Probleme

Gegeben sind zwei Kurven C_0 und C_e. Wir suchen die Kurve C_2, dass C_e die Äquidistant-Kurve von C_1 und C_2 ist. C_2 ist einfach die Hüllkurve der Kreise, die tangent zu C_1 sind, und ihre Mittelpunkte auf C_e liegen.

1. Sei C_1 die Linie der x-Achse und C_e der Kreis $x^2 + y^2 = 1$.

Die Gleichung der obigen Kreise lautet:

$(x - x_0)^2 + (y - y_0)^2 - y_0^2 = 0.$ (EK)

Ihre Mittelpunkte liegen auf C_e:

$x_0^2 + y_0^2 - 1 = 0.$ (EE)

Zuerst eliminieren wir x_0 aus EK und EE:

$R1 = Resultant[\text{EK}, \text{EE}, x_0]$,

dann y_0 aus $\partial R1/\partial y_0$:

$R2 = Resultant[R1, D[R1, y_0], y_0]$.

Wir erhalten so die Gleichung der Kurve C_2, sie ist die Nephroide $4(x^2 + y^2 - 1)^3 = 27y^2$, vgl. Abb. 18.

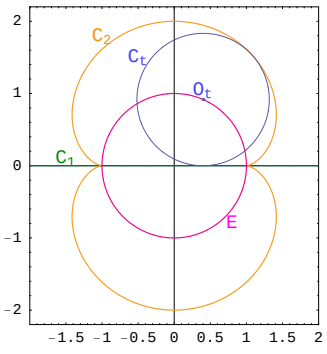

Abbildung 18

2. Sei C_1 die Konchoide $(x_0^2+y_0^2)(y_0-1)^2=y_0^2$ und C_e der Punkt $P_1(0,1)$. Wir suchen die Hüllkurve der Kreise $(x-x_0)^2+(y-y_0)^2=x_0^2+(y_0-1)^2$. Eliminierend x_0, y_0, erhalten wir:

$x^{10}+x^8(7-12y+5y^2)+2x^6(297-104y+42y^2-24y^3+5y^4)+2x^4(-61-492y+783y^2-304y^3+105y^4-36y^5+5y^6)+x^2(-1+y)^3(355+345y-242y^2+82y^3-33y^4+5y^5)+(-3+y)(-1+y)^9=0$

Die Konchoide ist die Äquidistant-Kurve der gelben Kurve und des Punktes P_1, vgl. Abb. 19.

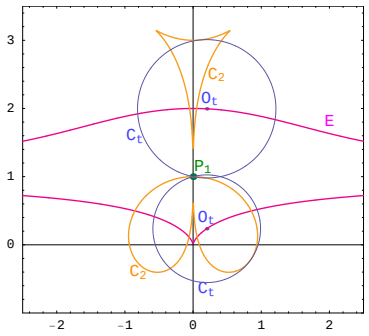

Abbildung 19

3. Wie wir schon gesehen haben, ist die Parabel die Eigen-Äquidistant-Kurve der Strophoide. Es gibt aber undendlich viele Kurven, deren Eigen-Äquidistant-Kurve auch einen Parabel-Bogen besitzt. Nehmen wir die folgende Kurve dritten Grades (grün) $8y^3+8y(x^2-1)+(2x-1)^2=0$. Wie die blauen Kreise zeigen, sind die Punkte der Parabel $y=x^2$ äquidistant, vgl. Abb. 20.

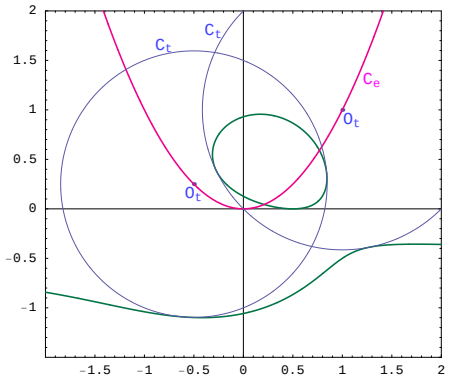

Abbildung 20

4. Die Frage der Anti-Selbst-Äquidistant-Kurve bleibt offen. Z.B. welche Kurve hat die Parabel als Selbst-Äquidistant-Kurve? Gibt es Kurven C_1, C_2 so, dass C_2 die Selbst-Äquidistant-Kurve von C_1 ist und C_1 die Selbst-Äquidistant-Kurve von C_2 ist?

Literatur

[1] DO CARMO, M., *Differential Geometry of Curves and Surfaces*. Prentice Hall, 1976.

[2] GRAY, A., *Differentialgeometrie*. Spektrum, 1994.

[3] DINGELDEY, H., *Die einfachsten Metridistanten*. Radebeul, 1914.

[4] LORIA, G., *Spezielle algebraische und transscendente ebene Kurve*. Teubner, Leipzig 1902., Seite: 711

[5] SCHMIDT, H., *Ausgewählte höhere Kurven*. Wiesbaden, 1949.

Tibor Dósa
Pi Software
Simon 3, 8300 Tapolca, Hungary
e-mail: dosa.tibor@t-online.de

Original scientific paper
Accepted 23. 12. 2010.

SONJA GORJANC
TIBOR SCHWARCZ
MIKLÓS HOFFMANN*

On Central Collineations which Transform a Given Conic to a Circle

On Central Collineations which Transform a Given Conic to a Circle

ABSTRACT

In this paper we prove that for a given axis the centers of all central collineations which transform a given proper conic c into a circle, lie on one conic cc confocal to the original one. The conics c and cc intersect into real points and their common diametral chord is conjugate to the direction of the given axis.

Furthermore, for a given center S the axes of all central collineations that transform conic c into a circle form two pencils of parallel lines. The directions of these pencils are conjugate to two common diametral chords of c and the confocal conic through S that cuts c at real points.

Finally, we formulate a theorem about the connection of the pair of confocal conics and the fundamental elements of central collineations that transform these conics into circles.

Key words: central collineation, confocal conics, Apollonian circles

MSC 2010: 51N05, 51A05, 51M15

O perspektivnim kolineacijama koje danu koniku preslikavaju u kružnice

SAŽETAK

U članku je dokazano da središta svih perspektivnih kolineacija koje s obzirom na zadanu os preslikavaju danu koniku c u kružnicu, leže na jednoj konici cc konfokalnoj s početnom konikom. Konike c i cc imaju realna sjecišta, a njihova zajednička dijametralna tetiva konjugirana je smjeru zadane osi kolineacije.

Nadalje je dokazano da osi svih prespektivnih kolineacija koje s obzirom na zadano središte S preslikavaju danu koniku c u kružnicu, čine dva pramena paralelnih pravaca. Smjerovi tih pramenova konjugirani su zajedničkim dijametralnim tetivama konike c i njoj konfokalne konike koja sadrži točku S i realno siječe c.

Na kraju je formuliran teorem koji govori o vezi para konfokalnih konika i temeljnih elemenata perspektivnih kolineacija koje te konike preslikavaju u kružnice.

Ključne riječi: perspektivna kolineacija, konfokalne konike, Apolonijeve kružnice

1 Introduction

Central collineation is a classical and widely studied transformation in projective geometry. Basic properties of this transformation can be found in any textbook of the field, including the well-known fact that it can transform any proper conic into a circle. The standard way of applying this fact in drawing is that a given conic c, the center S and the axis a of the central collineation is chosen in a proper way, using the most suitable, simplest transformation to transfer c to a circle.

In this paper we consider this problem in a more constrained way. Given a conic c and a line a, we try to find all the centers S with which the central collineation with center S and axis a transforms c into a circle. Alternatively, given a conic c and a point S, we try to find all the axes a with which the central collineation with center S and axis a transforms c into a circle. These two problems are solved in Section 3 and 4. Before these results, we briefly present the necessary facts about pencils of circles and confocal conics in Section 2.

The aim of this study is not purely theoretic. Our future purpose is to classify special transformations, called quadratic projections, which are geometric abstractions of omnidirectional vision tools and cameras [2]. This practical equipment is of central importance in robotics, and the geometry of these tools are heavily influenced by the projective geometric issues studied in the present paper.

* Supported by János Bolyai Scholarship of Hungarian Academy of Sciences.

2 Pencils of circles and confocal conics

In this section we collect some basic properties of a pencil of circles and a range of confocal conics. Both structures will be used throughout the following sections, so it may be worth to recall the necessary facts about them. These issues can be found in several books of the field, e.g. in [1], [3], [4], [5], [6], [7], [8].

A *pencil of circles* is the set of circles which pass through two given points. It is an elliptic, hyperbolic or parabolic pencil if these intersection points are real and different, imaginary or coinciding, respectively. See fig. 1.

The circles of elliptic, hyperbolic and parabolic pencils cut the central line into the pairs of elliptic, hyperbolic and parabolic involution, respectively. Every point on the radical axis has the same point's circle power with respect to all circles of the pencil. On the radical axis all circles of the pencil induce the same polar involution that is hyperbolic, elliptic or parabolic, if the pencil is elliptic, hyperbolic or parabolic, respectively. Every pencil contains its radical axis and the line at infinity as a splitting circle. Only the hyperbolic pencils contain two imaginary circles that are two pairs of isotropic lines with real intersection points that are called the Poncelet's points.

Appolonian circles are two pencils of circles such that every circle of the first pencil cuts every circle of the second pencil orthogonally, and vice versa. If the first pencil is elliptic, the second is hyperbolic. If the first pencil is parabolic, the second is parabolic, too. See figures 2, 3.

All circles of one pencil induce the same polar involution on its radical axis. This involution is the same as the intersection involution that the corresponding Apollonian pen-

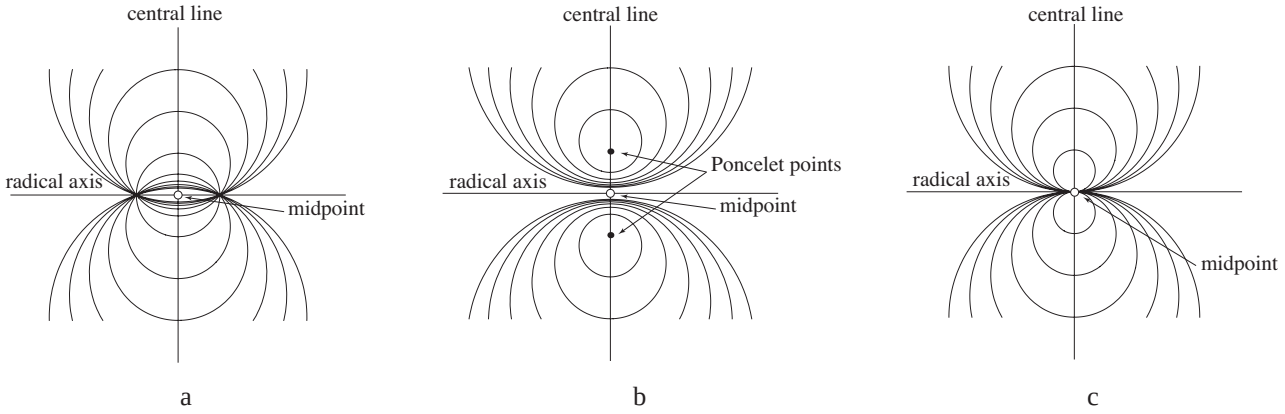

Figure 1: *An elliptic, hyperbolic and parabolic pencil of circles are shown in figures a, b and c, respectively.*

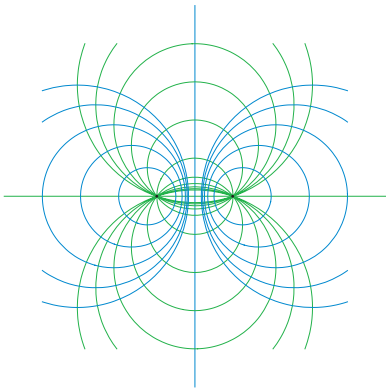

Figure 2: *One family of elliptic and hyperbolic pencils of orthogonal circles*

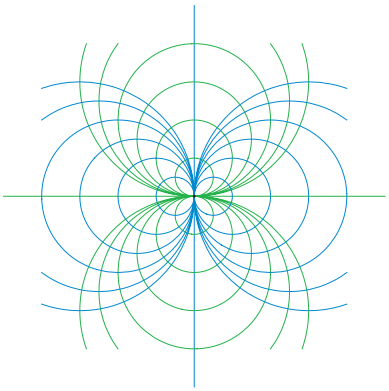

Figure 3: *One family of two orthogonal parabolic pencils*

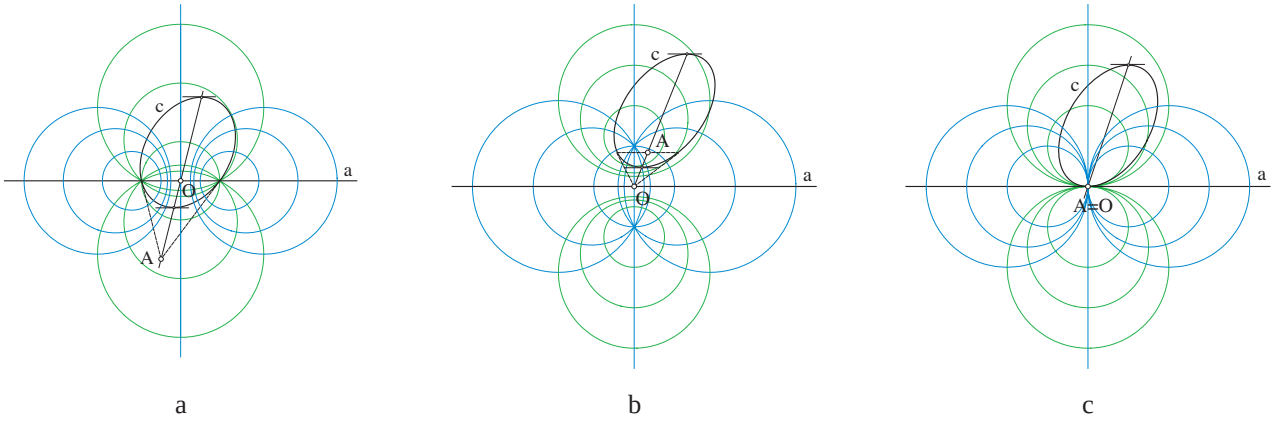

a b c

Figure 4: *A is the pole of a with respect to c, and O is the midpoint of the orthogonal pencils of circles. The conic c and the line a with real and different, imaginary or coinciding intersection points, together with the corresponding Apollonian circles, are shown in figures a, b and c, respectively.*

cil induces on its central line. For Apollonian circles the Poncelet's points of the hyperbolic pencil are the Laguerre's points of the elliptic pencil.

For every conic c and a line a such that A^∞ (the point at infinity of the line a) is an external point of c, exists one family of orthogonal circles such that one pencil cuts the line a at the same points as the conic c, and another cuts the line a into the pairs of polar involution induced by c on a, see fig. 4.

The family of *confocal conics* is a range of conics defined by two pairs of isotropic tangent lines that always have two real intersection points called real foci F_1, F_2. If one focus is the point at infinity, all confocal conics are parabolas. In all other cases a confocal range consists of ellipses and hyperbolas. Through every point P in the plane, two conics of a confocal range pass, and they cut orthogonally. If one of these conics is an ellipse, the other one is a hyperbola and vice versa.

The tangent lines at P to these conics bisect the angles between the tangents from P to any other conic of the confocal system (these tangents can be real and different, imaginary[1] or coinciding). The lines PF_1 and PF_2 are equally inclined to the tangents from P to any one of the conics of the system, see figures 5, 6.

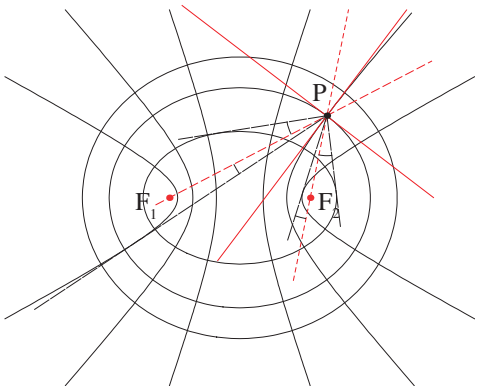

Figure 5: *The range of confocal ellipses and hyperbolas*

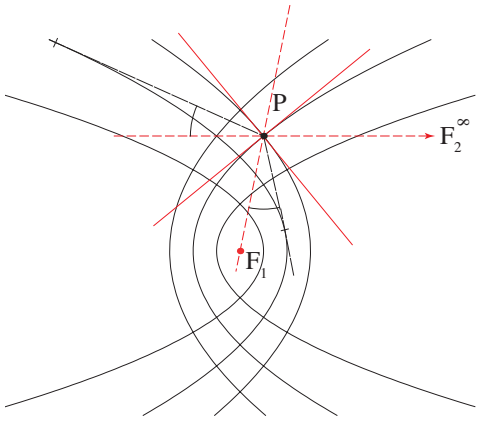

Figure 6: *The range of confocal parabolas*

[1] About the real bisectors of imaginary lines see [6, p. 70].

3 Collineations with given axis

Let c and a be a given conic and a line, and let A^∞ be the point at infinity on the line a. In this section we consider the following problem: where are the centers of all central collineations with a given axis a that transform a conic c into circles?

Lemma 1 *If a point A^∞ lies on the conic c or if it is an internal point of c, there does not exist any central collineation with the axis a that transforms c into a circle.*

PROOF: Since the real or imaginary character of points and lines is invariant under a central collineation, then it transforms interior and exterior of a given conic c into the interior and exterior of the image of c. For every circle, A^∞ is an external point. Therefore, all parabolas and hyperbolas that pass through A^∞ as well as all hyperbolas with A^∞ as an internal point, could not be transformed into a circle by any central collineation with the axis a. □

Theorem 1 *For a given straight line a and a conic c, where $A^\infty \in Ext\, c$, the centers of all central collineations with the axis a that transform c into circles lie on one conic cc that is confocal to c. If a is not parallel to any axis of c, the conic cc is an ellipse, hyperbola or parabola, if c is a hyperbola, ellipse or parabola, respectively.*

PROOF:
• Let a and c ($A^\infty \in Ext\, c$) intersect in two different points D_1, D_2, let $\mathcal{P}(c,a)$ be a pencil of circles that intersect the line a at the same points D_1 and D_2 and let O be the midpoint of $\mathcal{P}(c,a)$. The line a is the radical axis of $\mathcal{P}(c,a)$, the line aa through O orthogonal to a is its central line and the pencil is elliptic or hyperbolic if D_1, D_2 are real or imaginary points, respectively. Let A be the pole of a with respect to c. OA is the diameter of c conjugate to the direction of a. Let T and $\overline{T}$ be the intersection points of the diameter OA and the conic c. If c is a parabola one of these points is the point at infinity. See fig. 7.

For every circle $c' \in \mathcal{P}(c,a)$ there are two central collineations with the axis a that transform c into c'. These collineations transform the diametral chord $T\overline{T}$ of c into the diametral chord T_1T_2 of c' lying on aa. The intersections of corresponding rays TT_1, $\overline{T}T_2$ or TT_2, $\overline{T}T_1$ are the centers S^1 and S^2 of these collineations, respectively. S^1 and S^2 are collinear with A and A', where A' is the pole of c' with respect to a, because polarity is invariant under a central collineation. Since the points T_1 and T_2 correspond involutory (the pair of intersections of $c' \in \mathcal{P}(c,a)$ and aa), then varying c', the mappings $TT_1 \longrightarrow \overline{T}T_2$ and $TT_2 \longrightarrow \overline{T}T_1$ define the same projectivity $(T) \barwedge (\overline{T})$. The resulting curve of this projectivity is a conic cc that contains the centers of all central collineations with the axis a which transform c into circles. The points T and $\overline{T}$ that correspond to the splitting circle (c' breaks up into the line a and the line at infinity) are excluding as the centers of requested central collineations.

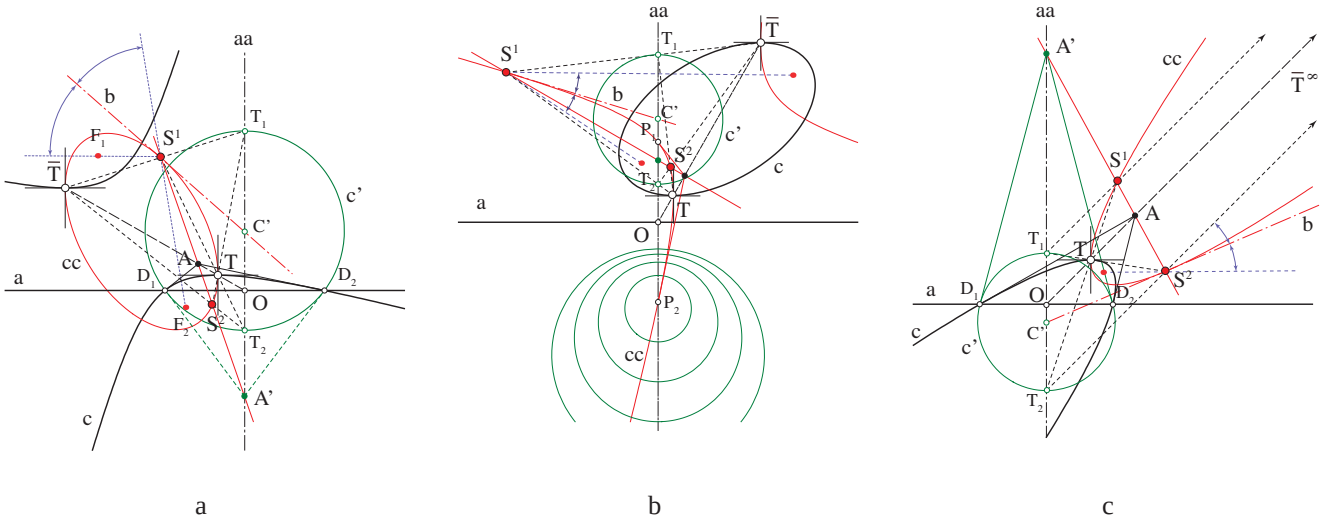

a b c

Figure 7: *In figure a, conic c is a hyperbola, D_1, D_2 are real points and cc is an ellipse that cuts aa at imaginary points. In figure b, conic c is an ellipse, D_1, D_2 are imaginary points and cc is a hyperbola that cuts aa at Poncelet's points of $\mathcal{P}(c,a)$. In figure c, conic c is a parabola, D_1, D_2 are real points and cc is a parabola that cuts the line aa at the pair of imaginary points.*

The point S^1 is the intersection of common tangents of c and c' that can be real or imaginary. Therefore, a line b that passes through S^1 and C', where C' is the center of the circle c', bisects the angle $\measuredangle F_1S^1F_2$ (where F_1, F_2 are the foci of c) and it is the tangent line of cc at S^1. Namely, if we suppose that b cuts cc at any other point $S \neq S^2$ (S^1S^2 cuts aa at $A' \neq C'$), then S would be the third solution that transform c into c' which is impossible according to the previous considerations. Thus, the tangent line at every point S^1 of the conic cc bisects the angle $\measuredangle F_1S^1F_2$, i.e. F_1 and F_2 are the foci of cc, see fig. 7. The conic cc cuts the line aa at two double points of the involution $T_1 \longleftrightarrow T_2$, that are imaginary if $\mathcal{P}(c,a)$ is elliptic or real Poncelet's points P_1, P_2 if it is hyperbolic.

Since the conics c and cc intersect each other in the real points T, $\overline{T}$, cc is a hyperbola, ellipse or parabola, if c is an ellipse, hyperbola or parabola, respectively.

• Let a be the tangent of c with a touching point O and let T be another intersection point of c and the diameter of c through O (if c is a parabola, T is the point at infinity). Let c' be a circle with the center C' that touches a at the point O and let T' be another intersection point of the diameter of c' through O and c'. It is clear that there exists a unique central collineation with the center S and the axis a that transform T and T' and the conic c into c', see fig. 8. Since the conics c and c' have common tangent lines t_1, t_2 through S (real and different, imaginary or coinciding) they also have a common bisector b of these tangents through S. This line b also bisects the angle $\measuredangle F_1SF_2$ and is the tangent at S of a conic cc that is confocal to c and passes through the points T and O. Thus, every point on the conic cc is the center of one central collineation that transforms c into a circle. On the other hand, every circle $c' \in \mathcal{P}(c,a)$ defines the unique solution S that is the touching point of the tangent b from C' to the conic cc (another tangent through C' to cc is the line aa with the touching point O), i.e. all solutions lie on the conic cc.

Since the conics c and cc intersect each other in the real points O and T, cc is a hyperbola, ellipse or parabola, if c is an ellipse, hyperbola or parabola, respectively.

• If the line a is perpendicular to one axis of the conic c, all centers of central collineations that transform c into circles lie on the central line aa of the pencil $\mathcal{P}(c,a)$. Namely, for every $c' \in \mathcal{P}(c,a)$ there exists $S \in aa$ that is the intersection of common tangent lines of c and c' (these tangent lines can be real or imaginary). The point S is the center of central collineation that transforms c into c'. The line aa is the part of a splitting conic that is confocal to c. In the cases when c is an ellipse or hyperbola, the confocal conic splits into the axes of c, and if c is a parabola it splits into its axis and the line at infinity. □

In the case when c is an ellipse, the conic cc is a hyperbola with two real points at infinity and the pencil of circles $\mathcal{P}(c,a)$ contains two circles into which the given ellipse is transformed by an affinity. The construction of these circles is a solution of a classical task in constructive geometry: The centers of these circles are the intersection points of the line aa and one circle, where the diameter of this circle is formed by the intersection points of the given line a and the axes of the ellipse.

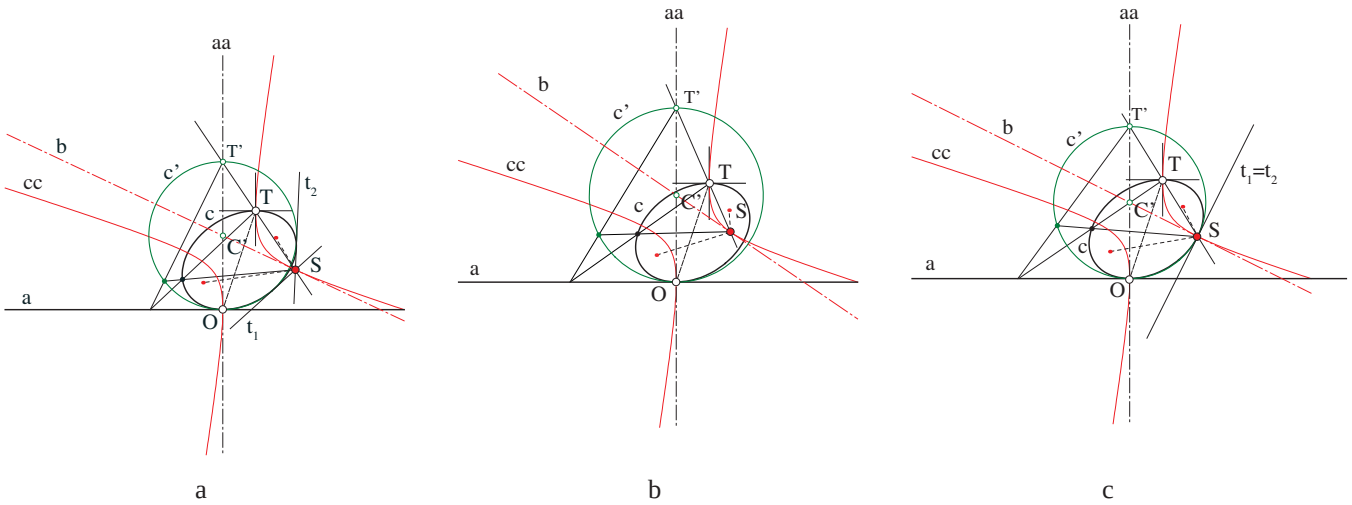

a b c

Figure 8: *The illustrations of the above described construction for $S \in Ext\, c$, $S \in Int\, c$ and $S \in c$ are shown in figures a, b and c, respectively.*

4 Collineations with given center

For a given point S and a conic c, the following problem is considered in this section: where are the axes of all central collineations with given center S that transform a given proper conic c into circles?

In the following, by cc_S we denote the confocal conic to c that passes through S and cuts c at real points.

Theorem 2 *For a given point S and a conic c, the axes of all central collineations with the center S that transform c into circles form two pencils of parallel lines with directions conjugate to two common diametral chords of c and* cc_S.

PROOF: Let c and S be any conic and a point and let b be the bisector of the tangent lines of c through S. If c is an ellipse or parabola, b bisects the internal angle $\measuredangle F_1SF_2$ and if c is a hyperbola b bisects the external angle $\measuredangle F_1SF_2$. For every point $C' \in b$ there exists one circle c' such that c and c' have common tangent lines t_1, t_2 through S (real and different, imaginary or coinciding). Let the common diametral chords of c and cc_S be $X\overline{X}$ and $Y\overline{Y}$ (if c is a parabola $\overline{X}$ and $\overline{Y}$ coincide with the point at infinity) and let x and y be the tangent lines at X and Y, respectively. The line b is the tangent line of cc_S at S. Let us consider any two lines $a_1 \parallel x$, $S \notin a_1$, and $a_2 \parallel y$, $S \notin a_2$ and let O_1 and O_2 be the midpoints of the polar involutions that conic c induces on a_1 and a_2, respectively. According to Theorem 1, there are two central collineations with the center S and axes a_1 and a_2 that transform c into circles c_1' and c_2', respectively. The centers of these circles are the intersection points of b and the lines aa_1 and aa_2, perpendicular to a_1 and a_2 through the points O_1 and O_2, respectively. Thus, for every c and S there are two pencils of parallel lines such that every central collineation with the center S and the axis that belongs to one of the pencils transforms c into a circle. See fig. 9.

On the other hand, if c is transformed to a circle by a central collineation with the center S then the polar involution induced by c on the vanishing line is transformed to the circular involution on the line at infinity. The isotropic lines through S cut c into four imaginary points and among six lines that join them only two are real. These two real sides of the complete quadrangle (determined with the four intersections of c and the isotropic lines through S) are the vanishing lines v_1 and v_2 of the requested central collineations. Thus, there are only two directions for axis of central collineatios with the center S that transform c into circles. The lines v_1, v_2 pass through the pole of b with respect to c and must be excluded from the pencils (a_1) and (a_2) as the axes of central collineations because they correspond with the isotropic lines through S in the correspondences $a_1 \longrightarrow c_1'$ and $a_2 \longrightarrow c_2'$, respectively. □

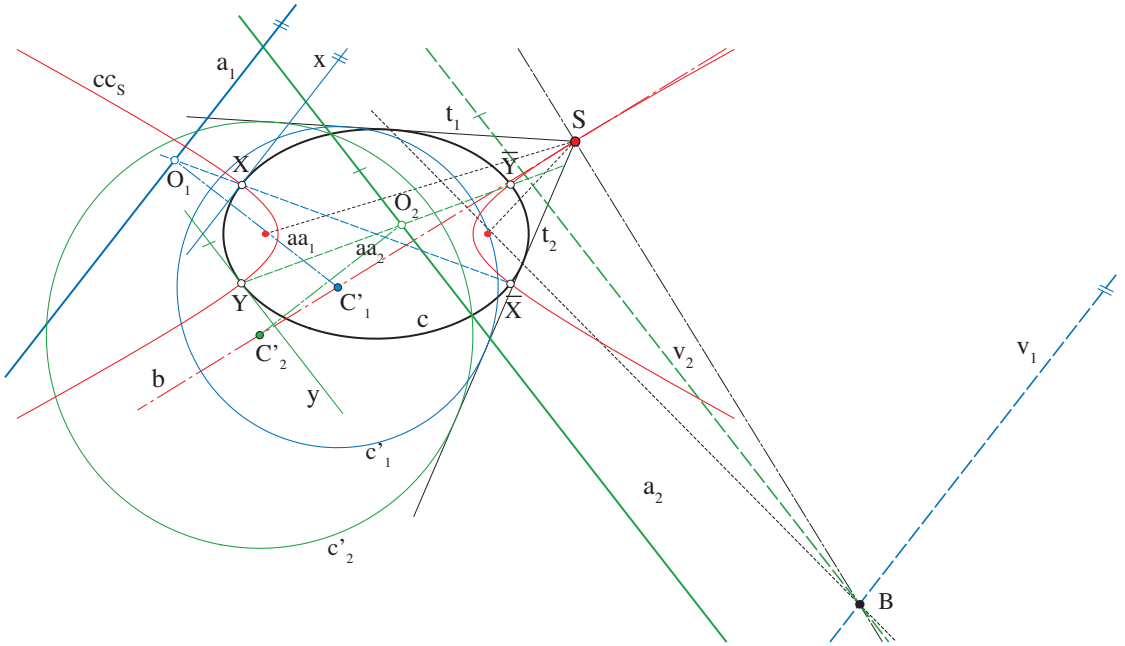

Figure 9: *Circles c_1' and c_2' are the images of c under the central collineations with the center S and axes a_1 and a_2 with vanishing lines v_1 and v_2, respectively. For any other central collineation with center S that transforms c into a circle, the vanishing line is either v_1 or v_2.*

5 Joint collineations of confocal conics

Finally we provide a consequence of the above discussed theorems proving a strong relationship among Apollonian circles, confocal conics and the fundamental elements of central collineations which transform them to circles.

If c_1 and c_2 are proper conics with a center C and common diametral chords $X\overline{X}$ and $Y\overline{Y}$, then for every point $A \in X\overline{X}$, $A \neq C$ ($B \in Y\overline{Y}$, $B \neq C$) the pair of polar lines a_1, a_2 (b_1, b_2) of A (B) with respect to c_1 and c_2, respectively, are orthogonal lines intersecting at a point $\overline{A} \in X\overline{X}$ ($\overline{B} \in Y\overline{Y}$) that is conjugate to A (B) with respect to the conics c_1 and c_2. See fig. 10.

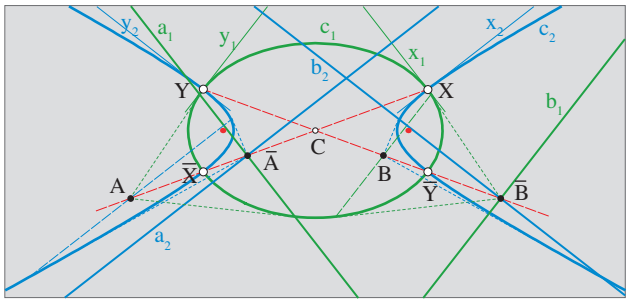

Figure 10: *The polar lines a_1 and a_2 (b_1 and b_2) are parallel to the tangent lines at X (Y) of conics c_1 and c_2, respectively.*

Theorem 3 *Let c_1 and c_2 be proper confocal conics with a center C and common diametral chords $X\overline{X}$ and $Y\overline{Y}$. Let a_1 and a_2 (b_1 and b_2) be any pair of lines conjugate to $X\overline{X}$ ($Y\overline{Y}$) with respect to c_1 and c_2, respectively, intersecting at a point $\overline{A} \in X\overline{X}$, $\overline{A} \neq C$ ($\overline{B} \in Y\overline{Y}$, $\overline{B} \neq C$). Then, the centers S_1, S_2 of all central collineations with axis a_1, a_2 (b_1, b_2) that transform c_1, c_2 into circles lie on the conic c_2, c_1, respectively.*

Varying $S_1 \in c_1$ and $S_2 \in c_2$ the image circles form Apollonian circles with central lines a_2, a_1 (b_2, b_1).

The tangent lines at S_1 and S_2 of conics c_1 and c_2 cut the central lines a_2, a_1 (b_2, b_1) into the centers of circles that correspond to the touching points S_1 and S_2 as the centers of collineations, respectively.

PROOF: The proof follows directly from the proof of theorem 1, properties that are illustrated in fig. 4 and fig. 10 and the fact that confocality of conics and orthogonality of circles are symmetric relations. See figures 11, 12 and 13. □

In the following figures the properties listed in theorem 3 are presented. These figures as well as all previous are produced in the program *Mathematica 7*.

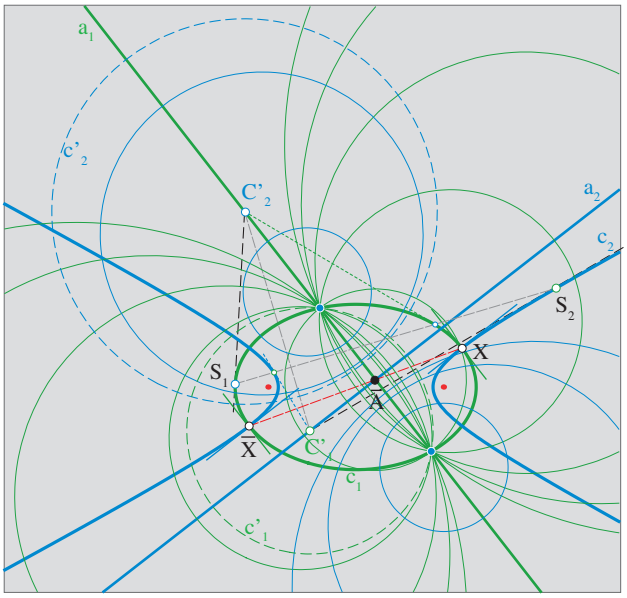

a

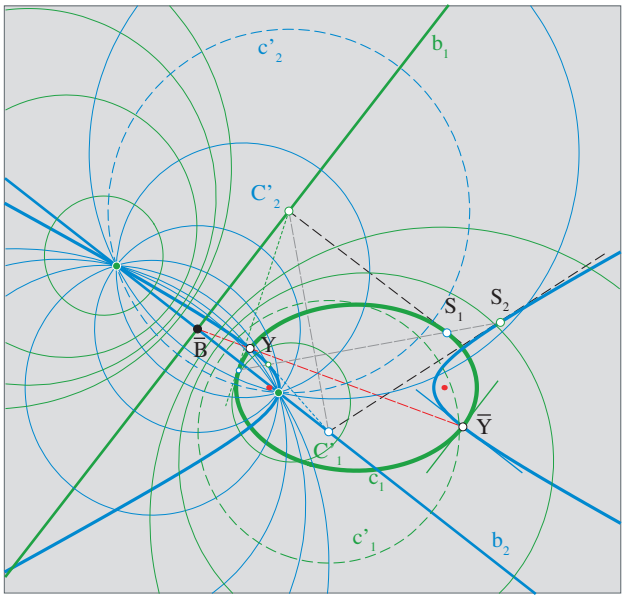

b

Figure 11: *All central collineations with the green (blue) axis and a center on the blue (green) conic transform the green (blue) conic into green (blue) circles. The directions of the axes in figures a and b are conjugate to the common diametral chords of confocal conics. In both figures, the property that the tangent line at a center of collineation passes through the center of image circle is pointed out for the points S_1 and S_2.*

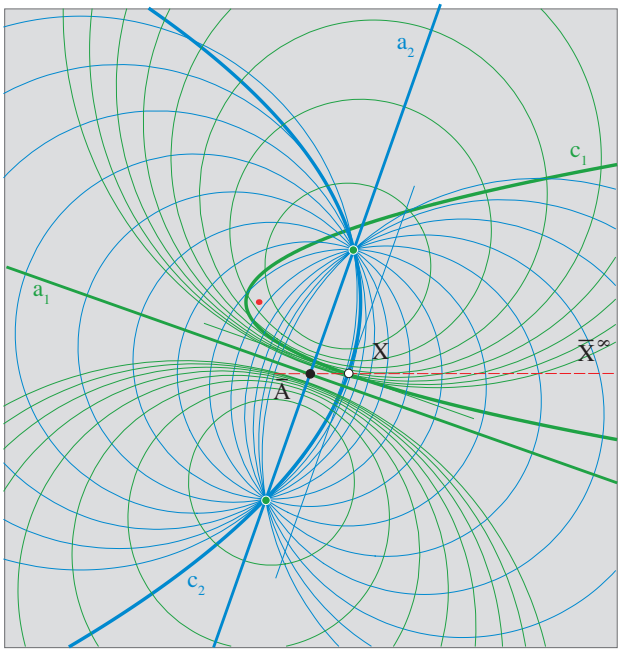

Figure 12: *The illustration of theorem 3 for confocal parabolas c_1 and c_2.*

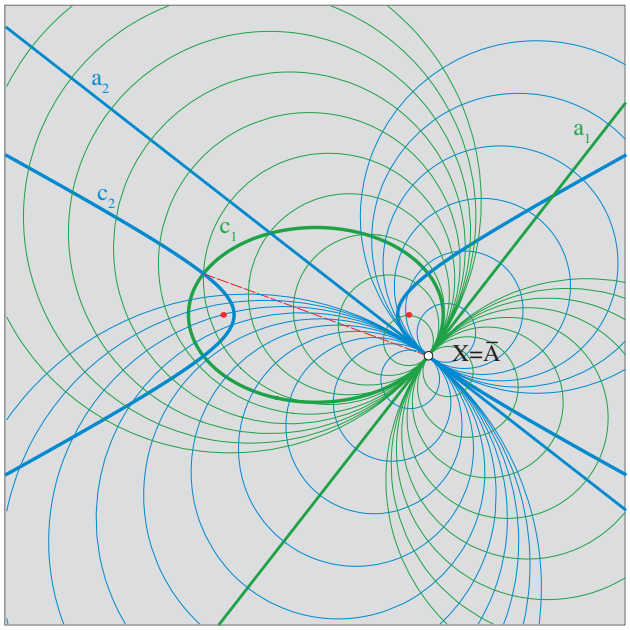

Figure 13: *If the axes a_1 and a_2 coincide with the tangent lines at the intersection point of c_1 and c_2, the image circles form the family of parabolic pencils.*

References

[1] R. CESAREC, Analitička geometrija, Školska knjiga, Zagreb, (1957) (in Croatian).

[2] C. GEYER, K. DANIILIDIS, Catadioptric projective geometry, Intl. Journal of Computer Vision, 45 (2001), 223—243.

[3] H. HILTON, Plane Algebraic Curves, Oxford Universtity Press, London, (1920)

[4] Encyclopaedia of Mathematics - SpringerLink. Edited by M. Hazewinkel, available on-line: http://eom.springer.de/s/s091970.htm

[5] V. NIČE, Sintetička geometrija, Školska knjiga, Zagreb, (1956) (in Croatian).

[6] G. SALMON, A Treatise on Conic Sections, Longmans, Green, Reader and Dyer, London, (1869), available on-line: http://books.google.com

[7] J. G. SEMPLE, G. T. KNEEBONE, Algebraic Projective geometry, Oxford University Press, Oxford, (1952)

[8] M. BERGER, Geometry I-II, Springer-Verlag, Berlin, (1977)

Sonja Gorjanc
Faculty of Civil Engineering
Kačićeva 26, 10000 Zagreb, Croatia
e-mail: sgorjanc@grad.hr

Tibor Schwarcz
Dept. of Computer Graphics and Image Proc.
University of Debrecen
Egyetem sqr. 1, H-4010 Debrecen, Hungary
e-mail: schwarcz@inf.unideb.hu

Miklós Hoffmann
Institute of Mathematics and Computer Science
Károly Eszterházy College
Leányka str. 4., H-3300 Eger, Hungary
e-mail: hofi@ektf.hu

How to get KoG?

The easiest way to get your copy of KoG is by contacting the editor's office:

Nikoleta Sudeta
nsudeta@arhitekt.hr
Faculty of Architecture
Kačićeva 26, 10 000 Zagreb, Croatia
Tel: (+385 1) 4639 219
Fax: (+385 1) 4639 465

The price of the issue is €15 + mailing expenses €5 for European countries and €10 for other parts of the world.

The amount is payable to:

ACCOUNT NAME: Hrvatsko društvo za geometriju i grafiku
Kačićeva 26, 10000 Zagreb, Croatia

IBAN: HR862360000-1101517436

Kako nabaviti KoG?

KoG je najjednostavnije nabaviti u uredništvu časopisa:

Nikoleta Sudeta
nsudeta@arhitekt.hr
Arhitektonski fakultet
Kačićeva 26, 10 000 Zagreb
Tel: (01) 4639 219
Fax: (01) 4639 465

Za Hrvatsku je cijena primjerka 100 KN + 10 KN za poštarinu.

Nakon uplate za:

HDGG (za KoG), Kačićeva 26, 10000 Zagreb
žiro račun broj **2360000-1101517436**

poslat ćemo časopis na Vašu adresu.

Ako Vas zanima tematika časopisa i rad našega društva, preporučamo Vam da postanete članom HDGG (godišnja članarina iznosi 150 KN). Za članove društva časopis je besplatan.

INSTRUCTIONS FOR AUTHORS

SCOPE. "KoG" publishes scientific and professional papers from the fields of geometry, applied geometry and computer graphics.

SUBMISSION. Scientific papers submitted to this journal should be written in English or German, professional papers should be written in Croatian, English or German. The papers have not been published or submitted for publication elsewhere.
The manuscript with wide margins and double spaced should be sent in PDF format via e-mail to the one of the editors:

Sonja Gorjanc
sgorjanc@grad.hr

Jelena Beban - Brkić
jbeban@geof.hr

The first page should contain the article title, authors and coauthors names, affiliation, a short abstract in English, a list of keywords and the Mathematical subject classification.

UPON ACCEPTANCE. After the manuscript has been accepted for publication authors are requested to send its LaTeX file via e-mail to the address:

sgorjanc@grad.hr

Figures should be included in EPS or PS formats.

OFFPRINTS. The corresponding author and coauthors will receive hard copies of the issue free of charge and a PDF file of the article via e-mail.

UPUTE ZA AUTORE

PODRUČJE. "KoG" objavljuje znanstvene i stručne radove iz područja geometrije, primijenjene geometrije i računalne grafike.

UPUTSTVA ZA PREDAJU RADA. Znanstveni radovi trebaju biti napisani na engleskom ili njemačkom jeziku, a stručni na hrvatskom, engleskom ili njemačkom. Rad ne smije biti objavljen niti predan na recenziju drugim časopisima.
Rukopis sa širokim marginama i dvostrukim proredom šalje se u PDF formatu elektronskom poštom na adresu jedne od urednica:

Sonja Gorjanc
sgorjanc@grad.hr

Jelena Beban - Brkić
jbeban@geof.hr

Prva stranica treba sadržavati naslov rada, imena autora i koautora, podatke o autoru i koautorima, sažetak na hrvatskom i engleskom, ključne riječi i MSC broj.

PO PRIHVAĆANJU RADA. Tekst prihvaćenog rada autor dostavlja elektronskom poštom kao LaTeX datoteku, a slike u EPS ili PS formatu, na adresu:

sgorjanc@grad.hr

POSEBNI OTISCI. Svaki autor i koautor dobiva po jedan tiskani primjerak časipisa i PDF datoteku svog članka.

ISSN 1331-1611